Greenhouse-gas emissions from inland waters modulated by wetlands: African systems with a special focus on Congo

Alberto V. Borges
University of Liège (Belgium)

www.co2.ulg.ac.be

Global cycles of CO_2 and CH_4
&
Climate Change

Introduction

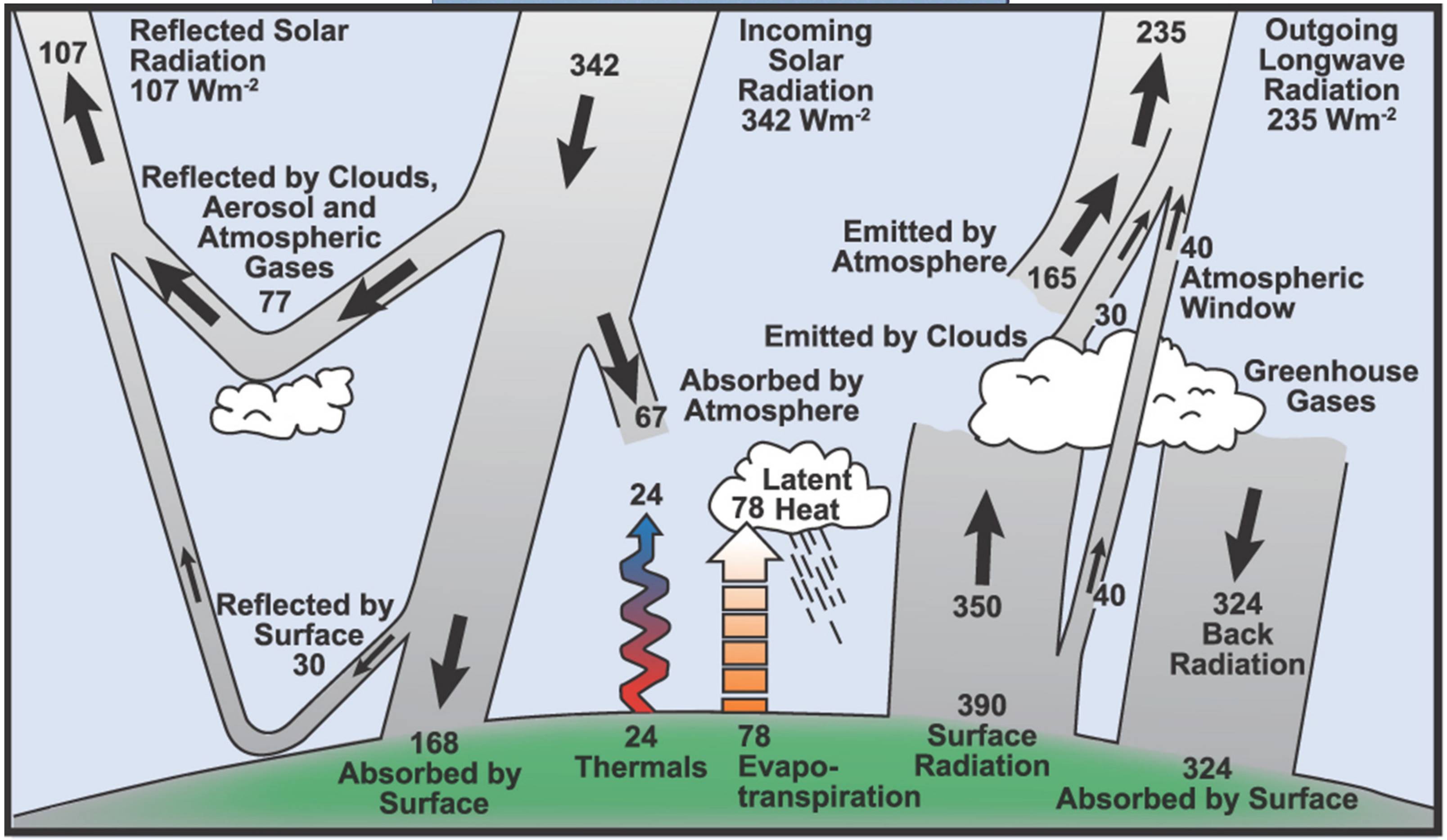

Introduction

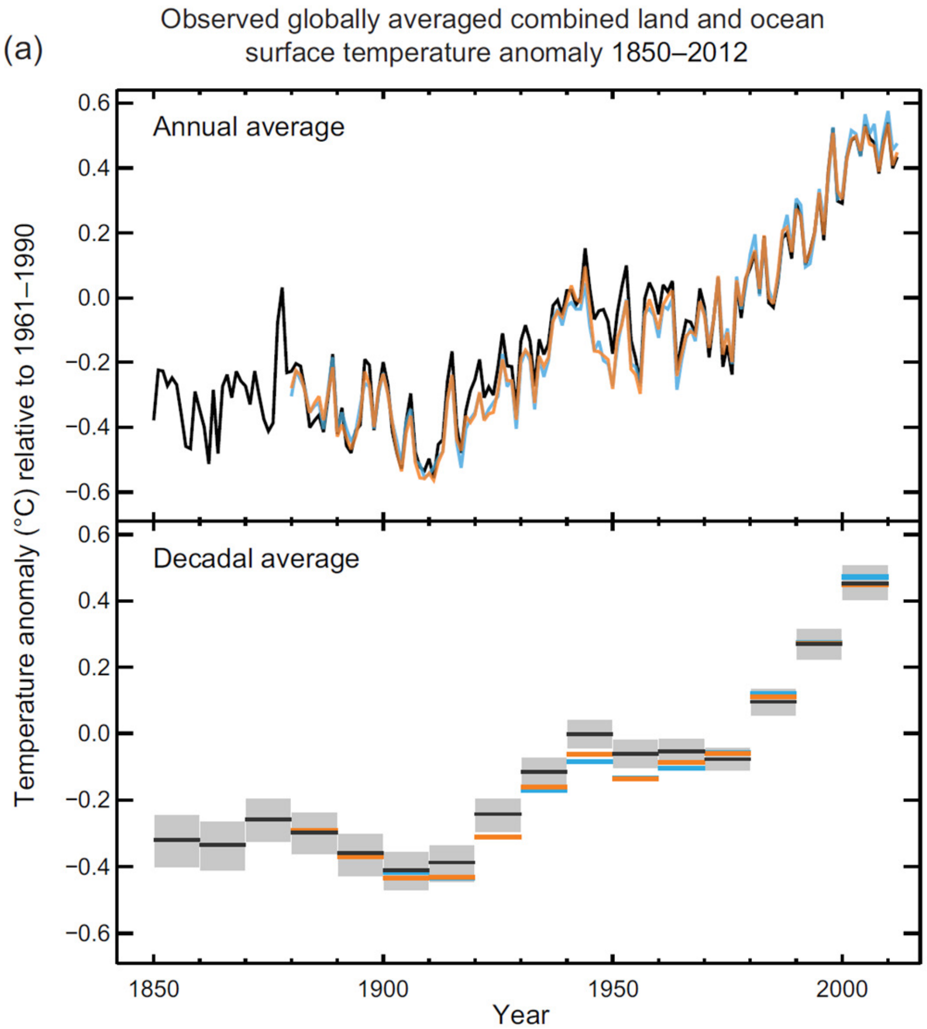

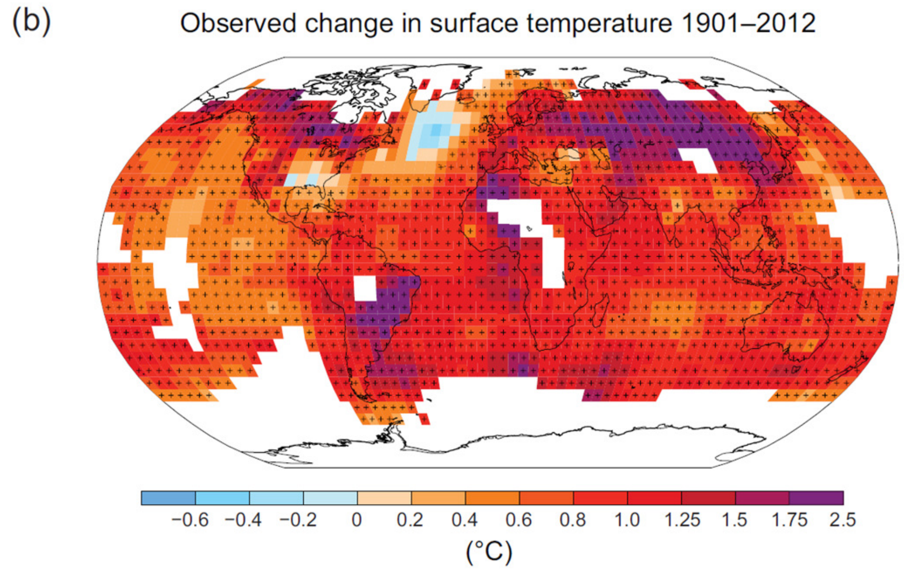

Figure SPM.1 | (a) Observed global mean combined land and ocean surface temperature anomalies, from 1850 to 2012 from three data sets. Top panel: annual mean values. Bottom panel: decadal mean values including the estimate of uncertainty for one dataset (black). Anomalies are relative to the mean of 1961–1990. (b) Map of the observed surface temperature change from 1901 to 2012 derived from temperature trends determined by linear regression from one dataset (orange line in panel a). Trends have been calculated where data availability permits a robust estimate (i.e., only for grid boxes with greater than 70% complete records and more than 20% data availability in the first and last 10% of the time period). Other areas are white. Grid boxes where the trend is significant at the 10% level are indicated by a + sign. For a listing of the datasets and further technical details see the Technical Summary Supplementary Material. {Figures 2.19–2.21; Figure TS.2}

Introduction

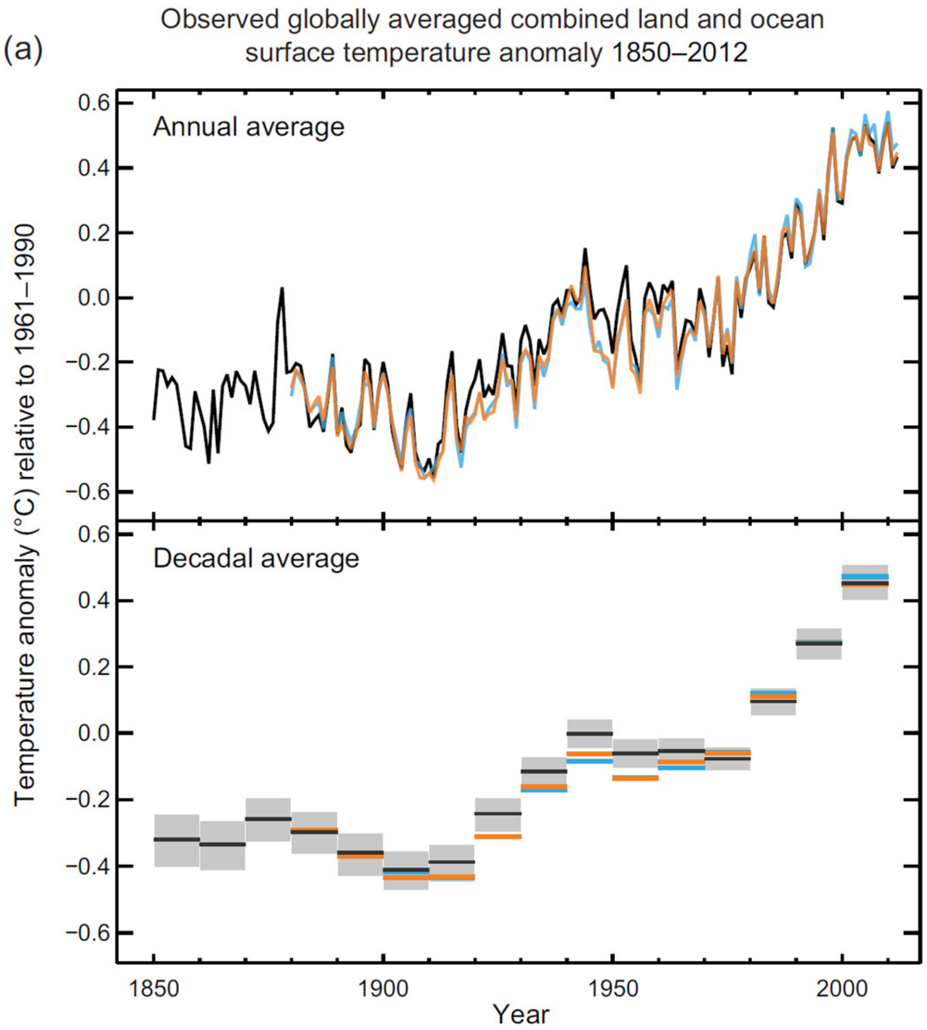

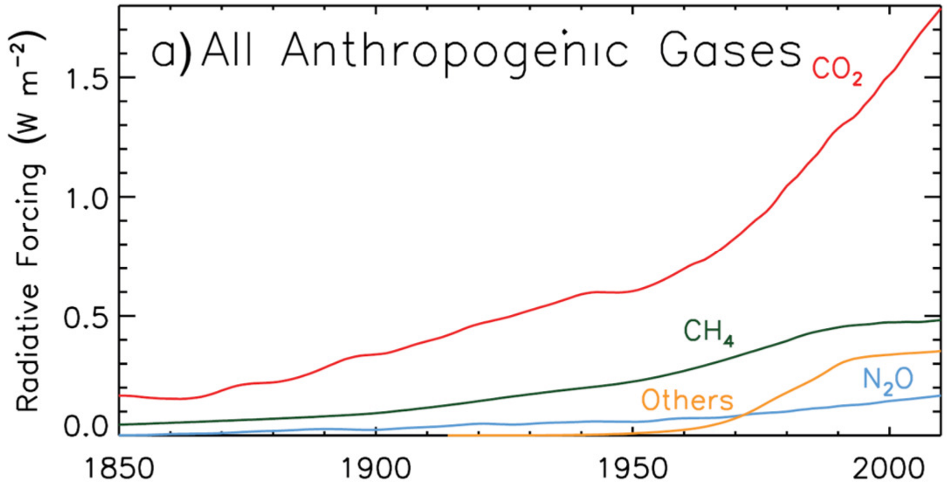

Figure SPM.1 | (a) Observed global mean combined land and ocean surface temperature anomalies, from 1850 to 2012 from three data sets. Top panel: annual mean values. Bottom panel: decadal mean values including the estimate of uncertainty for one dataset (black). Anomalies are relative to the mean of 1961–1990. (b) Map of the observed surface temperature change from 1901 to 2012 derived from temperature trends determined by linear regression from one dataset (orange line in panel a). Trends have been calculated where data availability permits a robust estimate (i.e., only for grid boxes with greater than 70% complete records and more than 20% data availability in the first and last 10% of the time period). Other areas are white. Grid boxes where the trend is significant at the 10% level are indicated by a + sign. For a listing of the datasets and further technical details see the Technical Summary Supplementary Material. {Figures 2.19–2.21; Figure TS.2}

Introduction

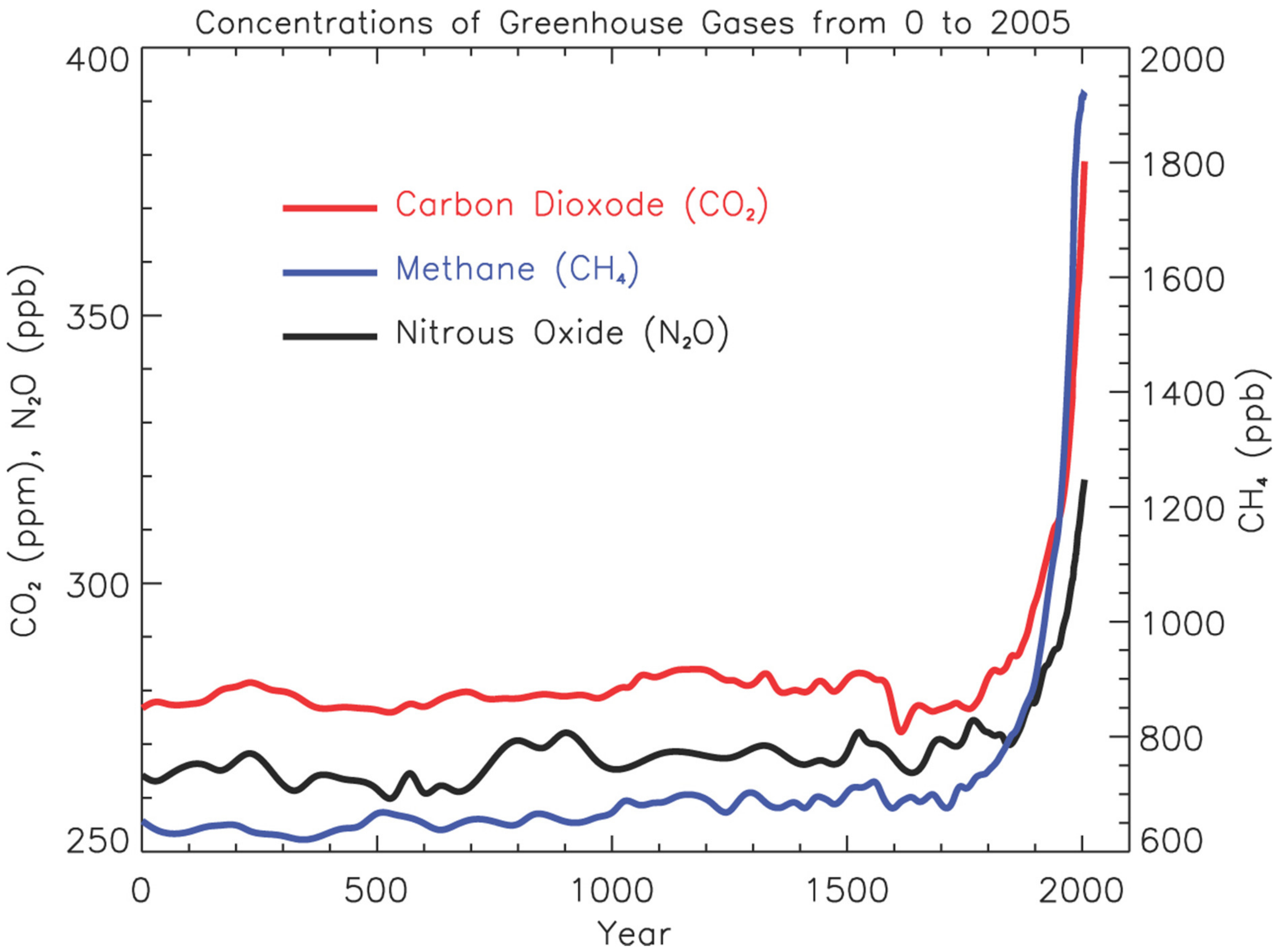

Introduction

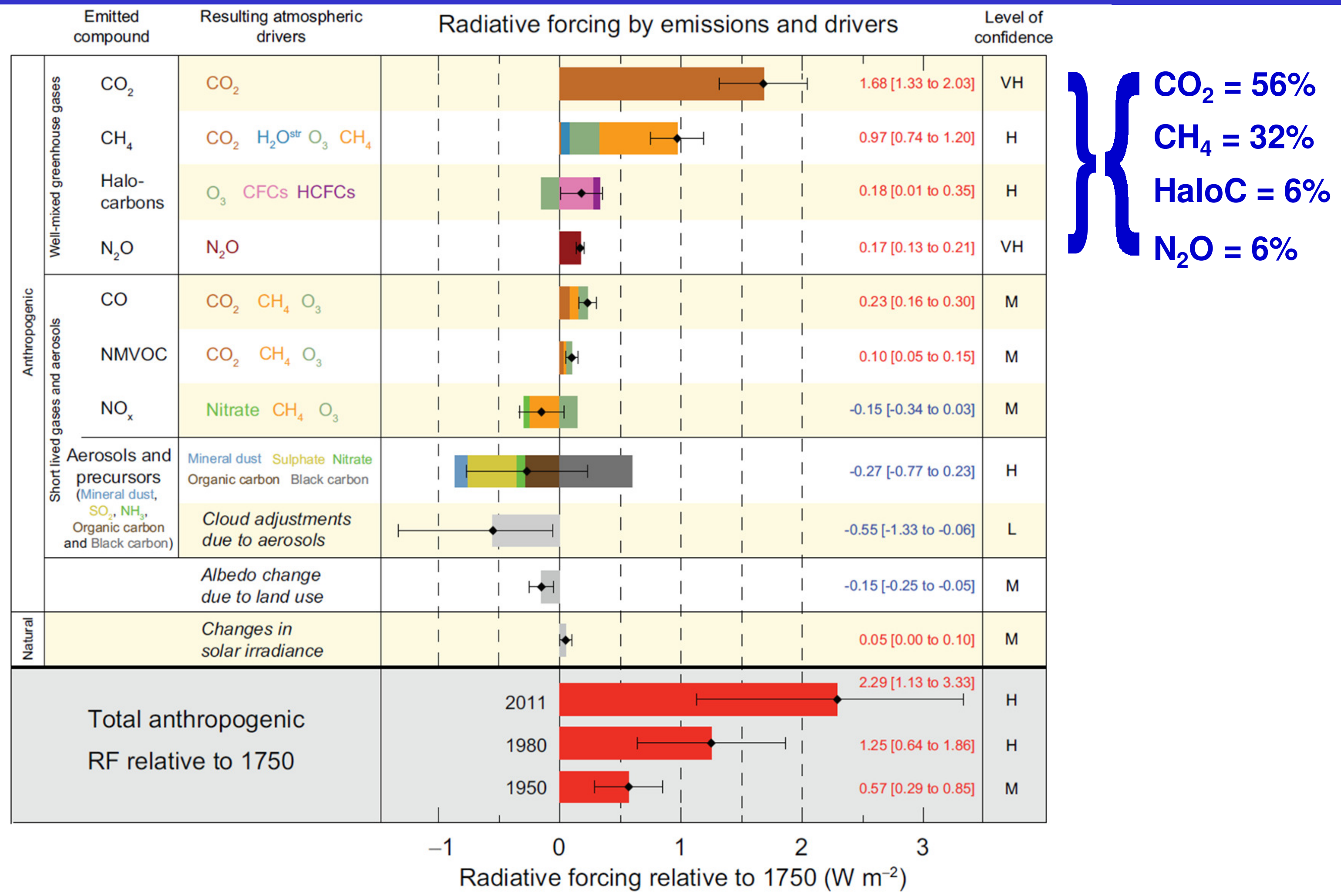

Figure SPM.5 | Radiative forcing estimates in 2011 relative to 1750 and aggregated uncertainties for the main drivers of climate change. Values are global average radiative forcing (RF[14]), partitioned according to the emitted compounds or processes that result in a combination of drivers. The best estimates of the net radiative forcing are shown as black diamonds with corresponding uncertainty intervals; the numerical values are provided on the right of the figure, together with the confidence level in the net forcing (VH – *very high*, H – *high*, M – *medium*, L – *low*, VL – *very low*). Albedo forcing due to black carbon on snow and ice is included in the black carbon aerosol bar. Small forcings due to contrails (0.05 W m^{-2}, including contrail induced cirrus), and HFCs, PFCs and SF_6 (total 0.03 W m^{-2}) are not shown. Concentration-based RFs for gases can be obtained by summing the like-coloured bars. Volcanic forcing is not included as its episodic nature makes is difficult to compare to other forcing mechanisms. Total anthropogenic radiative forcing is provided for three different years relative to 1750. For further technical details, including uncertainty ranges associated with individual components and processes, see the Technical Summary Supplementary Material. {8.5; Figures 8.14–8.18; Figures TS.6 and TS.7}

Introduction

Nitrous Oxide (N_2O): The Dominant Ozone-Depleting Substance Emitted in the 21st Century

A. R. Ravishankara,* John S. Daniel, Robert W. Portmann

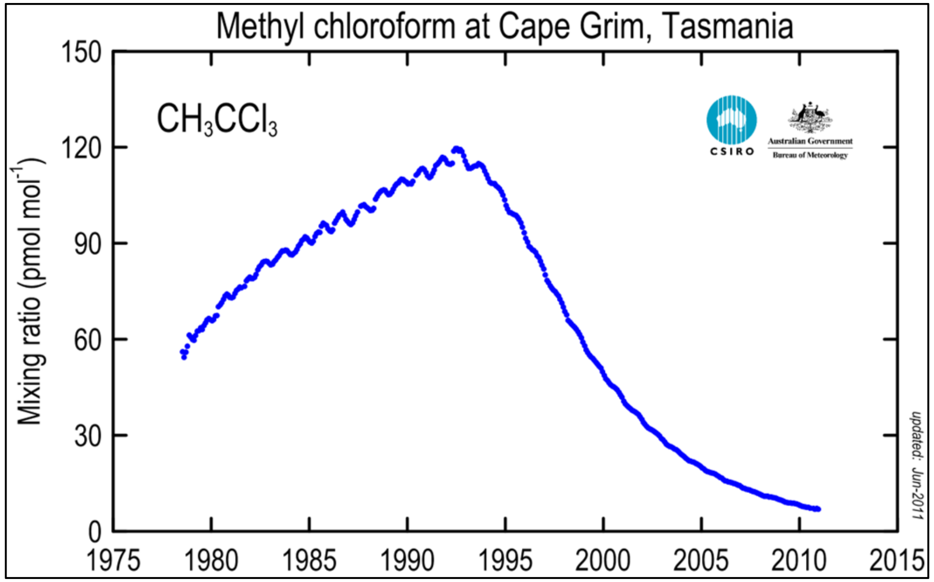

Montreal Protocol (1987)

Emergence of healing in the Antarctic ozone layer

Susan Solomon,[1]* Diane J. Ivy,[1] Doug Kinnison,[2] Michael J. Mills,[2] Ryan R. Neely III,[3,4] Anja Schmidt[3]

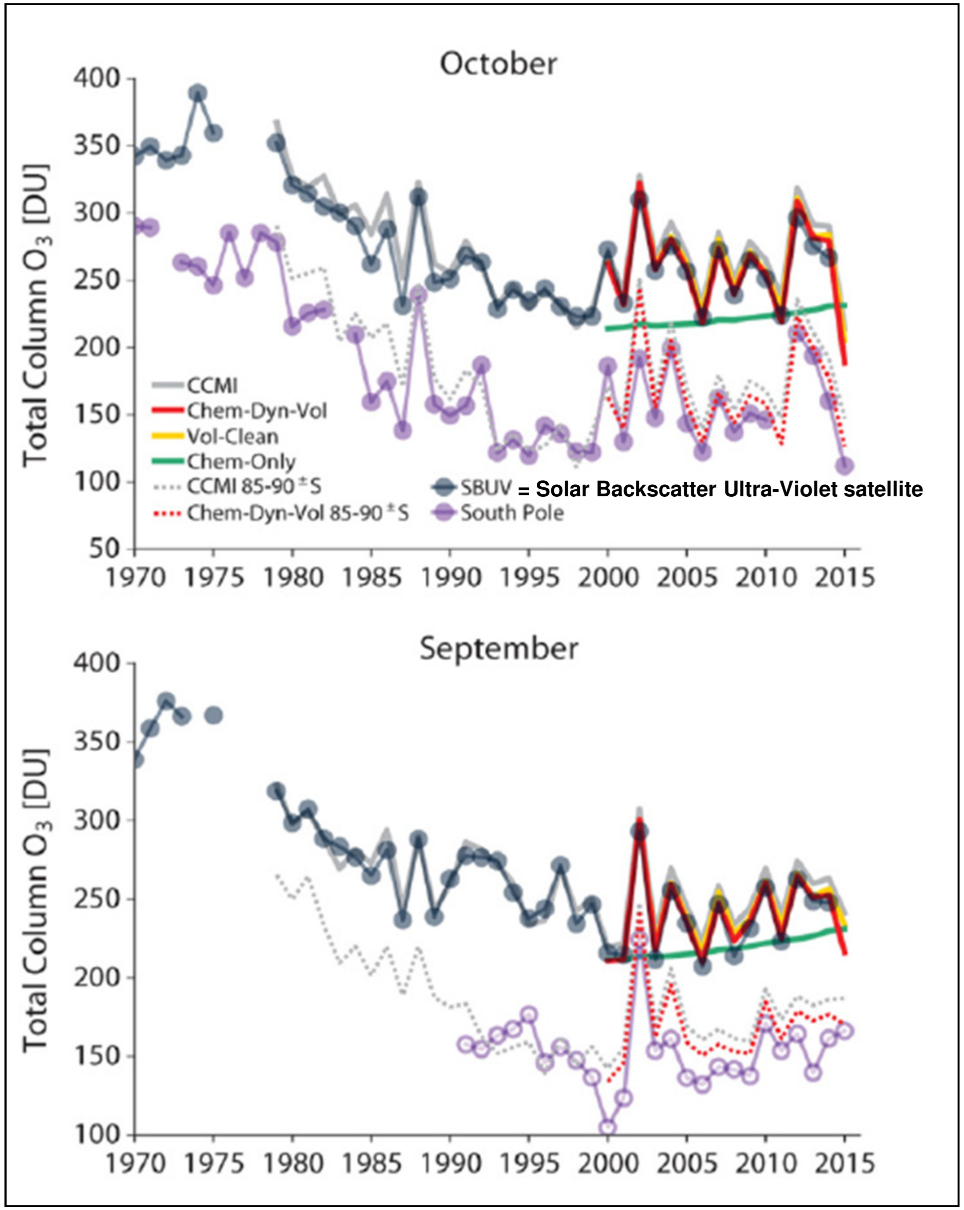

Introduction

Carbon dioxide (CO_2)

Introduction

Global anthropogenic CO_2 fluxes in 2010 ($PgC\ y^{-1} = 10^{15}\ gC\ y^{-1}$)

9.1±0.5 $PgC\ y^{-1}$

0.9±0.7 $PgC\ y^{-1}$ +

5.0±0.2 $PgC\ y^{-1}$
50%

2.6±1.0 $PgC\ y^{-1}$
26%
Calculated as the residual of all other flux components

24%
2.4±0.5 $PgC\ y^{-1}$
Average of 5 models

www.globalcarbonproject.org/

Introduction

Global anthropogenic CO_2 fluxes in 2010 ($PgC\ y^{-1} = 10^{15}\ gC\ y^{-1}$)

9.1 ± 0.5 PgC y^{-1}

United Nations
Framework Convention on
Climate Change

National Reports

0.9 ± 0.7 PgC y^{-1} +

Food and Agriculture
Organization of the
United Nations

www.globalcarbonproject.org/

5.0 ± 0.2 PgC y^{-1}

50%

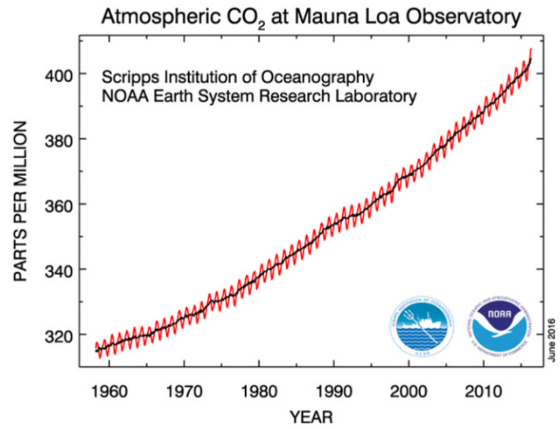

2.6 ± 1.0 PgC y^{-1}

26%

Calculated as the residual of all other flux components

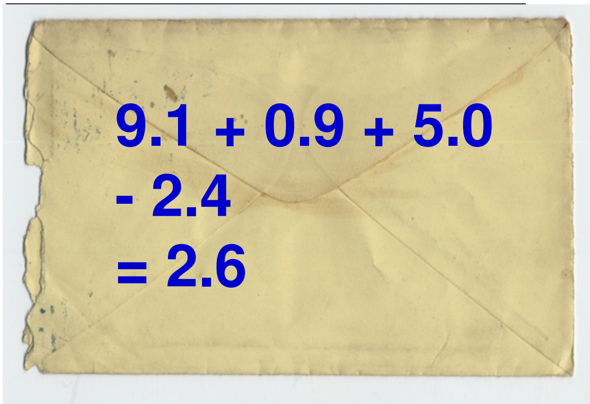

24%

2.4 ± 0.5 PgC y^{-1}

Average of 5 models

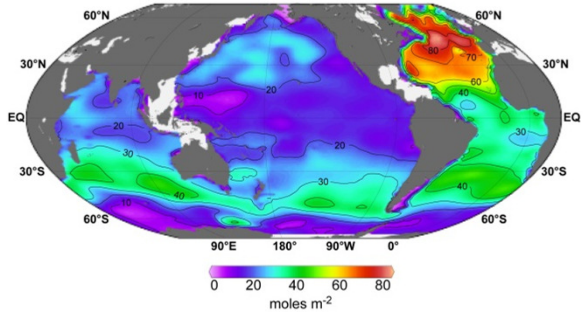

Why is the terrestrial biosphere a CO_2 sink ?

PERSPECTIVE
PUBLISHED ONLINE: 29 MAY 2013 | DOI: 10.1038/NCLIMATE1804
nature climate change

Untangling the confusion around land carbon science and climate change mitigation policy

Brendan Mackey[1]*, I. Colin Prentice[2,3], Will Steffen[4], Joanna I. House[5], David Lindenmayer[4], Heather Keith[4] and Sandra Berry[4]

Depletion of ecosystem carbon stocks is a significant source of atmospheric CO_2 and reducing land-based emissions and maintaining land carbon stocks contributes to climate change mitigation. We summarize current understanding about human perturbation of the global carbon cycle, examine three scientific issues and consider implications for the interpretation of international climate change policy decisions, concluding that considering carbon storage on land as a means to 'offset' CO_2 emissions from burning fossil fuels (an idea with wide currency) is scientifically flawed. The capacity of terrestrial ecosystems to store carbon is finite and the current sequestration potential primarily reflects depletion due to past land use. Avoiding emissions from land carbon stocks and refilling depleted stocks reduces atmospheric CO_2 concentration, but the maximum amount of this reduction is equivalent to only a small fraction of potential fossil fuel emissions.

Introduction

The top four emitters in 2013 covered 58% of global emissions
China (28%), United States (14%), EU28 (10%), India (7%)

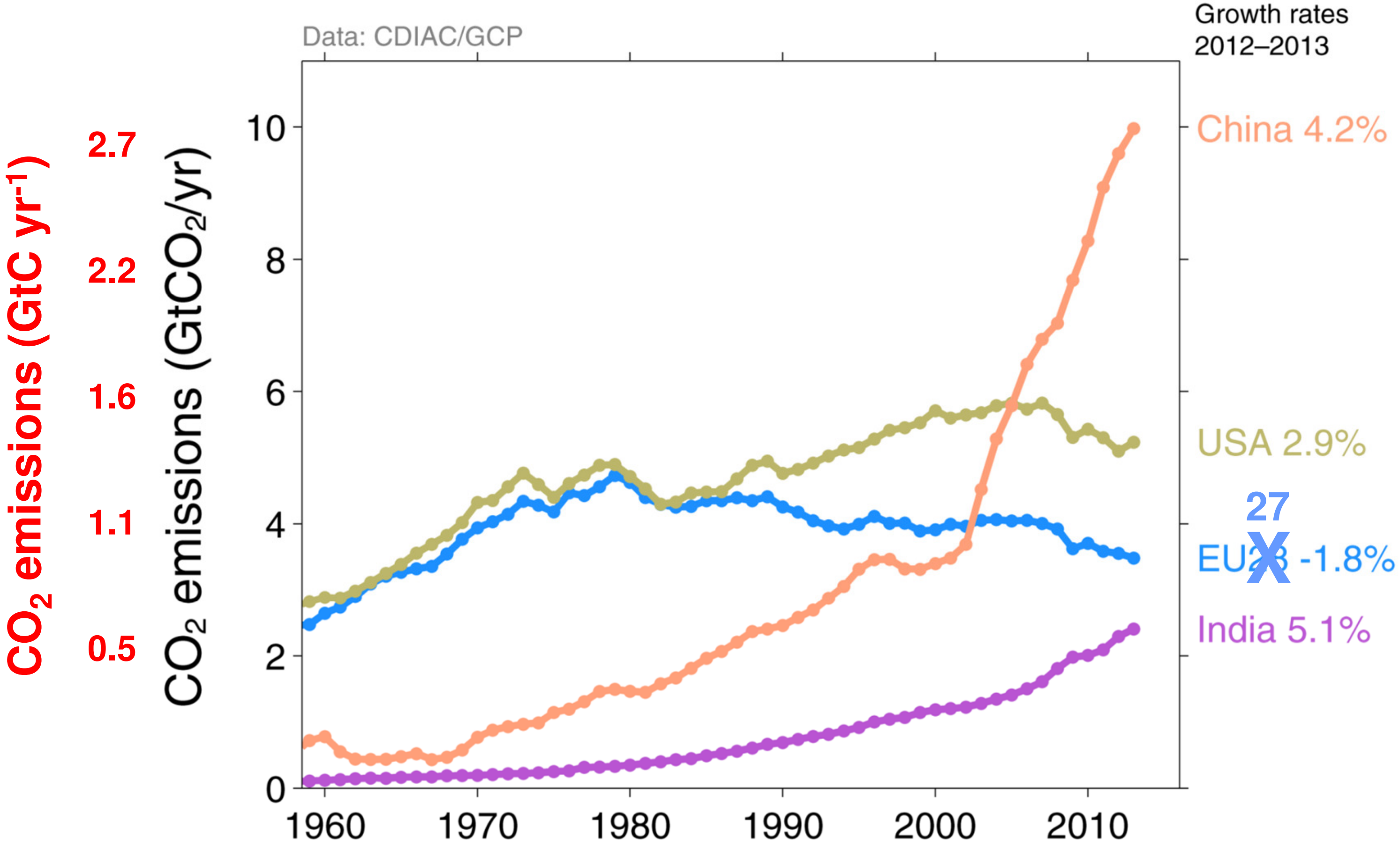

www.globalcarbonproject.org/

Introduction

China's per capita emissions have passed the EU28 and are 45% above the global average

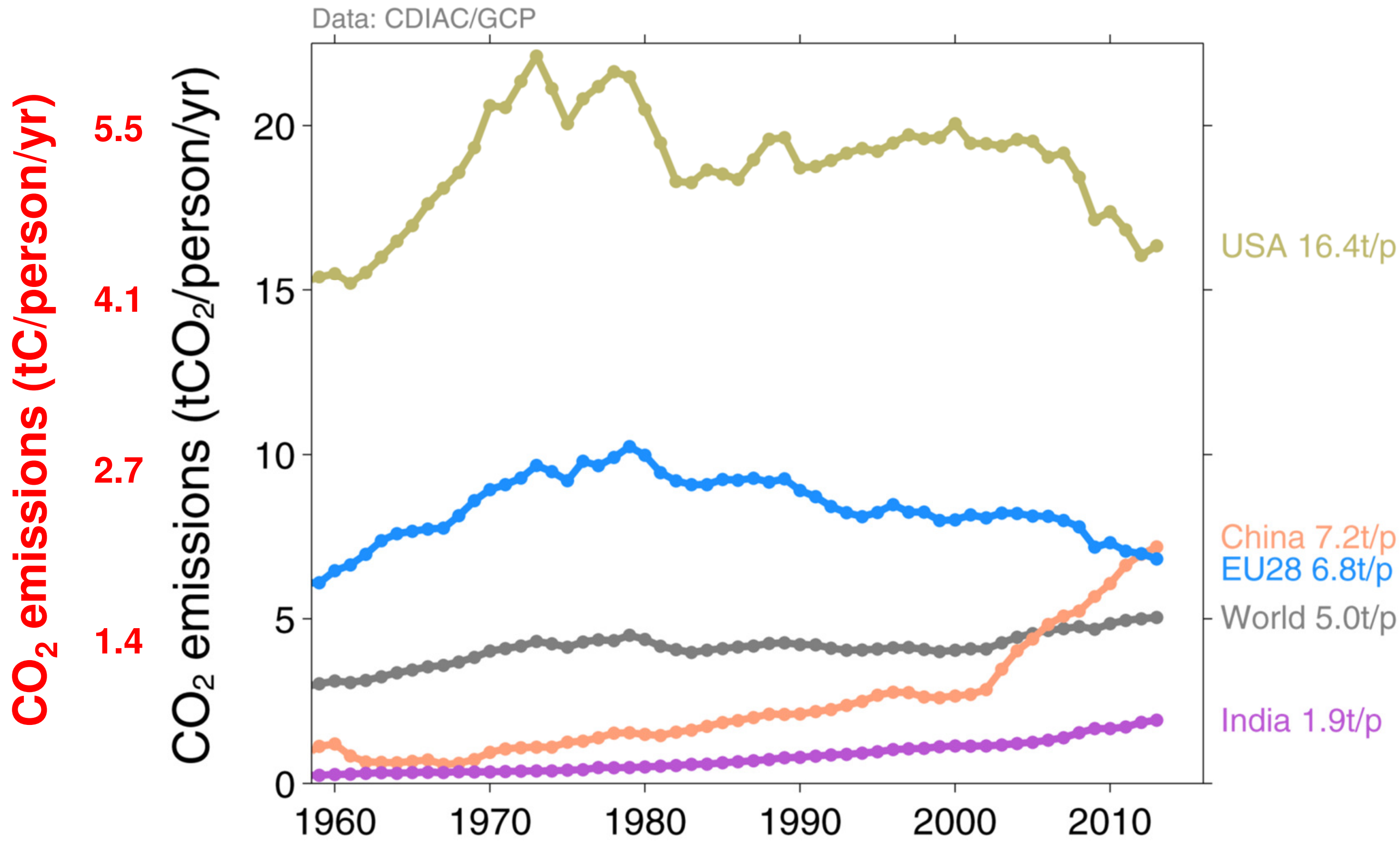

www.globalcarbonproject.org/

Methane (CH_4)

Introduction

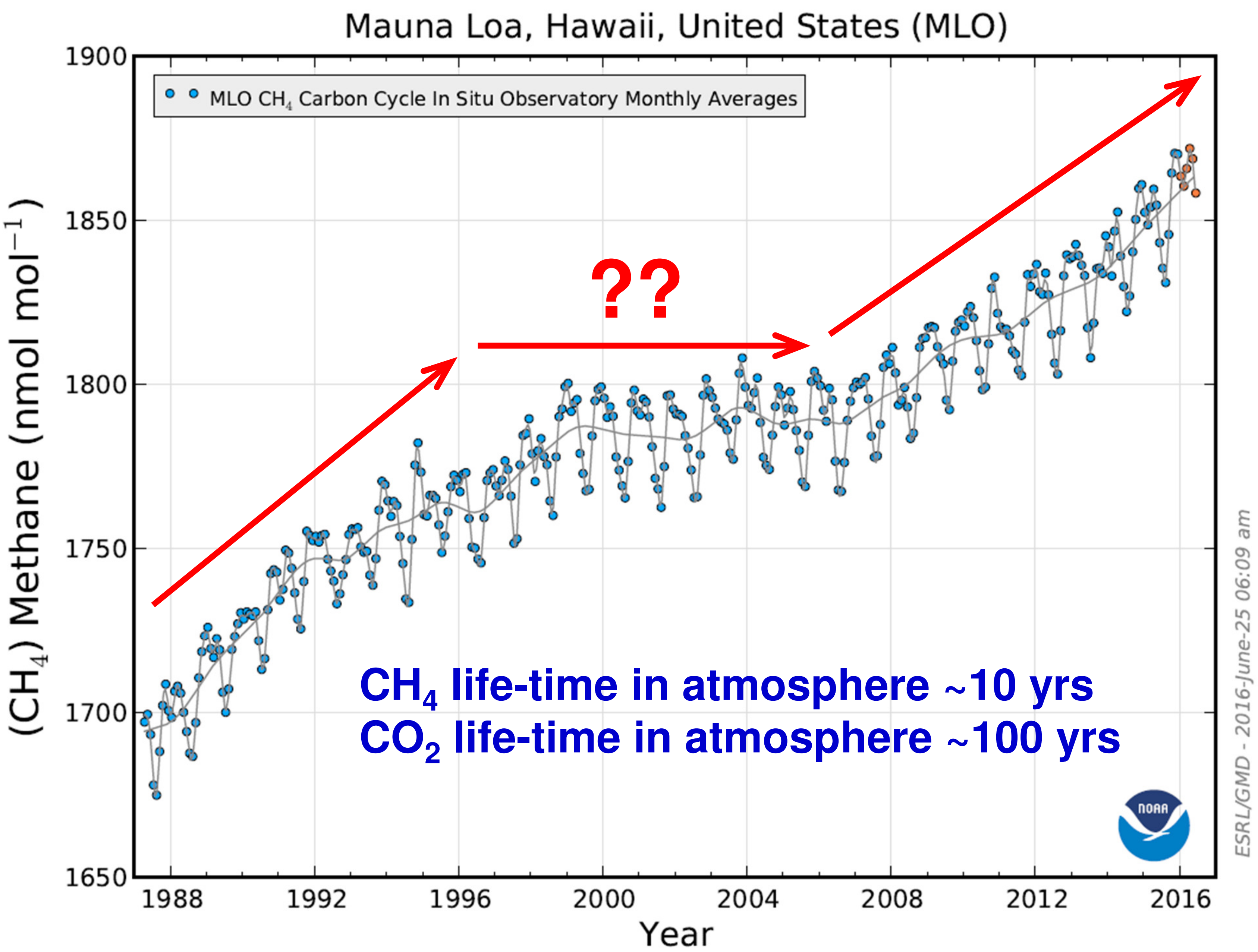

Introduction

Sources and sinks of CH_4 in Tg CH_4 yr^{-1}

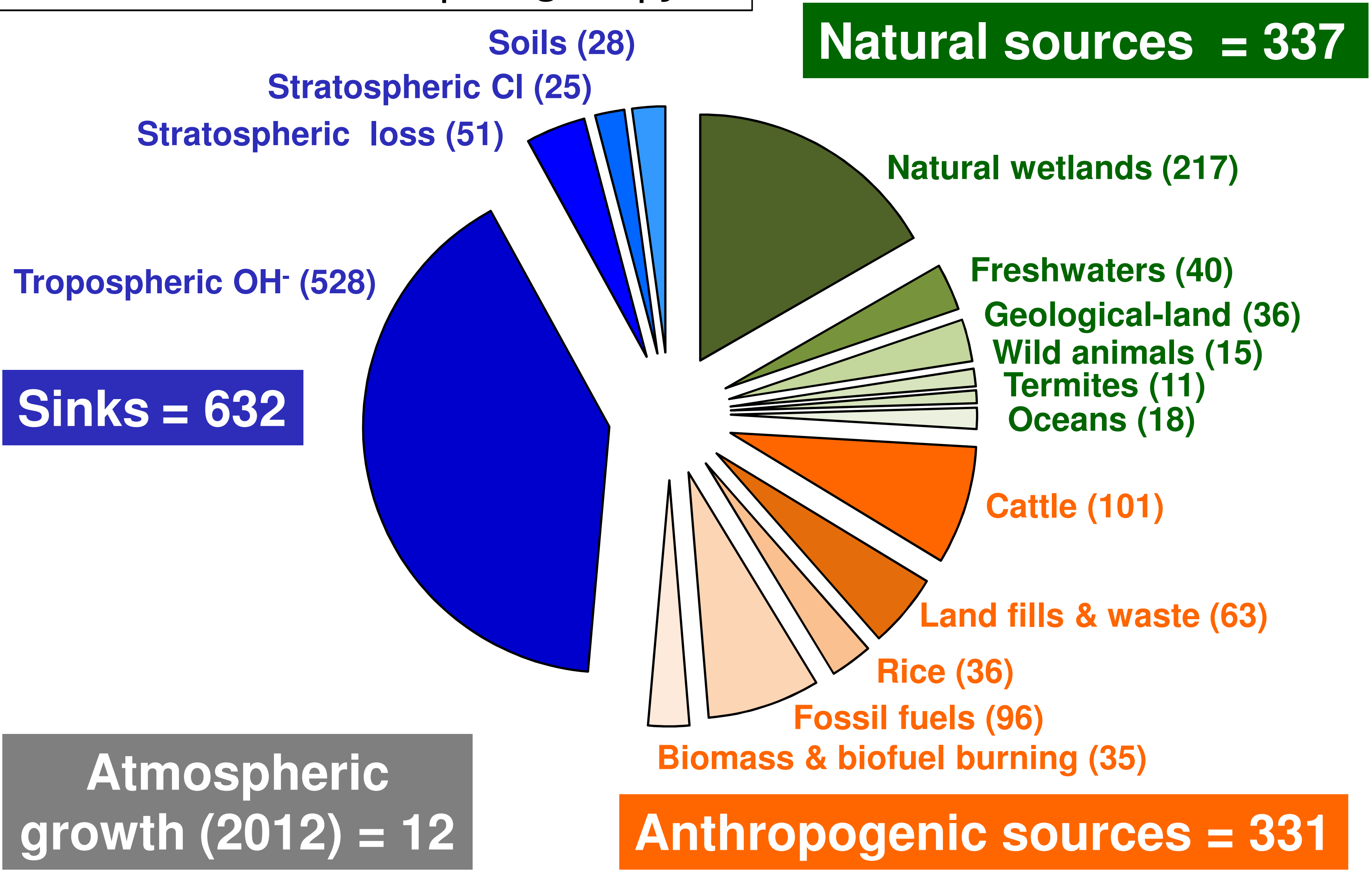

Kirschke et al. (2013) Nature Geoscience, 6, 813-823

Introduction

Sources and sinks of CH_4 in Tg CH_4 yr^{-1}

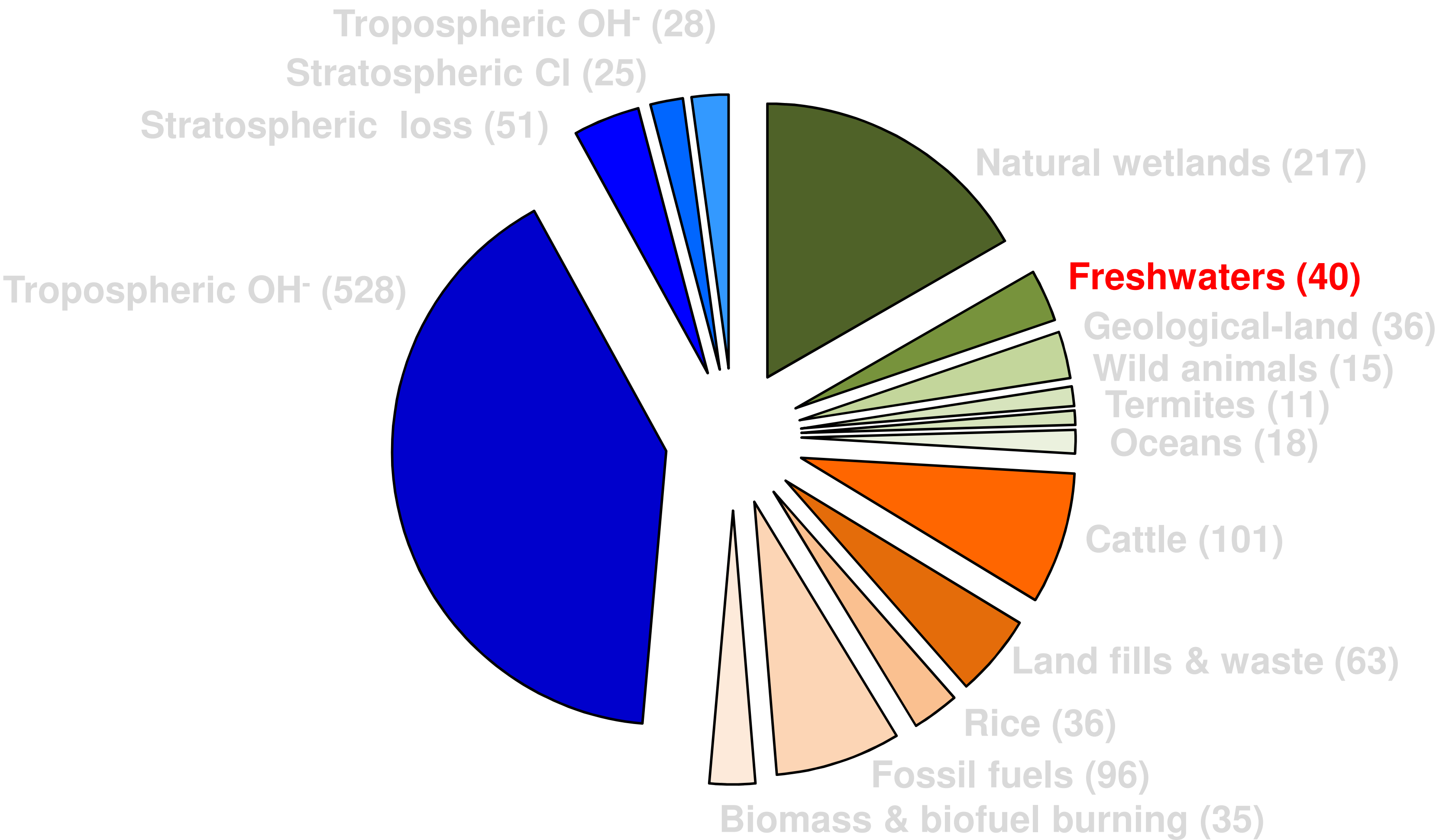

Kirschke et al. (2013) Nature Geoscience, 6, 813-823

Introduction

Freshwater Methane Emissions Offset the Continental Carbon Sink

David Bastviken,[1*] Lars J. Tranvik,[2] John A. Downing,[3] Patrick M. Crill,[4] Alex Enrich-Prast[5]

Latitude	Fluxes												Area (km^2)
	Total open water			Ebullition			Diffusive			Stored			
	Emiss.	*n*	CV	Emiss.	*n*	CV	Emiss.	*n*	CV	Emiss.	*n*	CV	
						Lakes							
>66°	6.8	17	72	6.4	17	74	0.7	60	37				288,318
>54°–66°	6.6	5	155	9.1	9	60	1.1	271	185	0.1	217	2649	1,533,084
25°–54°	31.6	15	127	15.8	15	177	4.8	33	277	3.7	36	125	1,330,264
<24°	26.6	29	51	22.2	28	54	3.1	29	97	21.3	1		585,536*
						Reservoirs							
>66°	0.2†												35,289
>54°–66°	1.0	24	176	1.8	2	140	0.2	4	93				161,352
25°–54°	0.7‡												116,922
<24°	18.1	11	87										186,437
						Rivers							
>66°	0.1	1											38,895
>54°–66°	0.2†												80,009
25°–54°	0.3	20	302										61,867
<24°	0.9‡												176,856
Sum open water	93.1	116		55.3	71		9.9	397		25.1	254		
Plant flux	10.2												
Sum all	103.3												

Total = 1.5 $TgCH_4\ yr^{-1}$

*Likely underestimated. For comparison, the mean flooded areas for the major South American savanna wetlands and the lowland Amazon (below 500 m above sea level) are 115,620 km^2 and 750,000 km^2, respectively (*14*). †Estimated assuming similar emissions per area unit at latitudes >54°. ‡Estimated assuming similar emissions per area unit at latitudes from 0° to 54°.

Introduction

The ecology of methane in streams and rivers: patterns, controls, and global significance

Emily H. Stanley,[1,4] Nora J. Casson,[1,3] Samuel T. Christel,[1] John T. Crawford,[2] Luke C. Loken,[1] and Samantha K. Oliver[1]

[1]*Center for Limnology, University of Wisconsin, 680 North Park Street, Madison, Wisconsin 53706 USA*
[2]*U.S. Geological Survey, 3215 Marine Street Suite E127, Boulder, Colorado 80303 USA*

Abstract. Streams and rivers can substantially modify organic carbon (OC) inputs from terrestrial landscapes, and much of this processing is the result of microbial respiration. While carbon dioxide (CO_2) is the major end-product of ecosystem respiration, methane (CH_4) is also present in many fluvial environments even though methanogenesis typically requires anoxic conditions that may be scarce in these systems. Given recent recognition of the pervasiveness of this greenhouse gas in streams and rivers, we synthesized existing research and data to identify patterns and drivers of CH_4, knowledge gaps, and research opportunities. This included examining the history of lotic CH_4 research, creating a database of concentrations and fluxes (MethDB) to generate a global-scale estimate of fluvial CH_4 efflux, and developing a conceptual framework and using this framework to consider how human activities may modify fluvial CH_4 dynamics. Current understanding of CH_4 in streams and rivers has been strongly influenced by goals of understanding OC processing and quantifying the contribution of CH_4 to ecosystem C fluxes. Less effort has been directed towards investigating processes that dictate in situ CH_4 production and loss. CH_4 makes a meager contribution to watershed or landscape C budgets, but streams and rivers are often significant CH_4 sources to the atmosphere across these same spatial extents. Most fluvial systems are supersaturated with CH_4 and we estimate an annual global emission of 26.8 Tg CH_4, equivalent to ~15-40% of wetland and lake effluxes, respectively. Less

Introduction

Sources and sinks of CH_4 in Tg CH_4 yr^{-1}

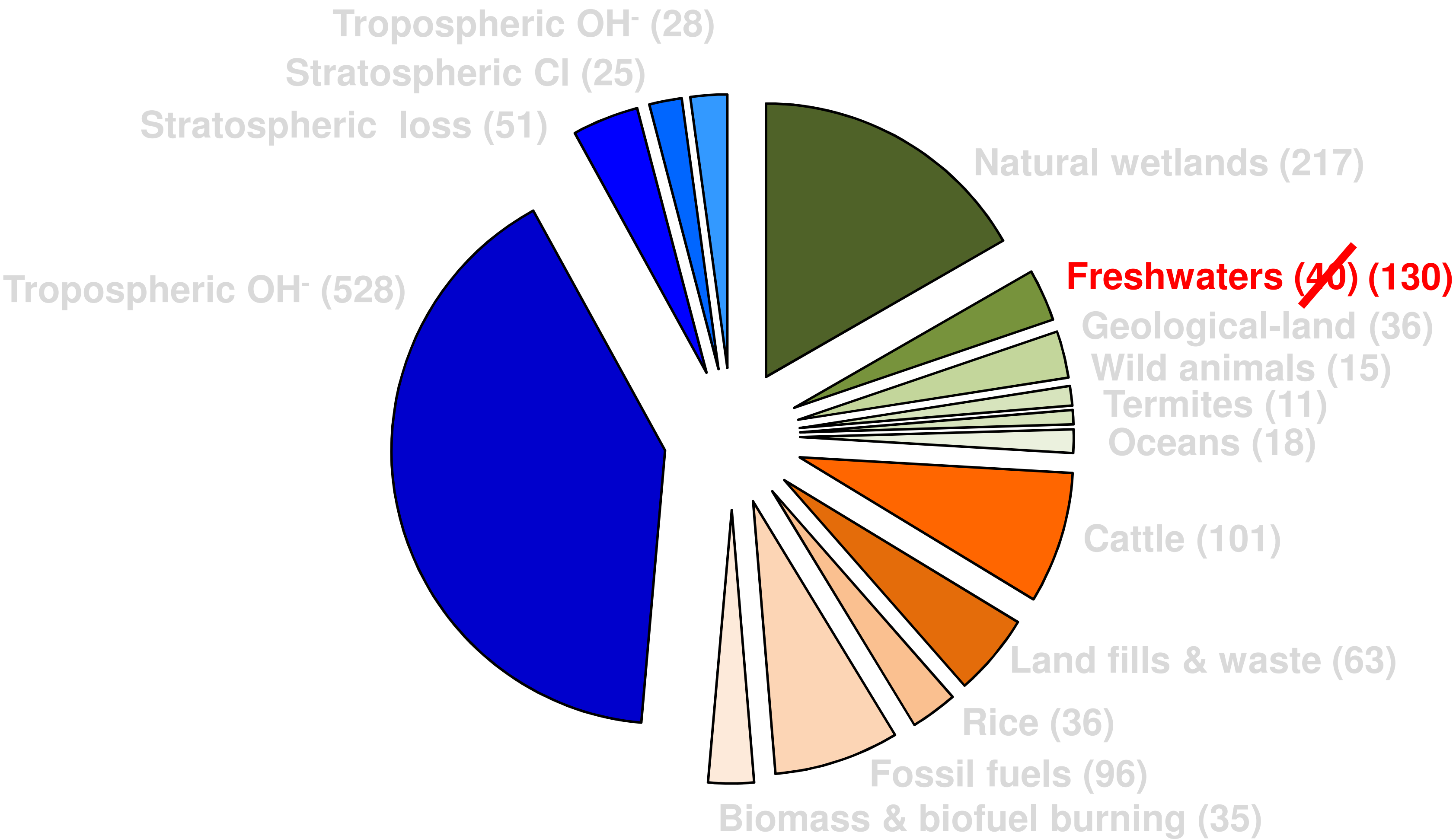

Kirschke et al. (2013) Nature Geoscience, 6, 813-823

Introduction

Sources and sinks of CH_4 in Tg CH_4 yr^{-1}

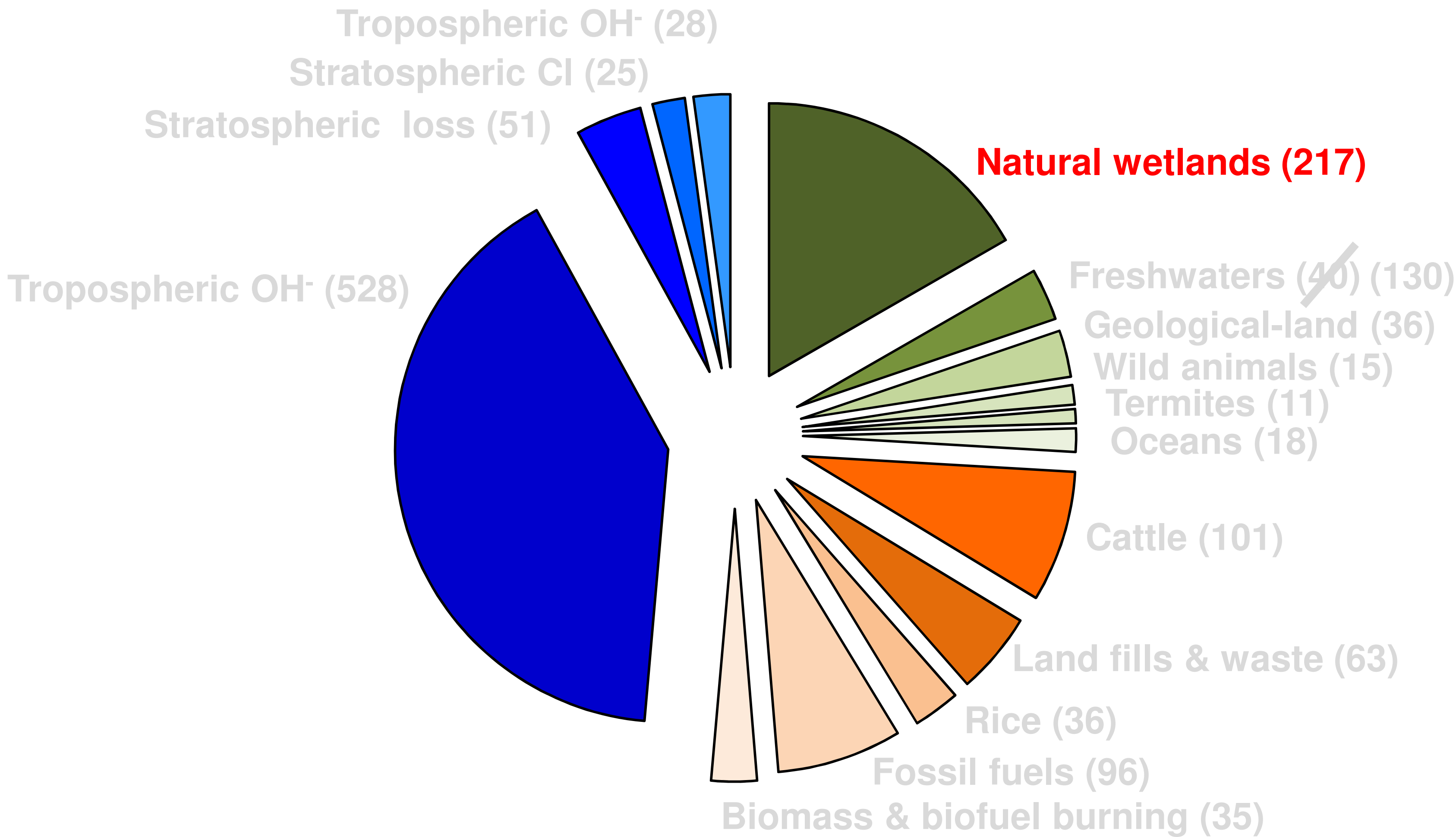

Kirschke et al. (2013) Nature Geoscience, 6, 813-823

Introduction

Bottom-Up approach

Regionalization of methane emissions in the Amazon Basin with microwave remote sensing

JOHN M. MELACK*†, LAURA L. HESS†, MARY GASTIL†, BRUCE R. FORSBERG‡, STEPHEN K. HAMILTON§, IVAN B.T. LIMA¶ and EVLYN M.L.M. NOVO¶

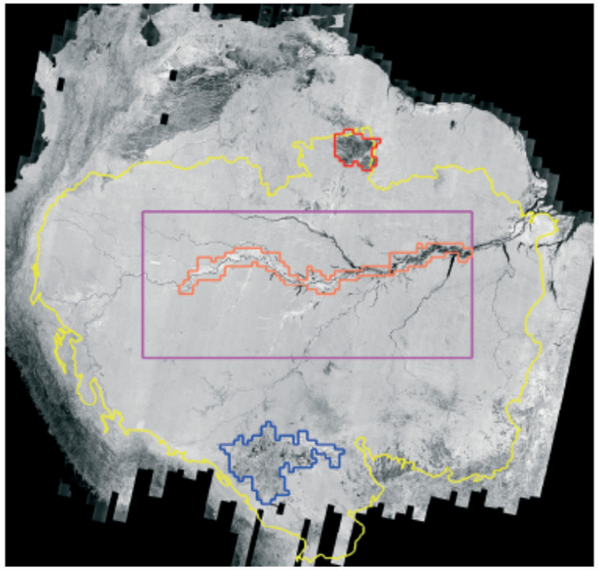

Fig. 1 Location of Amazon regions used for calculations of methane emission. The background image is the high-water Japanese Earth Resources Satellite-1 (JERS-1) mosaic displayed as a gray scale of radar backscatter (Siqueira *et al*., 2000). Yellow line indicates boundary of the lowland Amazon basin less than 500 m above sea level; rectangle in magenta delimits 1.77 million square kilometers area examined by Richey *et al*. (2002) and Hess *et al*. (2003) and used as part of our analyses. Areas for which inundation mapping from the passive microwave data were used are shown in orange (Solimões/Amazon mainstem floodplain; vertical line at 58.5°W delineates western and eastern reaches), dark blue (Llanos de Mojos) and red (Roraima wetlands). Three wetland regions outside of Amazon basin for which emissions were estimated (Bananal, Pantanal and Llanos del Orinoco) are not shown here.

Table 1 Means and Monte Carlo-based uncertainties expressed as standard deviations (SD) of the means for habitat-specific methane emissions calculated from individual measurements, where *n* is the number of measurements (A. Devol, personal communication; Devol *et al*., 1990)

Aquatic habitat	*n*	Methane emission ($kg\,C\,km^{-2}\,day^{-1}$) Mean	SD
Aquatic macrophyte (high)	66	243	54
Aquatic macrophyte (low)	55	92	25
Flooded forest	58	91	40
Open water	165	38	6

High and low refer to values during high and low water levels as designated in Devol *et al*. (1990).

Table 3 Annual methane emission ($Tg\,C\,yr^{-1}$) from each floodplain aquatic habitat and from the river channel of the Solimões/Amazon mainstem

Aquatic habitat	Methane emission ($Tg\,C\,yr^{-1}$) Mean	SD
Aquatic macrophyte	0.63	0.1
Flooded forest	0.61	0.2
Open water	0.087	0.02
River channel	0.0078	0.001
Total	1.3	0.3

Means and standard deviation (SD) of the means (derived from Monte Carlo error analysis) are presented.

Introduction

Bottom-Up approach

Tropical wetlands: A missing link in the global carbon cycle?

Sofie Sjögersten[1], Colin R. Black[1], Stephanie Evers[2], Jorge Hoyos-Santillan[1], Emma L. Wright[1], and Benjamin L. Turner[3]

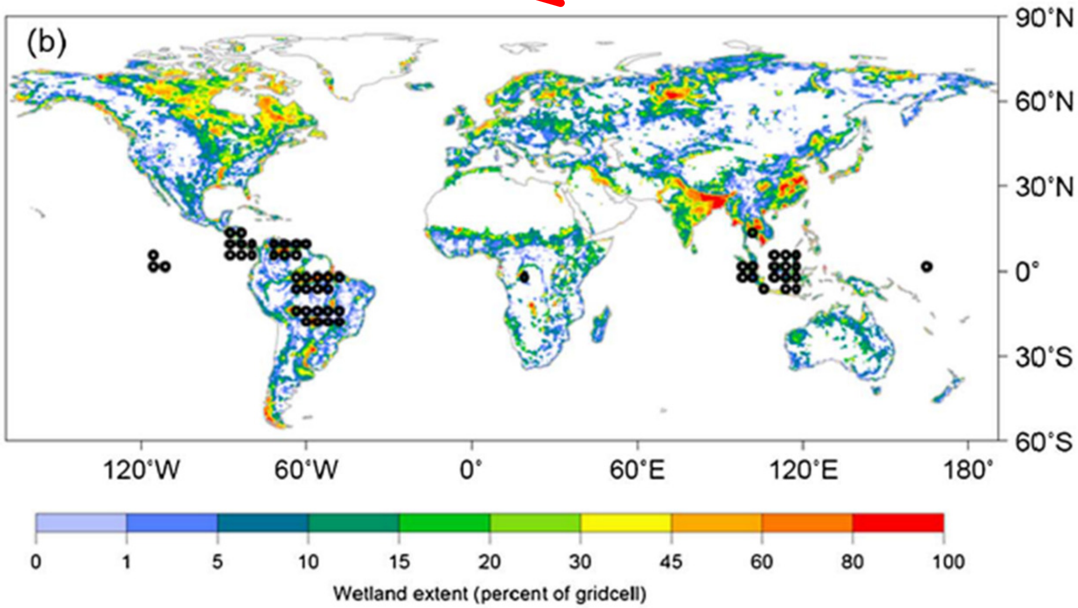

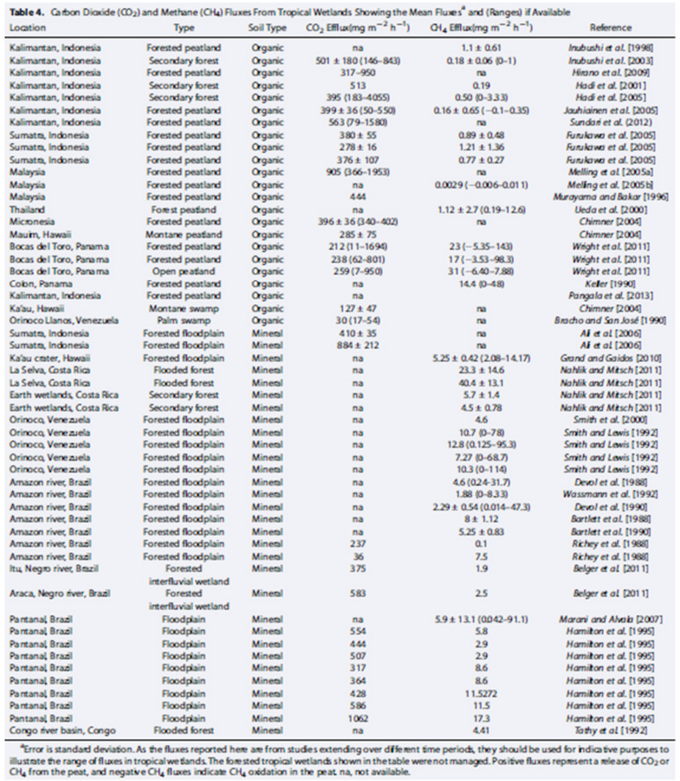

Table 4. Carbon Dioxide (CO_2) and Methane (CH_4) Fluxes From Tropical Wetlands Showing the Mean Fluxes[a] and (Ranges) if Available

Location	Type	Soil Type	CO_2 Efflux (mg m^{-2} h^{-1})	CH_4 Efflux (mg m^{-2} h^{-1})	Reference
Kalimantan, Indonesia	Forested peatland	Organic	na	1.1 ± 0.61	*Inubushi et al.* [1998]
Kalimantan, Indonesia	Secondary forest	Organic	501 ± 180 (146–843)	0.18 ± 0.06 (0–1)	*Inubushi et al.* [2003]
Kalimantan, Indonesia	Forested peatland	Organic	317–950	na	*Hirano et al.* [2009]
Kalimantan, Indonesia	Secondary forest	Organic	513	0.19	*Hadi et al.* [2001]
Kalimantan, Indonesia	Secondary forest	Organic	395 (183–4055)	0.50 (0–3.33)	*Hadi et al.* [2005]
Kalimantan, Indonesia	Forested peatland	Organic	399 ± 36 (50–550)	0.16 ± 0.65 (−0.1–0.35)	*Jauhiainen et al.* [2005]
Kalimantan, Indonesia	Forested peatland	Organic	563 (79–1580)	na	*Sundari et al.* (2012)
Sumatra, Indonesia	Forested peatland	Organic	380 ± 55	0.89 ± 0.48	*Furukawa et al.* [2005]
Sumatra, Indonesia	Forested peatland	Organic	278 ± 16	1.21 ± 1.36	*Furukawa et al.* [2005]
Sumatra, Indonesia	Forested peatland	Organic	376 ± 107	0.77 ± 0.27	*Furukawa et al.* [2005]
Malaysia	Forested peatland	Organic	905 (366–1953)	na	*Melling et al.* [2005a]
Malaysia	Forested peatland	Organic	na	0.0029 (−0.006–0.011)	*Melling et al.* [2005b]
Malaysia	Forested peatland	Organic	444		*Murayama and Bakar* [1996]
Thailand	Forest peatland	Organic	na	1.12 ± 2.7 (0.19–12.6)	*Ueda et al.* [2000]
Micronesia	Forested peatland	Organic	396 ± 36 (340–402)	na	*Chimner* [2004]
Mauim, Hawaii	Montane peatland	Organic	285 ± 75		*Chimner* [2004]
Bocas del Toro, Panama	Forested peatland	Organic	212 (11–1694)	23 (−5.35–143)	*Wright et al.* [2011]
Bocas del Toro, Panama	Forested peatland	Organic	238 (62–801)	17 (−3.53–98.3)	*Wright et al.* [2011]
Bocas del Toro, Panama	Open peatland	Organic	259 (7–950)	31 (−6.40–7.88)	*Wright et al.* [2011]
Colon, Panama	Forested peatland	Organic	na	14.4 (0–48)	*Keller* [1990]
Kalimantan, Indonesia	Forested peatland	Organic	na		*Pangala et al.* [2013]
Ka'au, Hawaii	Montane swamp	Organic	127 ± 47	na	*Chimner* [2004]
Orinoco Llanos, Venezuela	Palm swamp	Organic	30 (17–54)	na	*Bracho and San José* [1990]
Sumatra, Indonesia	Forested floodplain	Mineral	410 ± 35	na	*Ali et al.* [2006]
Sumatra, Indonesia	Forested floodplain	Mineral	884 ± 212	na	*Ali et al.* [2006]
Ka'au crater, Hawaii	Forested floodplain	Mineral	na	5.25 ± 0.42 (2.08–14.17)	*Grand and Gaidos* [2010]
La Selva, Costa Rica	Flooded forest	Mineral	na	23.3 ± 14.6	*Nahlik and Mitsch* [2011]
La Selva, Costa Rica	Flooded forest	Mineral	na	40.4 ± 13.1	*Nahlik and Mitsch* [2011]
Earth wetlands, Costa Rica	Secondary forest	Mineral	na	5.7 ± 1.4	*Nahlik and Mitsch* [2011]
Earth wetlands, Costa Rica	Secondary forest	Mineral	na	4.5 ± 0.78	*Nahlik and Mitsch* [2011]
Orinoco, Venezuela	Forested floodplain	Mineral	na	4.6	*Smith et al.* [2000]
Orinoco, Venezuela	Forested floodplain	Mineral	na	10.7 (0–78)	*Smith and Lewis* [1992]
Orinoco, Venezuela	Forested floodplain	Mineral	na	12.8 (0.125–95.3)	*Smith and Lewis* [1992]
Orinoco, Venezuela	Forested floodplain	Mineral	na	7.27 (0–68.7)	*Smith and Lewis* [1992]
Orinoco, Venezuela	Forested floodplain	Mineral	na	10.3 (0–114)	*Smith and Lewis* [1992]
Amazon river, Brazil	Forested floodplain	Mineral	na	4.6 (0.24–31.7)	*Devol et al.* [1988]
Amazon river, Brazil	Forested floodplain	Mineral	na	1.88 (0–8.33)	*Wassmann et al.* [1992]
Amazon river, Brazil	Forested floodplain	Mineral	na	2.29 ± 0.54 (0.014–47.3)	*Devol et al.* [1990]
Amazon river, Brazil	Forested floodplain	Mineral	na	8 ± 1.12	*Bartlett et al.* [1988]
Amazon river, Brazil	Forested floodplain	Mineral	na	5.25 ± 0.83	*Bartlett et al.* [1990]
Amazon river, Brazil	Forested floodplain	Mineral	237	0.1	*Richey et al.* [1988]
Amazon river, Brazil	Forested floodplain	Mineral	36	7.5	*Richey et al.* [1988]
Itu, Negro river, Brazil	Forested interfluvial wetland	Mineral	375	1.9	*Belger et al.* [2011]
Araca, Negro river, Brazil	Forested interfluvial wetland	Mineral	583	2.5	*Belger et al.* [2011]
Pantanal, Brazil	Floodplain	Mineral	na	5.9 ± 13.1 (0.042–91.1)	*Marani and Alvala* [2007]
Pantanal, Brazil	Floodplain	Mineral	554	5.8	*Hamilton et al.* [1995]
Pantanal, Brazil	Floodplain	Mineral	444	2.9	*Hamilton et al.* [1995]
Pantanal, Brazil	Floodplain	Mineral	507	2.9	*Hamilton et al.* [1995]
Pantanal, Brazil	Floodplain	Mineral	317	8.6	*Hamilton et al.* [1995]
Pantanal, Brazil	Floodplain	Mineral	364	8.6	*Hamilton et al.* [1995]
Pantanal, Brazil	Floodplain	Mineral	428	11.5272	*Hamilton et al.* [1995]
Pantanal, Brazil	Floodplain	Mineral	586	11.5	*Hamilton et al.* [1995]
Pantanal, Brazil	Floodplain	Mineral	1062	17.3	*Hamilton et al.* [1995]
Congo river basin, Congo	Flooded forest	Mineral	na	4.41	*Tathy et al.* [1992]

[a]Error is standard deviation. As the fluxes reported here are from studies extending over different time periods, they should be used for indicative purposes to illustrate the range of fluxes in tropical wetlands. The forested tropical wetlands shown in the table were not managed. Positive fluxes represent a release of CO_2 or CH_4 from the peat, and negative CH_4 fluxes indicate CH_4 oxidation in the peat. na, not available.

Pantropical wetland emission of 92 $TgCH_4$ yr^{-1}

Extrapolation of ~40 measurements to 1.4 10^6 km^2

Introduction

Top-down approach

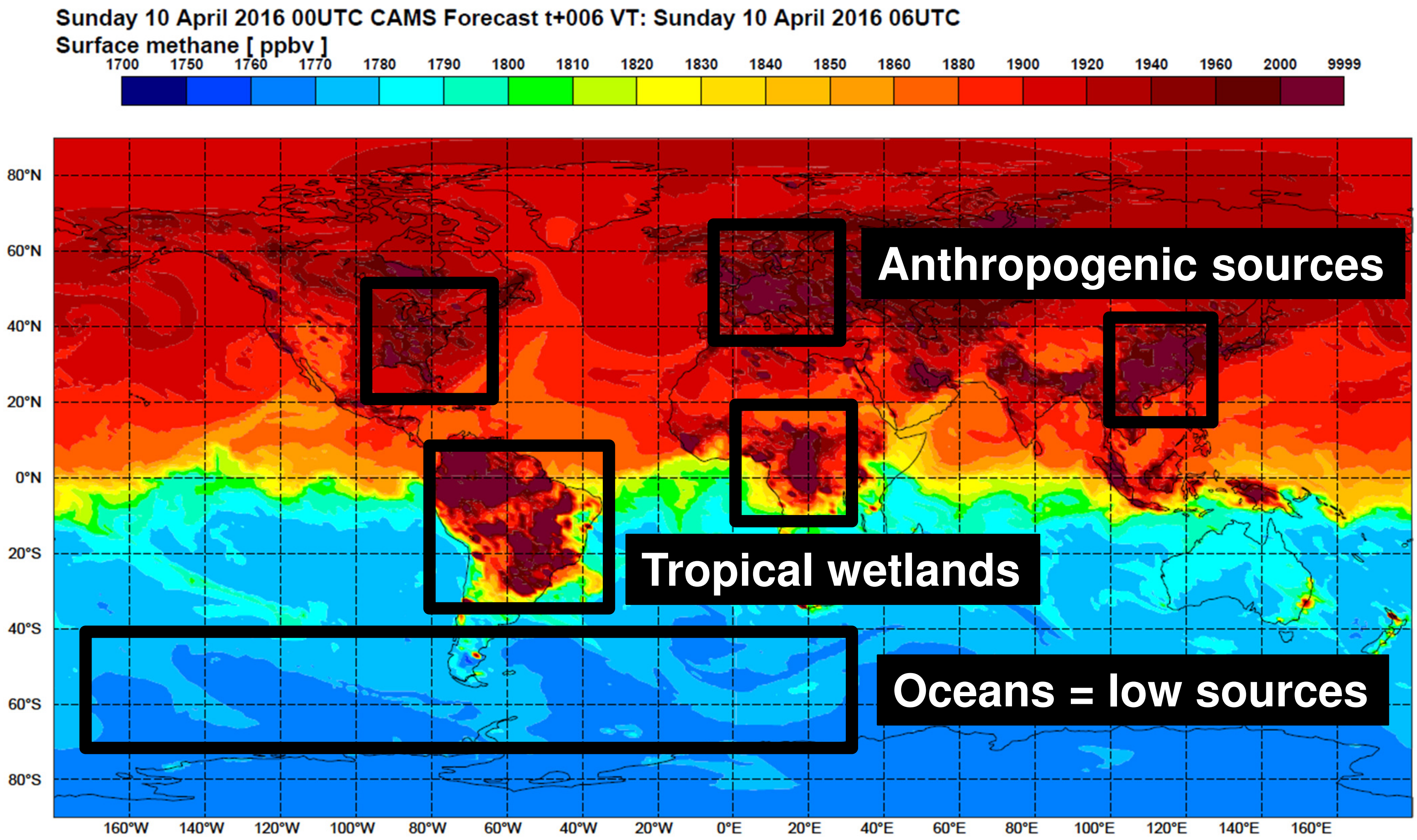

Introduction

Top-down approach

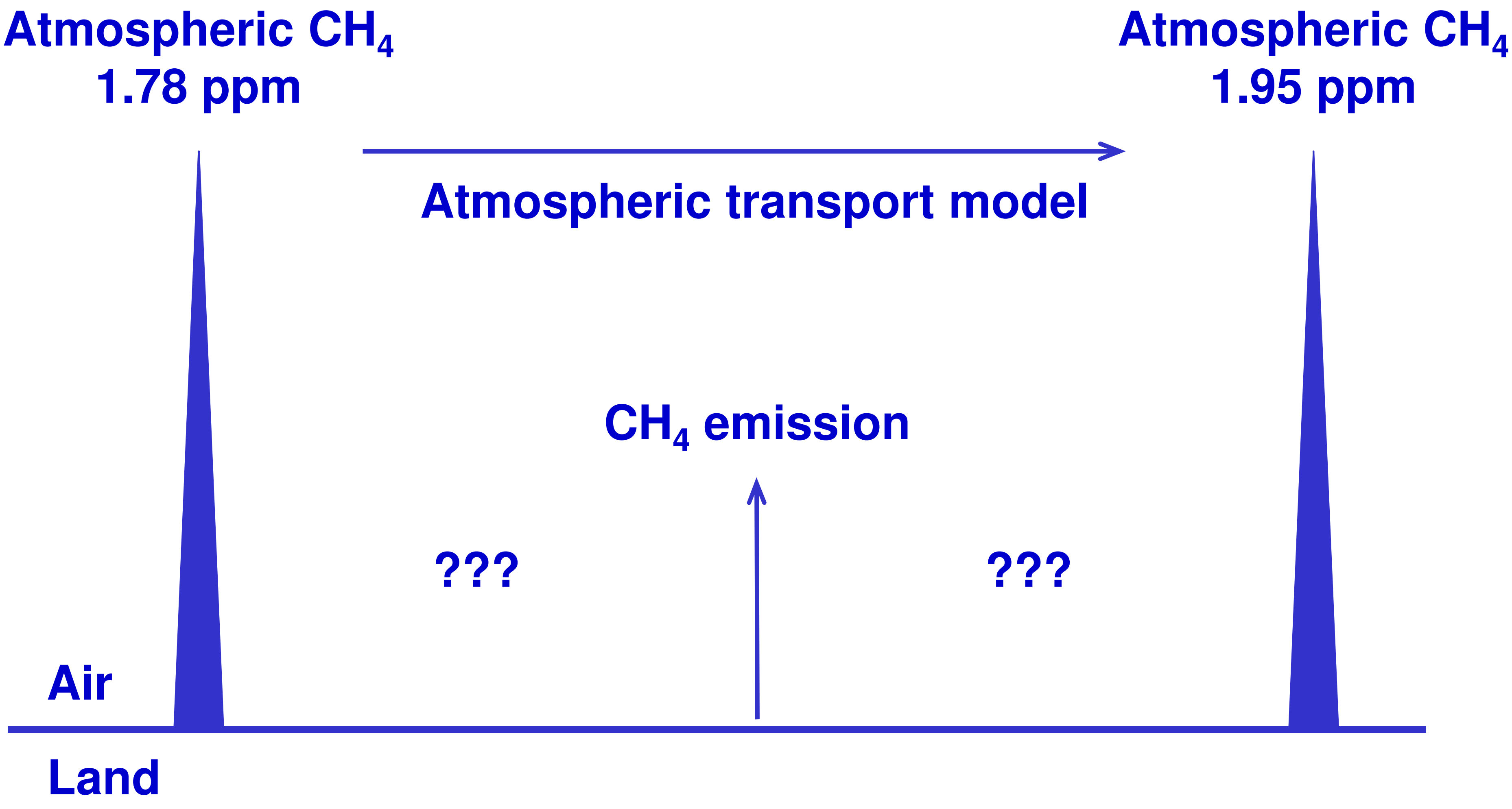

Introduction

Top-down approach

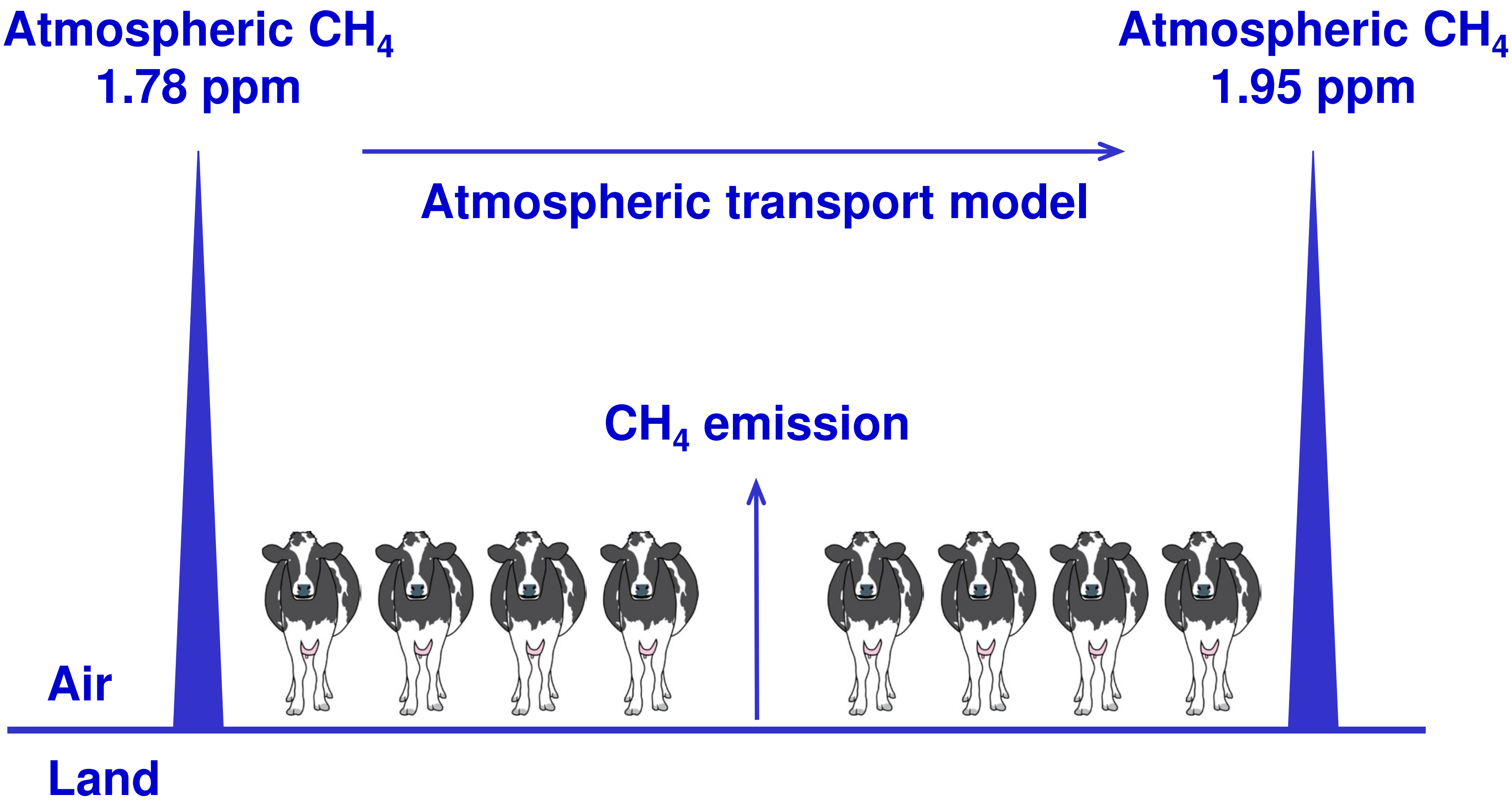

Introduction

Top-down approach

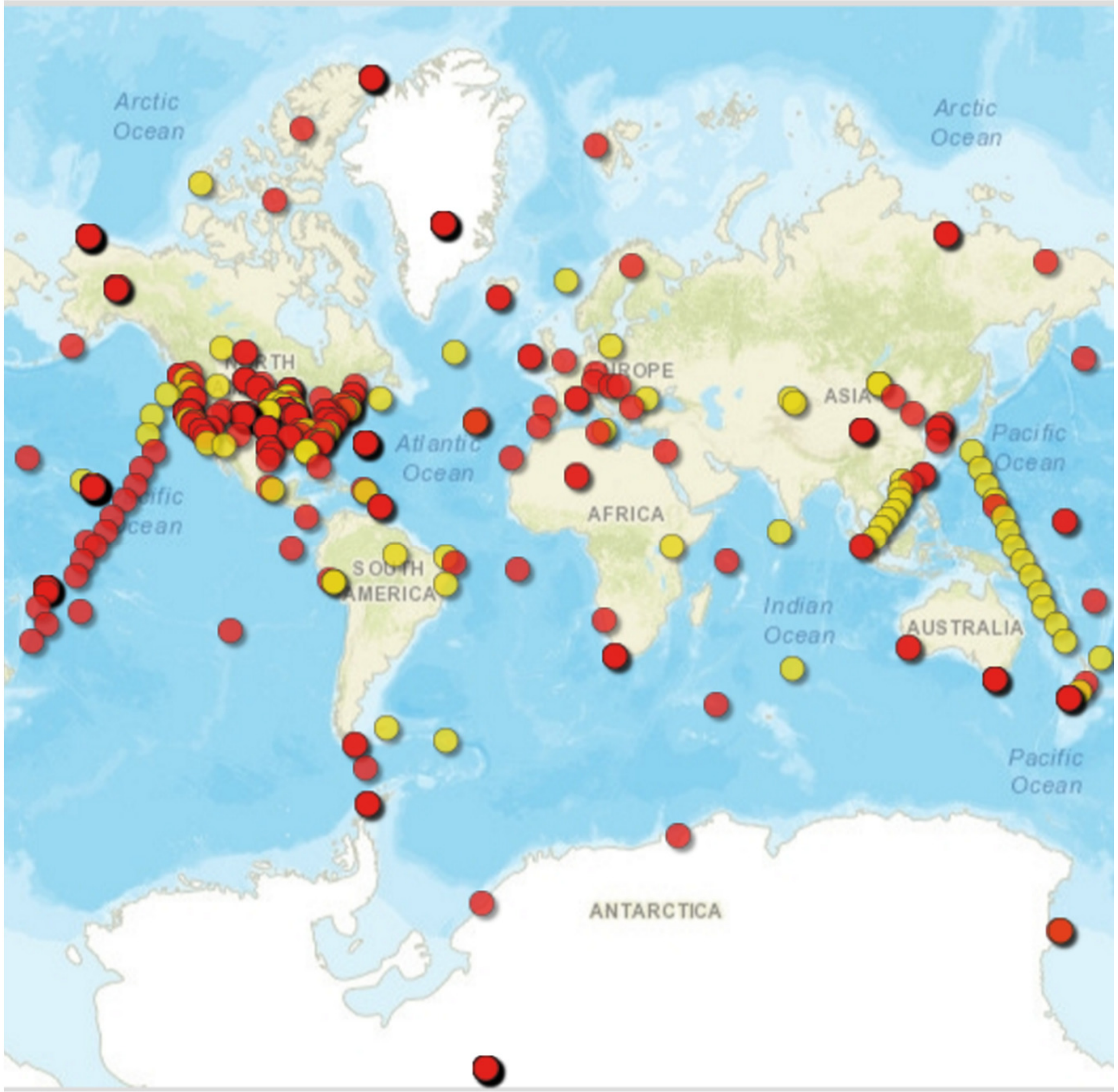

Introduction

Top-down approach

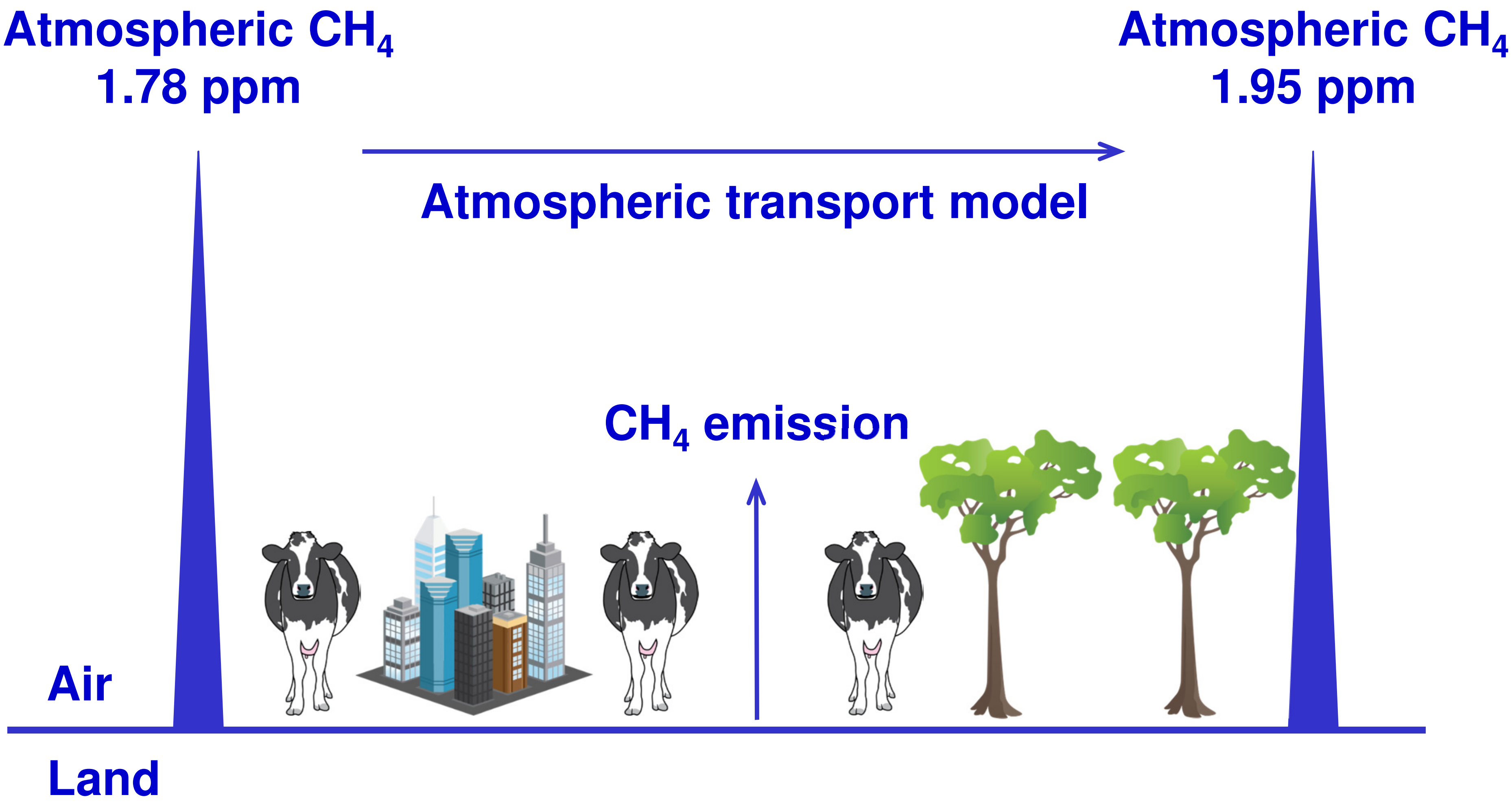

Large variety of CH_4 sources that overlap geographically

Introduction

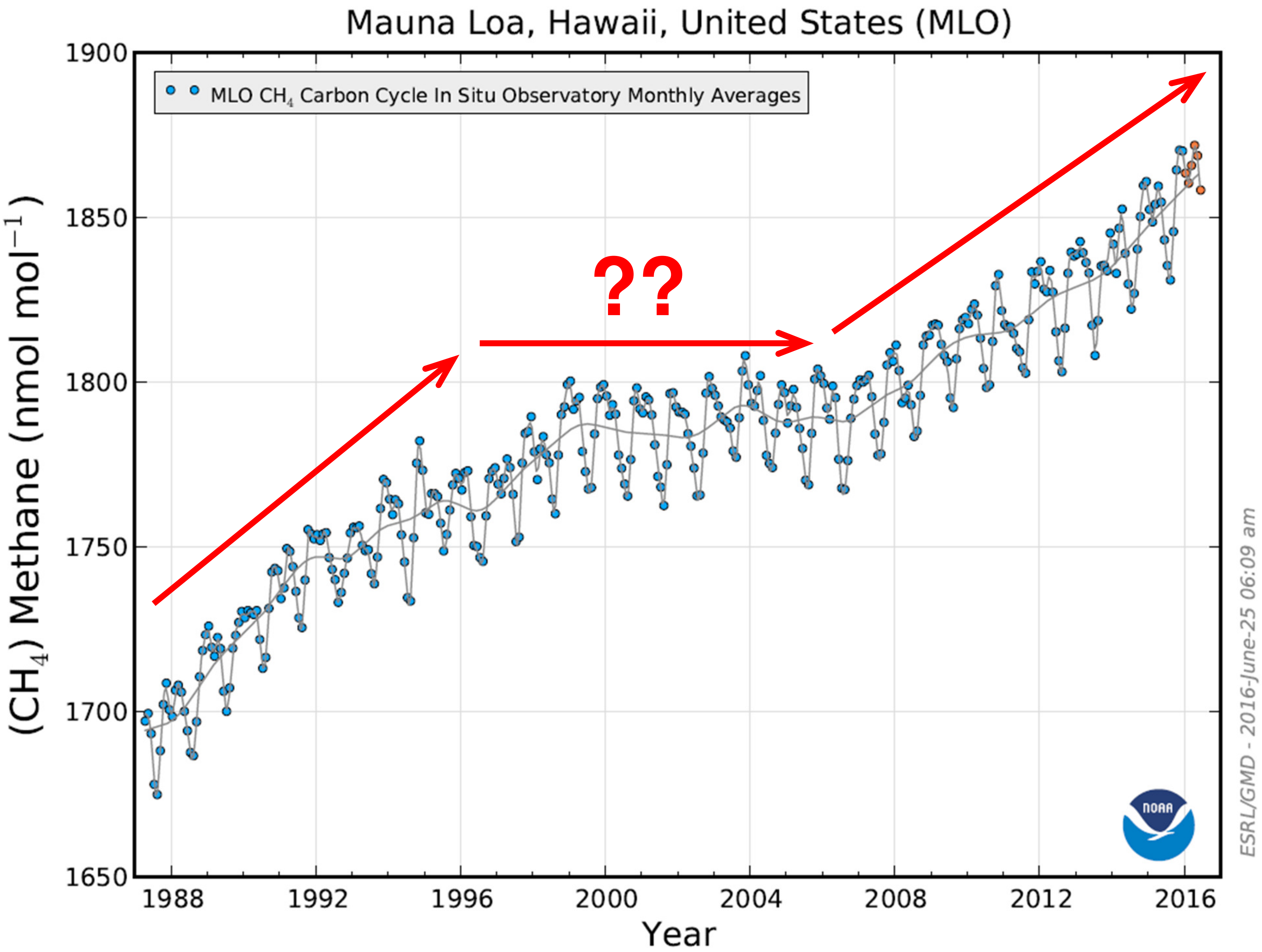

Introduction

ATMOSPHERIC SCIENCE

Methane on the Rise—Again

Euan G. Nisbet,[1] Edward J. Dlugokencky,[2] Philippe Bousquet[3]

Atmospheric concentrations of the greenhouse gas methane are rising, but the reasons remain incompletely understood.

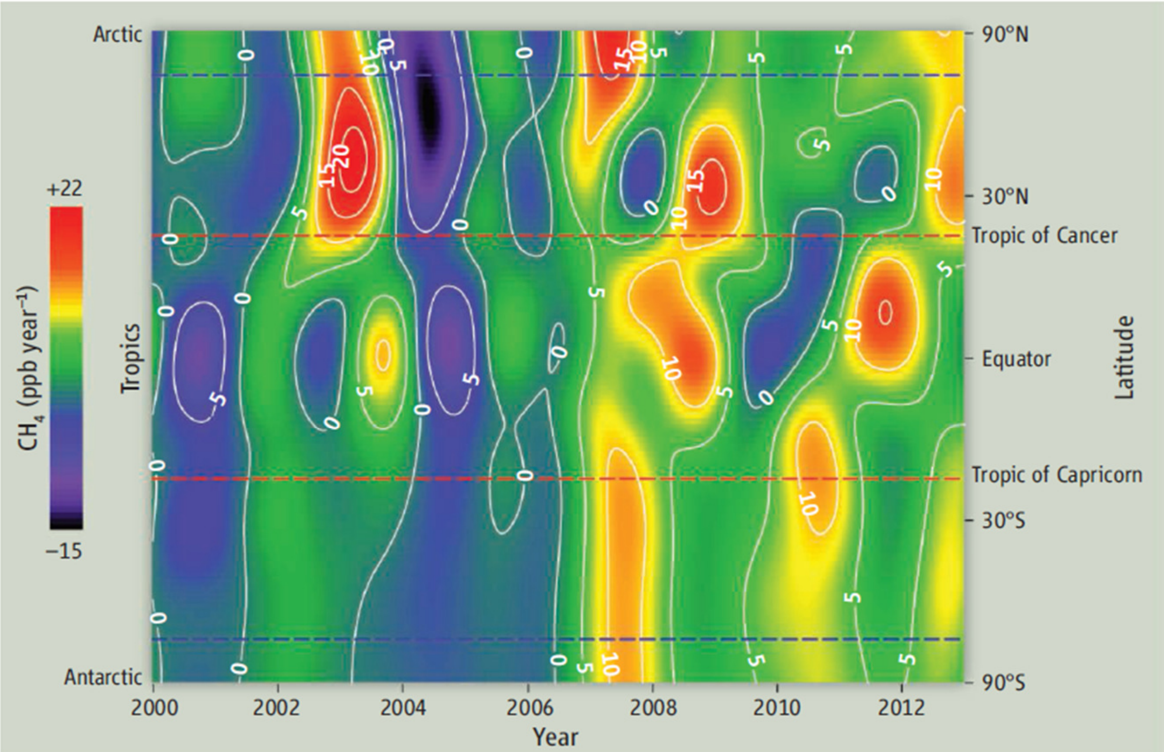

Methane growth rate by latitude. Contours of methane growth rate with sine of latitude. Plotting by sine of degree of latitude equally weights the results for surface area with latitude. Data from www.esrl.noaa.gov/gmd/ccgg/mbl/.

Atmospheric data show that global emissions were ~15 to 22 Tg (million tons) CH_4 per year greater in 2010 than in 2005. Global-scale modeling of these methane observations (*4*, *5*, *11*) suggests that in 2007, tropical wetland emissions dominated growth, with output from high northern latitudes also important. Since then, the increase has mostly been driven by the tropics (9 to 14 Tg/year) and northern mid-latitudes (6 to 8 Tg/year) (*11*).

Introduction

Science

REPORTS

Cite as: H. Schaefer *et al.*, *Science* 10.1126/science.aad2705 (2016).

A 21st century shift from fossil-fuel to biogenic methane emissions indicated by $^{13}CH_4$

Hinrich Schaefer,[1*] Sara E. Mikaloff Fletcher,[1] Cordelia Veidt,[2] Keith R. Lassey,[1†] Gordon W. Brailsford,[1] Tony M. Bromley,[1] Edward J. Dlugokencky,[3] Sylvia E. Michel,[4] John B. Miller,[3] Ingeborg Levin,[2] Dave C. Lowe,[1‡] Ross J. Martin,[1] Bruce H. Vaughn,[4] James W. C. White[4]

[1]National Institute of Water and Atmospheric Research, Wellington 6021, New Zealand. [2]Institut für Umweltphysik, Heidelberg University, Germany. [3]National Oceanic and Atmospheric Administration, Earth System Research Laboratory, Boulder, CO, USA. [4]Institute of Arctic and Alpine Research, Boulder, CO, USA.

*Corresponding author. E-mail: hinrich.schaefer@niwa.co.nz

†Present address: Lassey Research & Education, Wellington, New Zealand.

‡Present address: LoweNZ, Plimmerton, New Zealand.

Between 1999 and 2006, a plateau interrupted the otherwise continuous increase of atmospheric methane concentration [CH_4] since pre-industrial times. Causes could be sink variability or a temporary reduction in industrial or climate sensitive sources. We reconstruct the global history of [CH_4] and its stable carbon isotopes from ice cores, archived air and a global network of monitoring stations. A box-model analysis suggests that diminishing thermogenic emissions, probably from the fossil-fuel industry, and/or variations in the hydroxyl CH_4-sink caused the [CH_4]-plateau. Thermogenic emissions didn't resume to cause the renewed [CH_4]-rise after 2006, which contradicts emission inventories. Post-2006 source increases are predominantly biogenic, outside the Arctic, and arguably more consistent with agriculture than wetlands. If so, mitigating CH_4-emissions must be balanced with the need for food production.

Introduction

How important are emissions of greenhouse-gas from inland waters ?

Introduction

Global carbon dioxide emissions from inland waters

Peter A. Raymond[1], Jens Hartmann[2*], Ronny Lauerwald[2,3*], Sebastian Sobek[4*], Cory McDonald[5], Mark Hoover[1], David Butman[1,6], Robert Striegl[6], Emilio Mayorga[7], Christoph Humborg[8], Pirkko Kortelainen[9], Hans Dürr[10], Michel Meybeck[11], Philippe Ciais[12] & Peter Guth[13]

Carbon dioxide (CO_2) transfer from inland waters to the atmosphere, known as CO_2 evasion, is a component of the global carbon cycle. Global estimates of CO_2 evasion have been hampered, however, by the lack of a framework for estimating the inland water surface area and gas transfer velocity and by the absence of a global CO_2 database. Here we report regional variations in global inland water surface area, dissolved CO_2 and gas transfer velocity. We obtain global CO_2 evasion rates of $1.8^{+0.25}_{-0.25}$ petagrams of carbon (Pg C) per year from streams and rivers and $0.32^{+0.52}_{-0.26}$ Pg C yr^{-1} from lakes and reservoirs, where the upper and lower limits are respectively the 5th and 95th confidence interval percentiles. The resulting global evasion rate of 2.1 Pg C yr^{-1} is higher than previous estimates owing to a larger stream and river evasion rate. Our analysis predicts global hotspots in stream and river evasion, with about 70 per cent of the flux occurring over just 20 per cent of the land surface. The source of inland water CO_2 is still not known with certainty and new studies are needed to research the mechanisms controlling CO_2 evasion globally.

Source of 2.1 PgC yr^{-1}

Raymond et al. (2013)

Global anthropogenic CO_2 fluxes in 2010 ($PgC\ y^{-1} = 10^{15}\ gC\ y^{-1}$)

$9.1 \pm 0.5\ PgC\ y^{-1}$

$0.9 \pm 0.7\ PgC\ y^{-1}$ +

$5.0 \pm 0.2\ PgC\ y^{-1}$

50%

$2.6 \pm 1.0\ PgC\ y^{-1}$

26%

Calculated as the residual of all other flux components

24%

$2.4 \pm 0.5\ PgC\ y^{-1}$

Average of 5 models

www.globalcarbonproject.org/

Introduction

Spatial patterns in CO_2 evasion from the global river network

Ronny Lauerwald[1,2,3], Goulven G. Laruelle[1,4], Jens Hartmann[3], Philippe Ciais[5], and Pierre A. G. Regnier[1]

[1]Department of Earth and Environmental Sciences, Université Libre de Bruxelles, Brussels, Belgium, [2]Institut Pierre-Simon Laplace, Paris, France, [3]Institute for Geology, University of Hamburg, Hamburg, Germany, [4]Department of Earth Sciences-Geochemistry, Utrecht University, Utrecht, Netherlands, [5]LSCE IPSL, Gif Sur Yvette, France

Abstract CO_2 evasion from rivers (FCO_2) is an important component of the global carbon budget. Here we present the first global maps of CO_2 partial pressures (pCO_2) in rivers of stream orders 3 and higher and the resulting FCO_2 at 0.5° resolution constructed with a statistical model. A geographic information system based approach is used to derive a pCO_2 prediction function trained on data from 1182 sampling locations. While data from Asia and Africa are scarce and the training data set is dominated by sampling locations from the Americas, Europe, and Australia, the sampling locations cover the full spectrum from high to low latitudes. The predictors of pCO_2 are net primary production, population density, and slope gradient within the river catchment as well as mean air temperature at the sampling location ($r^2 = 0.47$). The predicted pCO_2 map was then combined with spatially explicit estimates of stream surface area A_{river} and gas exchange velocity k calculated from published empirical equations and data sets to derive the FCO_2 map. Using Monte Carlo simulations, we assessed the uncertainties of our estimates. At the global scale, we estimate an average river pCO_2 of 2400 (2019–2826) μatm and a FCO_2 of 650 (483–846) Tg C yr^{-1} (5th and 95th percentiles of confidence interval). Our global CO_2 evasion is substantially lower than the recent estimate of 1800 Tg C yr^{-1} although the training set of pCO_2 is very similar in both studies, mainly due to lower tropical pCO_2 estimates in the present study. Our maps reveal strong latitudinal gradients in pCO_2, A_{river}, and FCO_2. The zone between 10°N and 10°S contributes about half of the global CO_2 evasion. Collection of pCO_2 data in this zone, in particular, for African and Southeast Asian rivers is a high priority to reduce uncertainty on FCO_2.

Lauerwald et al. (2015)

3 x lower than Raymond et al.

Introduction

Raymond et al. (2013)

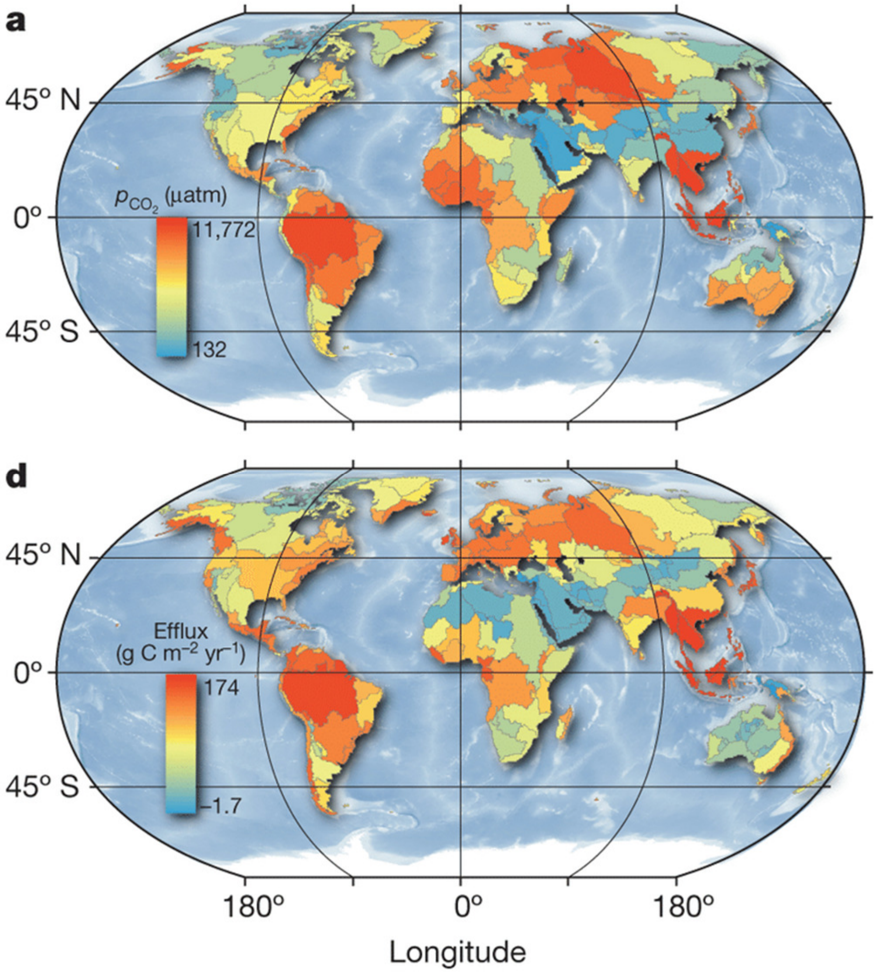

Lauerwald et al. (2015)

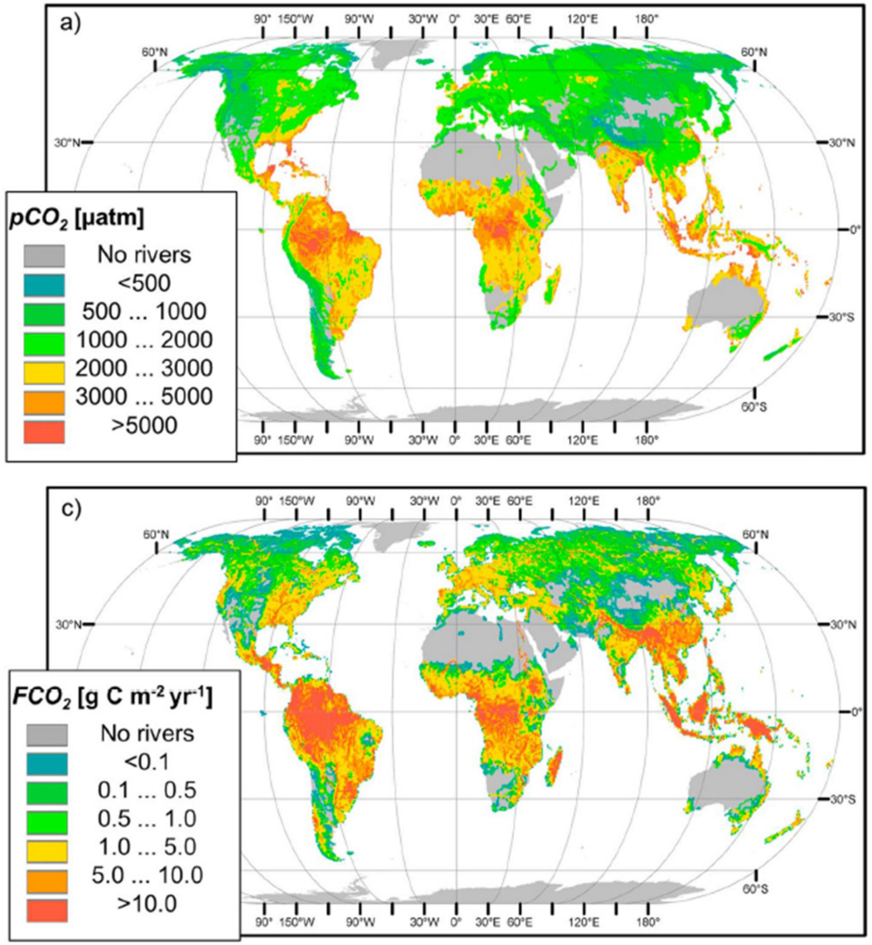

Introduction

Raymond et al. (2013)

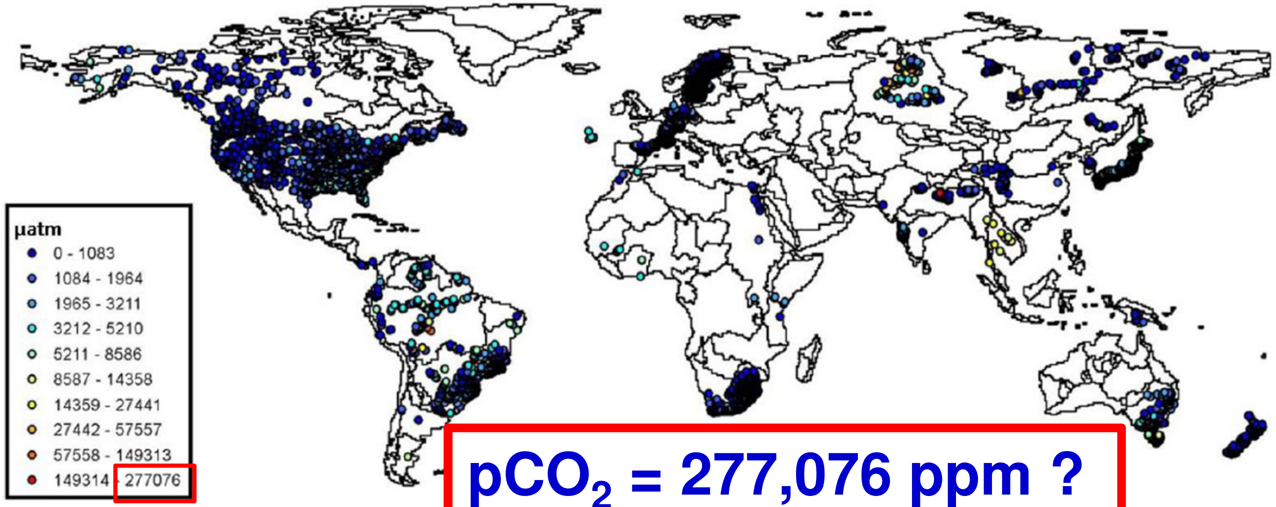

pCO_2 = 277,076 ppm ?

Lauerwald et al. (2015)

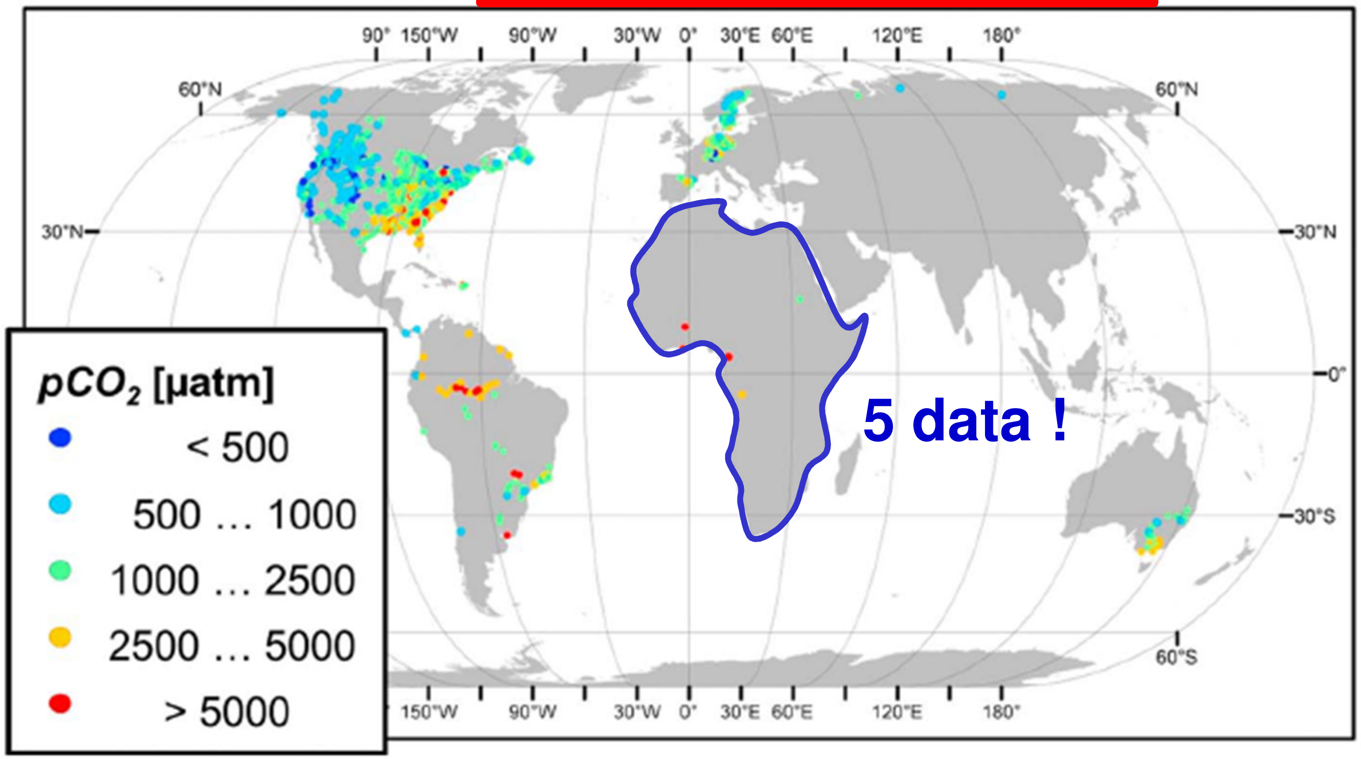

5 data !

Raymond et al. (2013) & Lauerwald et al. (2015) used pCO_2 computed from pH and total alkalinity

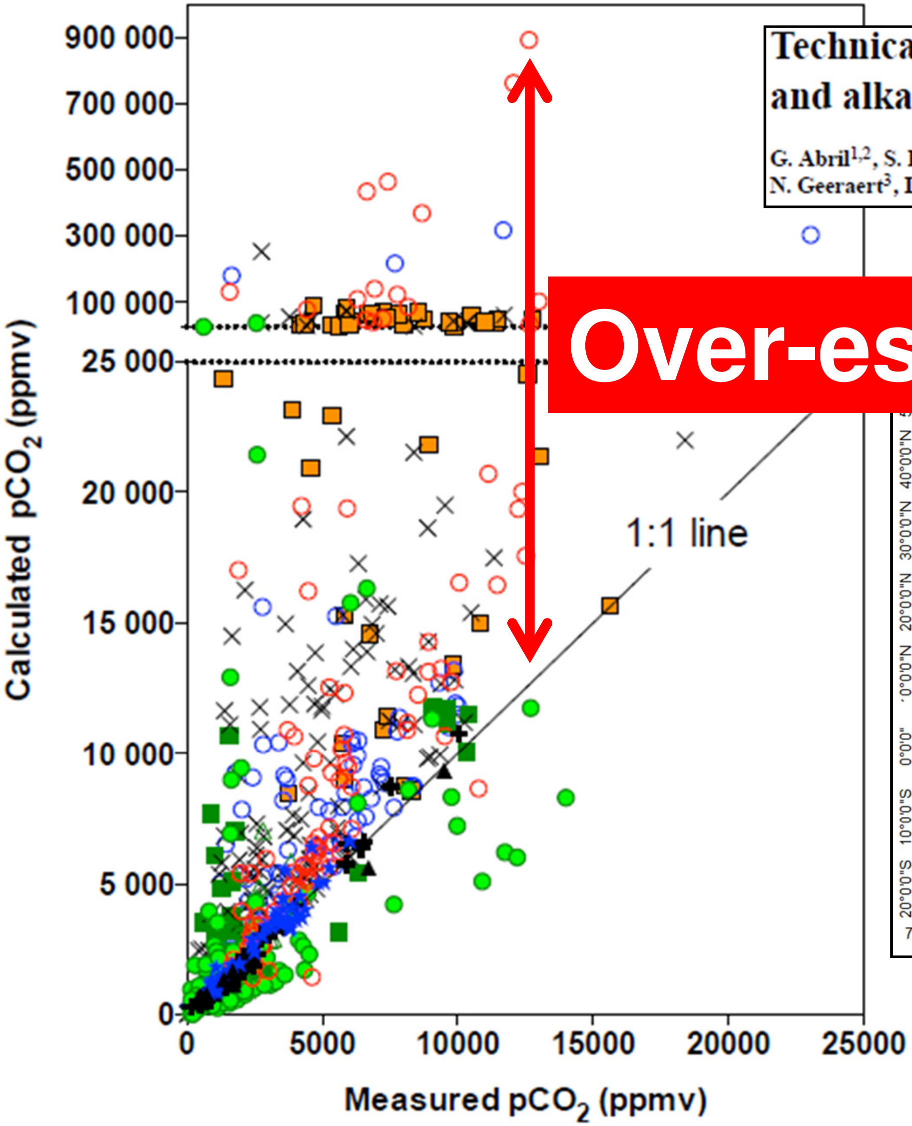

Technical Note: Large overestimation of pCO_2 calculated from pH and alkalinity in acidic, organic-rich freshwaters

G. Abril[1,2], S. Bouillon[3], F. Darchambeau[4], C. R. Teodoru[3], T. R. Marwick[3], F. Tamooh[3], F. Ochieng Omengo[3], N. Geeraert[3], L. Deirmendjian[1], P. Polsenaere[1], and A. V. Borges[4]

Over-estimation up to 75 x

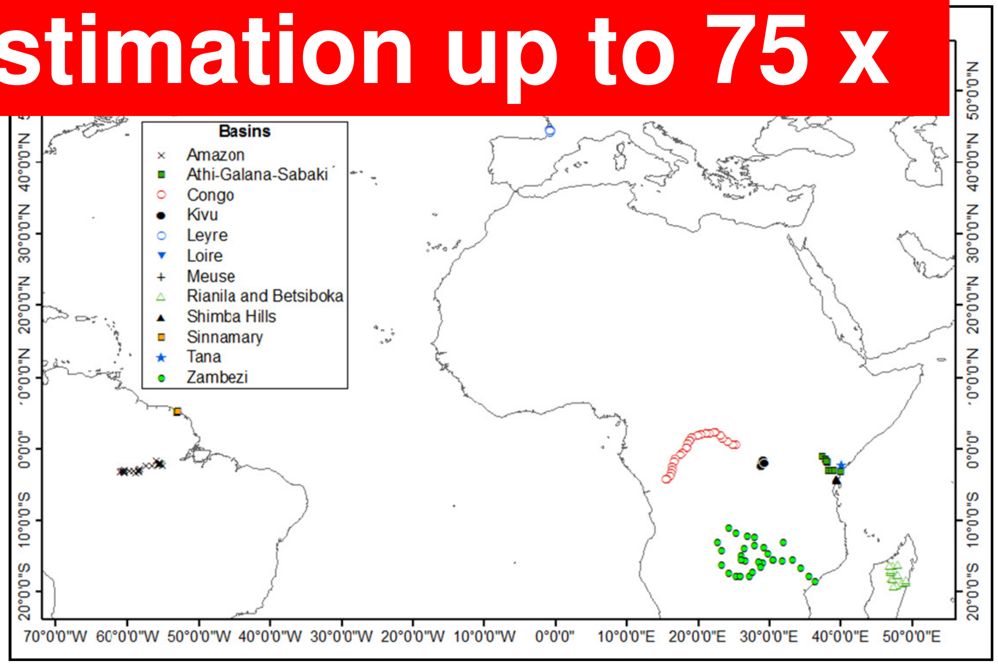

Introduction

$CO_2 + H_2O = HCO_3^- + H^+$ $K_1 = [CO_2] / ([HCO_3^-] + [H^+]) = f(S,T)$

$HCO_3^- = CO_3^{2-} + H^+$ $K_2 = [HCO_3^-] / ([CO_3^{2-}] + [H^+]) = f(S,T)$

pH = -log[H+]

Total Alkalinity = $[HCO_3^-] + 2 [CO_3^{2-}]$ + borate **+ organic alkalinity = humic acids**

borate = f(S)

Carbonate Alkalinity (CA) = $[HCO_3^-] + 2 [CO_3^{2-}]$

4 equations = K_1, K_2, pH, Total Alkalinity

4 unknows = $[CO_2]$, $[HCO_3^-]$, $[CO_3^{2-}]$, $[H^+]$

$[CO_2] = CA*[H^+]^2 / (K_1*([H^+]^2 + 2K_2)$

$pCO_2 = [CO_2] / K_H$ (Henry's Law)

Unaccounted fifth variable ⇒ solution is wrong

Introduction

Where's the river/lake CO_2 coming from ?

Plumbing the Global Carbon Cycle: Integrating Inland Waters into the Terrestrial Carbon Budget

J. J. Cole,[1] Y. T. Prairie,[2,*] N. F. Caraco,[1] W. H. McDowell,[3] L. J. Tranvik,[4] R. G. Striegl,[5] C. M. Duarte,[6] P. Kortelainen,[7] J. A. Downing,[8] J. J. Middelburg,[9] and J. Melack,[10]

Introduction

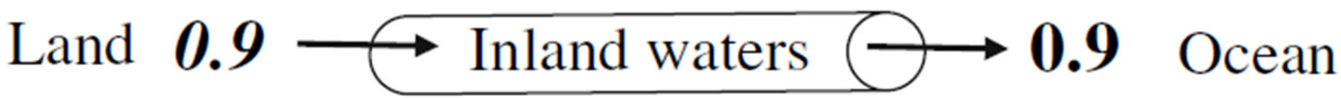

Fluxes in PgC yr^{-1}

Introduction

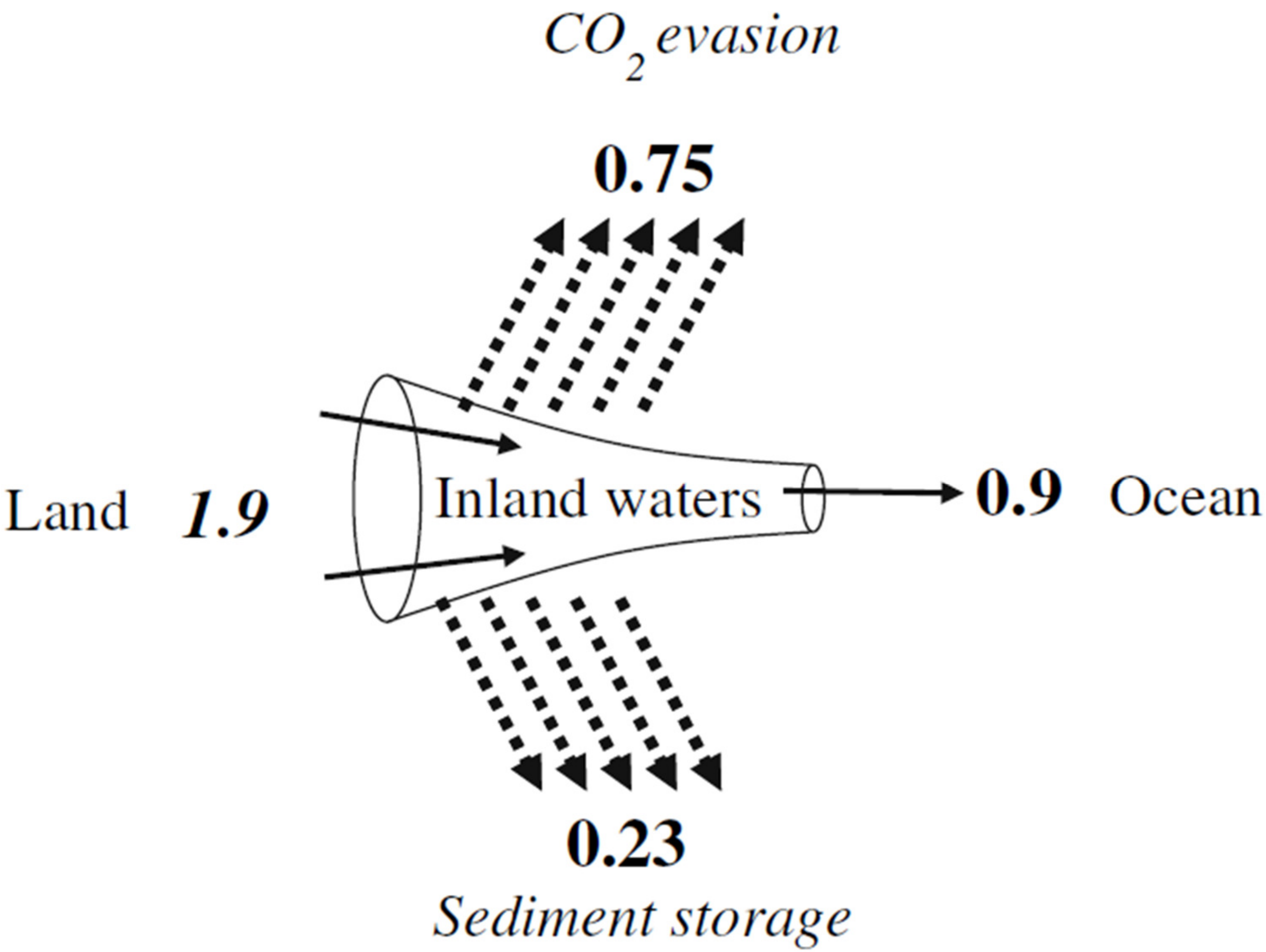

Fluxes in PgC yr^{-1}

Amazon River carbon dioxide outgassing fuelled by wetlands

Gwenaël Abril[1,2], Jean-Michel Martinez[2], L. Felipe Artigas[3], Patricia Moreira-Turcq[2], Marc F. Benedetti[4], Luciana Vidal[5], Tarik Meziane[6], Jung-Hyun Kim[7], Marcelo C. Bernardes[8], Nicolas Savoye[1], Jonathan Deborde[1], Edivaldo Lima Souza[9], Patrick Albéric[10], Marcelo F. Landim de Souza[11] & Fabio Roland[5]

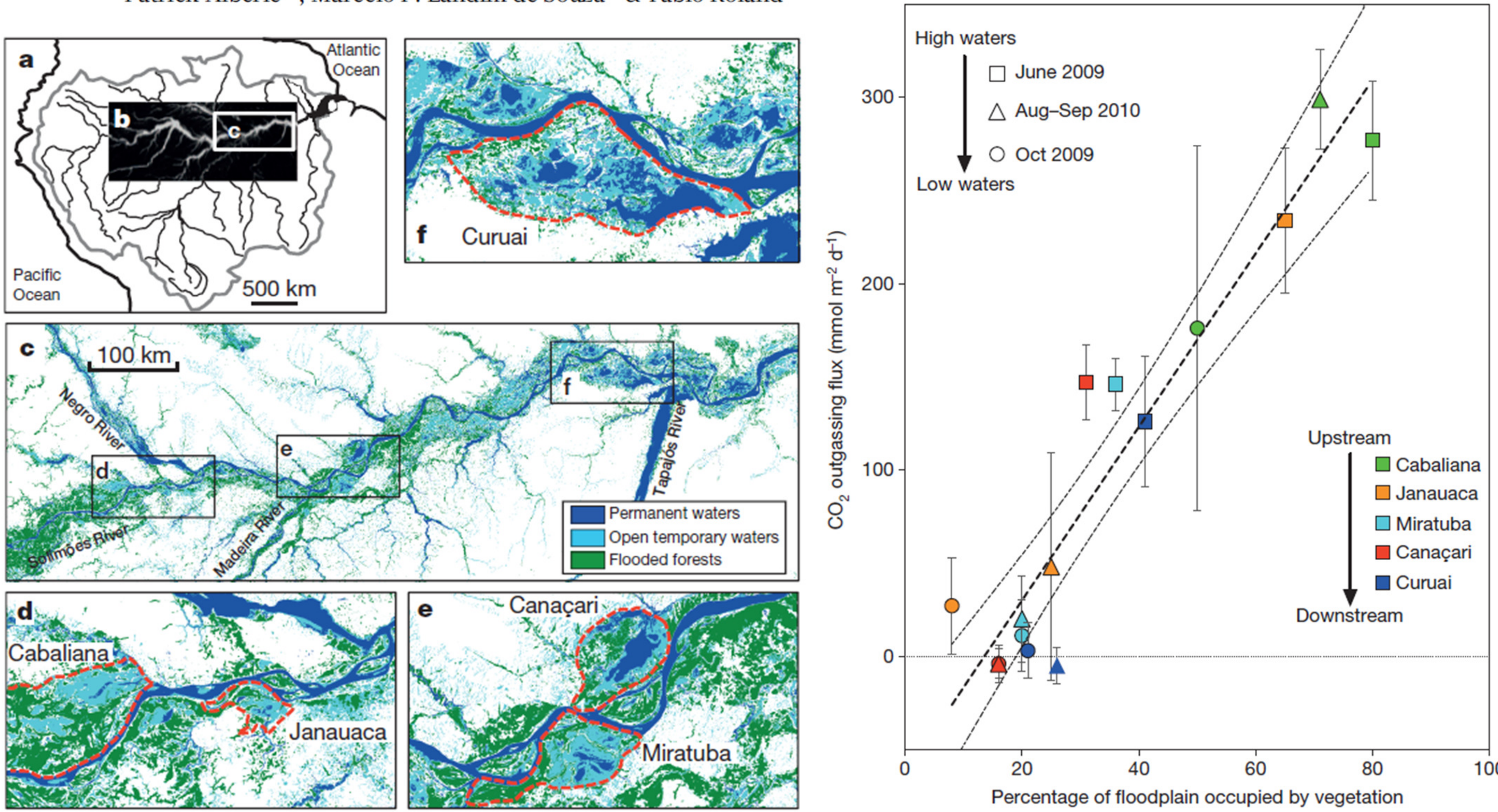

Catchment productivity controls CO_2 emissions from lakes

Stephen C. Maberly[1]*, Philip A. Barker[2], Andy W. Stott[3] and Mitzi M. De Ville[1]

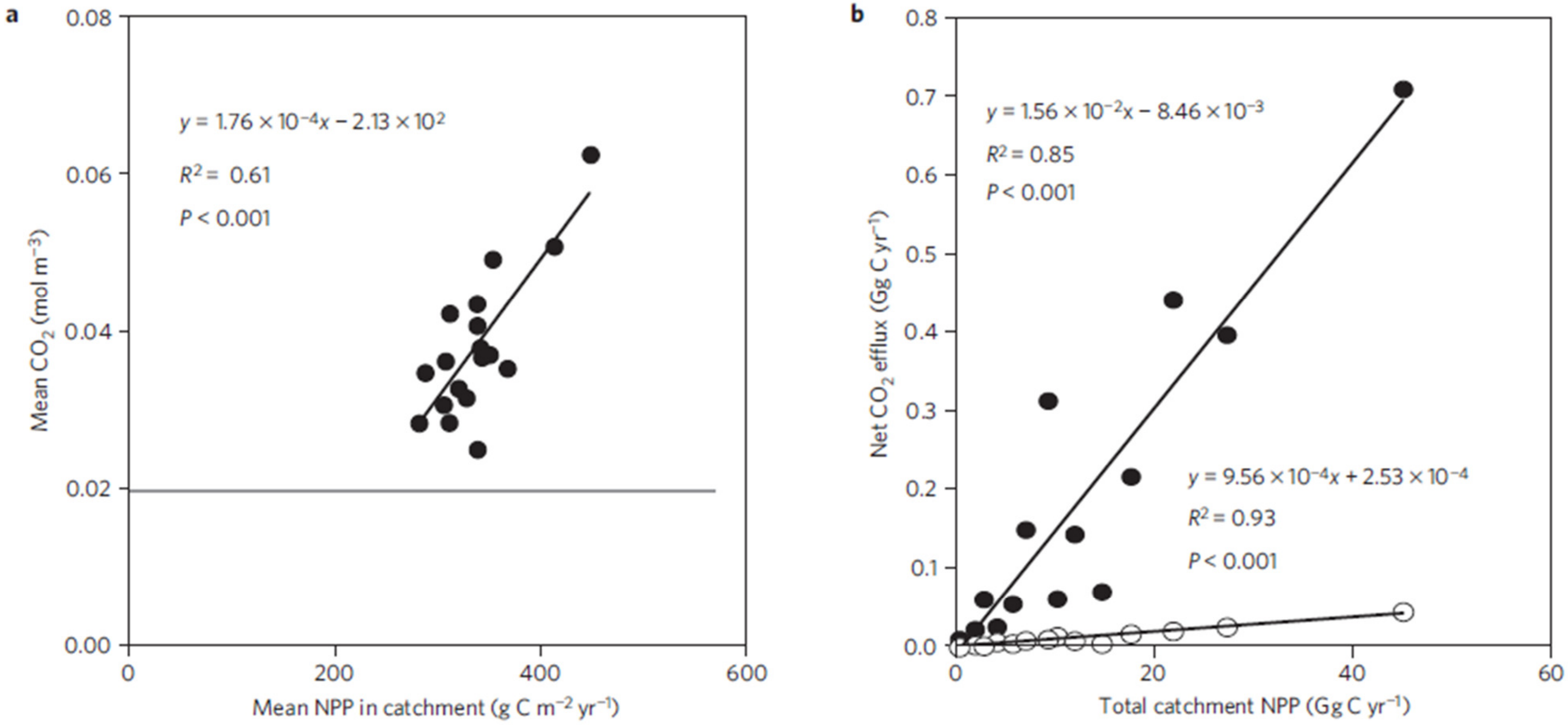

Figure 3 | Links between lake CO_2 concentration, CO_2 efflux and catchment productivity. a, Relationship between mean CO_2 concentration measured four times a year in 1984, 1991, 1995, 2000, 2005 and 2010 and mean NPP estimated from area of different land cover categories in the catchment. **b**, Estimated CO_2 efflux from the lake surface (filled circles) and loss of CO_2 to the downstream river (open circles) for lakes without another major lake upstream. The grey horizontal line in **a** is the approximate mean air-equilibrium concentration.

Introduction

nature geoscience
LETTERS
PUBLISHED ONLINE: 10 AUGUST 2015 | DOI: 10.1038/NGEO2507

Sources of and processes controlling CO_2 emissions change with the size of streams and rivers

E. R. Hotchkiss[1*†], R. O. Hall Jr[2], R. A. Sponseller[1], D. Butman[3], J. Klaminder[1], H. Laudon[4], M. Rosvall[5] and J. Karlsson[1]

nature geoscience
LETTERS
PUBLISHED ONLINE: 9 NOVEMBER 2015 | DOI: 10.1038/NGEO2582

Significant fraction of CO_2 emissions from boreal lakes derived from hydrologic inorganic carbon inputs

Gesa A. Weyhenmeyer[1*], Sarian Kosten[2], Marcus B. Wallin[1,3], Lars J. Tranvik [1], Erik Jeppesen[4,5] and Fabio Roland[6]

Introduction

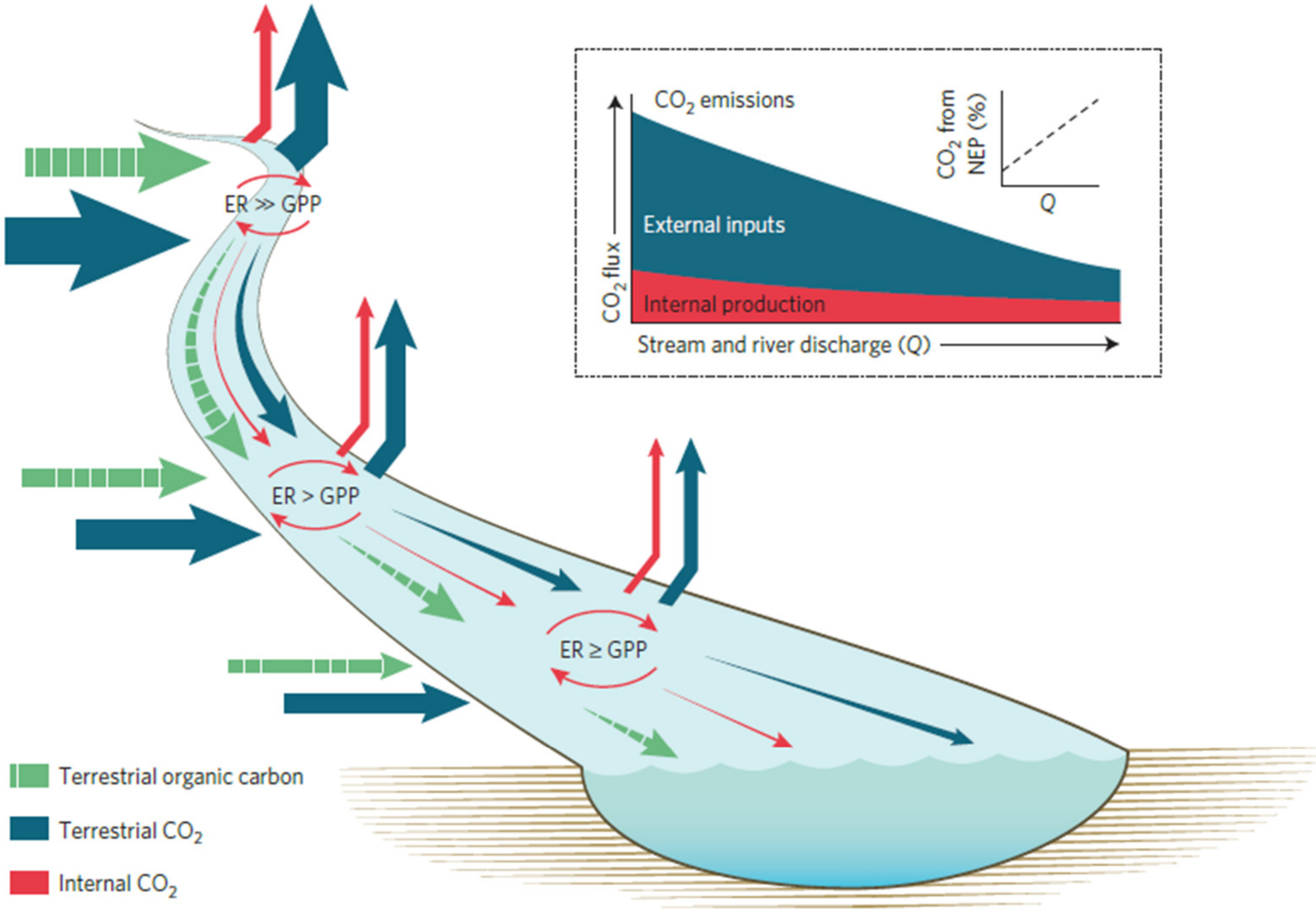

Figure 3 | Sources and magnitude of net CO_2 emissions along a theoretical stream–river continuum. Terrestrially derived CO_2 and organic carbon inputs per unit aquatic area decline downstream, decreasing net CO_2 emission rates in rivers compared to streams. Rapid loss of CO_2 results in a downstream shift in the source contributions to CO_2 emissions, from dominance of external CO_2 in streams to a more balanced supply of internal and external sources in rivers. Thus, aquatic mineralization of terrestrial OC (CO_2 from NEP) should contribute to a higher proportion of annual net CO_2 emissions in large rivers relative to small streams.

Introduction

Meuse Bassin

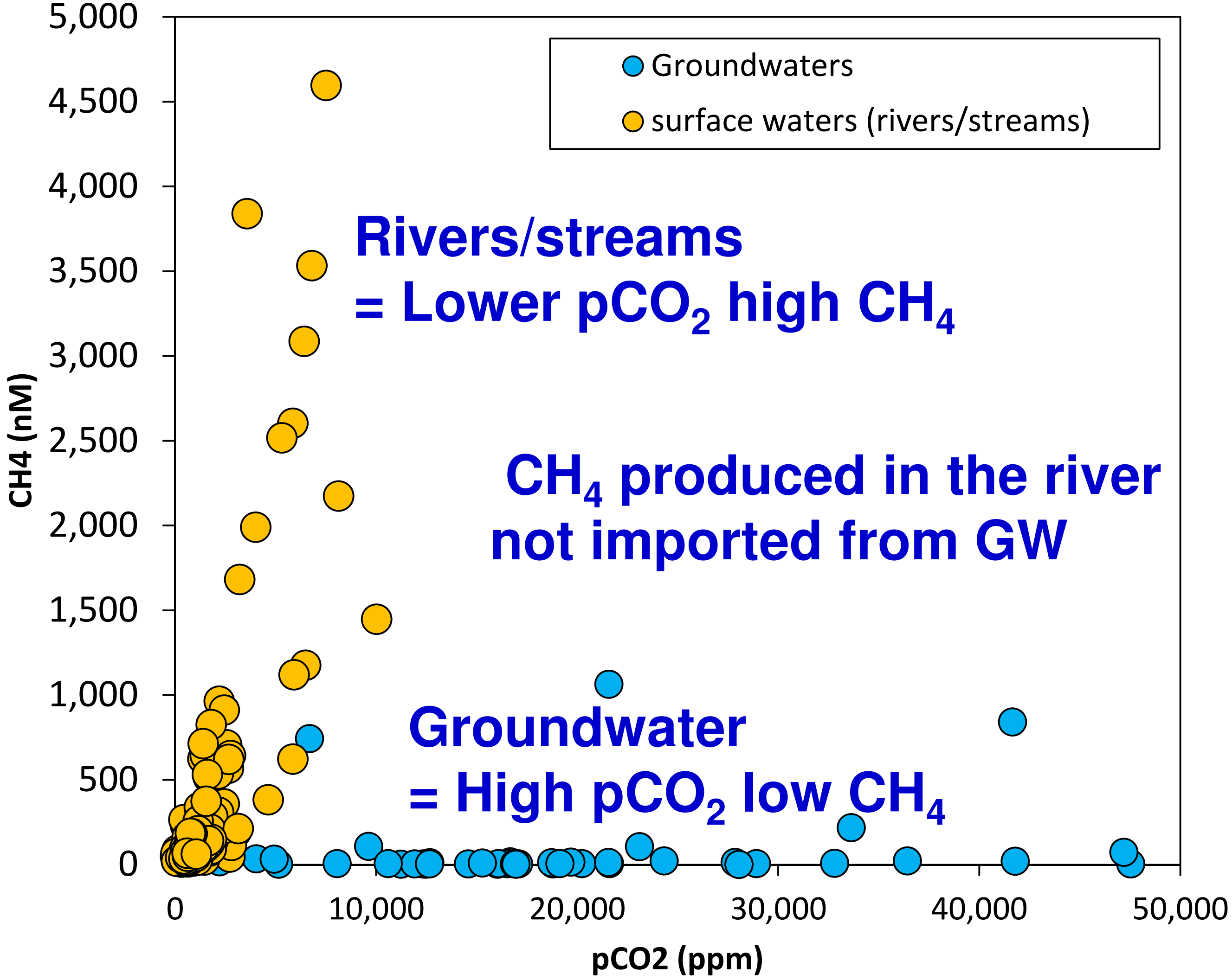

A.V. Borges (unpublished)

Introduction

Africa and global GHGs budgets

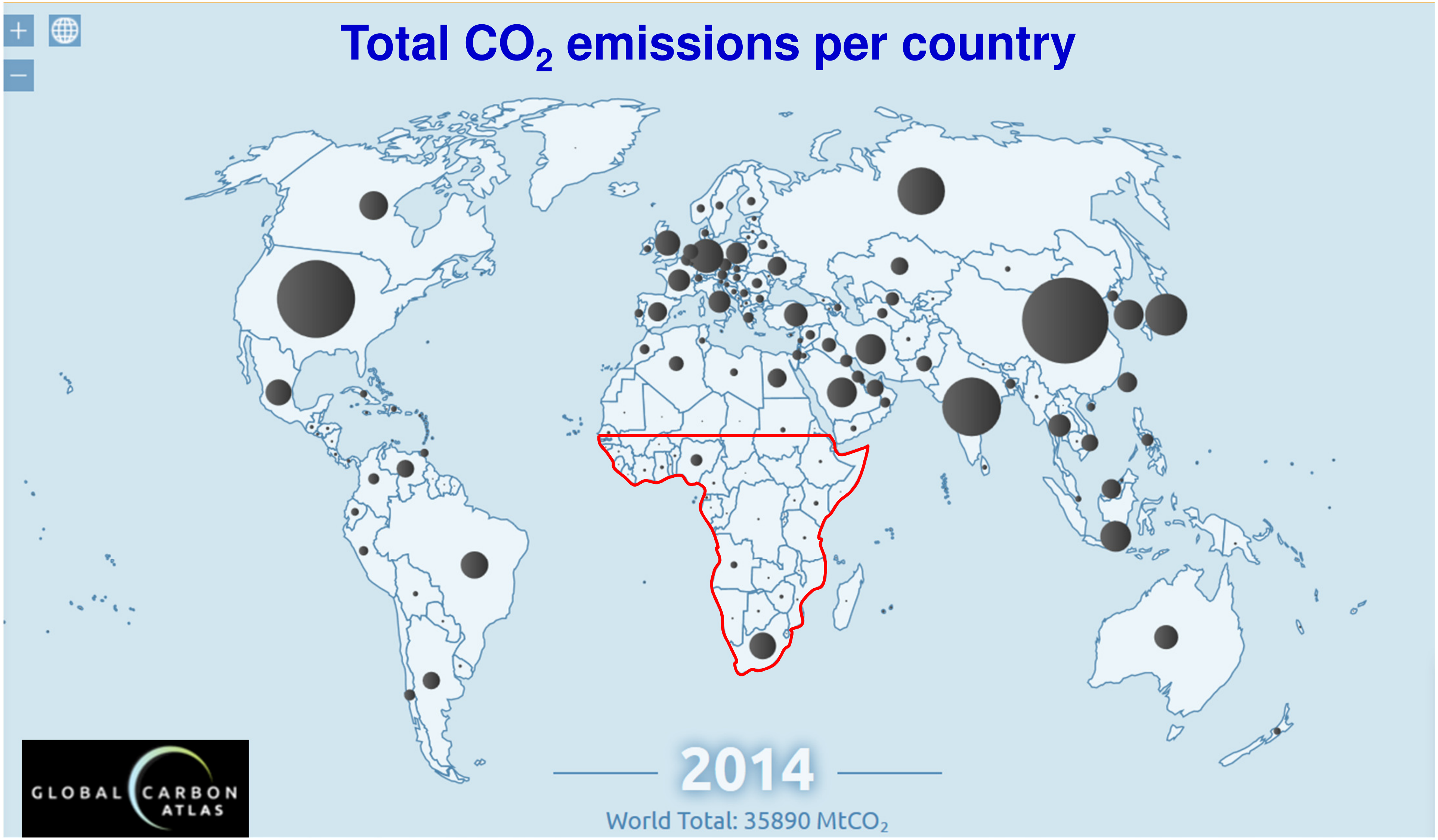
Total CO_2 emissions per country
GLOBAL CARBON ATLAS
2014
World Total: 35890 $MtCO_2$

Total CO_2 emissions per person

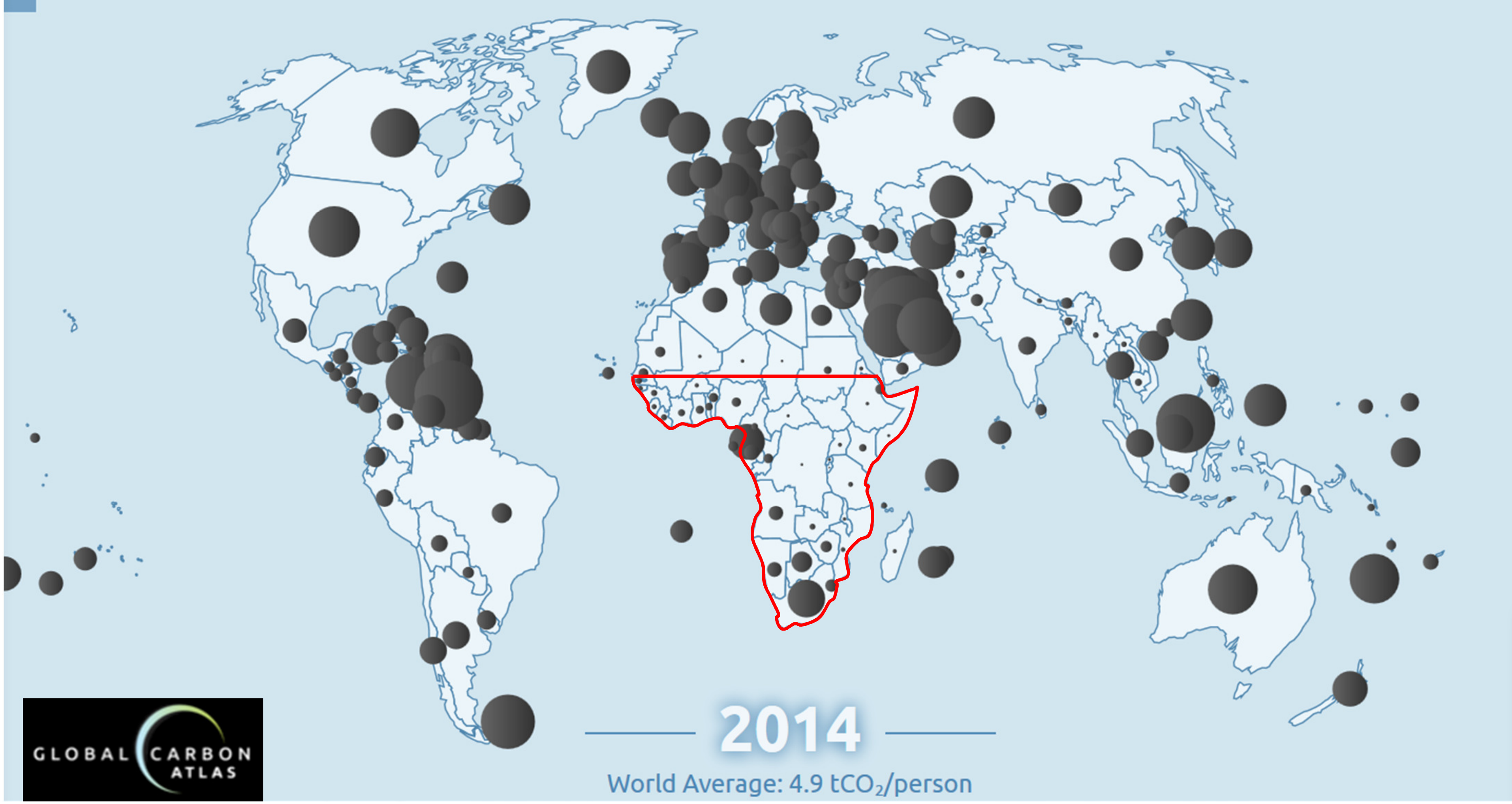

Introduction

The terrestrial biosphere as a net source of greenhouse gases to the atmosphere

Hanqin Tian[1], Chaoqun Lu[1,2], Philippe Ciais[3], Anna M. Michalak[4], Josep G. Canadell[5], Eri Saikawa[6], Deborah N. Huntzinger[7], Kevin R. Gurney[8], Stephen Sitch[9], Bowen Zhang[1], Jia Yang[1], Philippe Bousquet[3], Lori Bruhwiler[10], Guangsheng Chen[11], Edward Dlugokencky[10], Pierre Friedlingstein[12], Jerry Melillo[13], Shufen Pan[1], Benjamin Poulter[14], Ronald Prinn[15], Marielle Saunois[3], Christopher R. Schwalm[7,16] & Steven C. Wofsy[17]

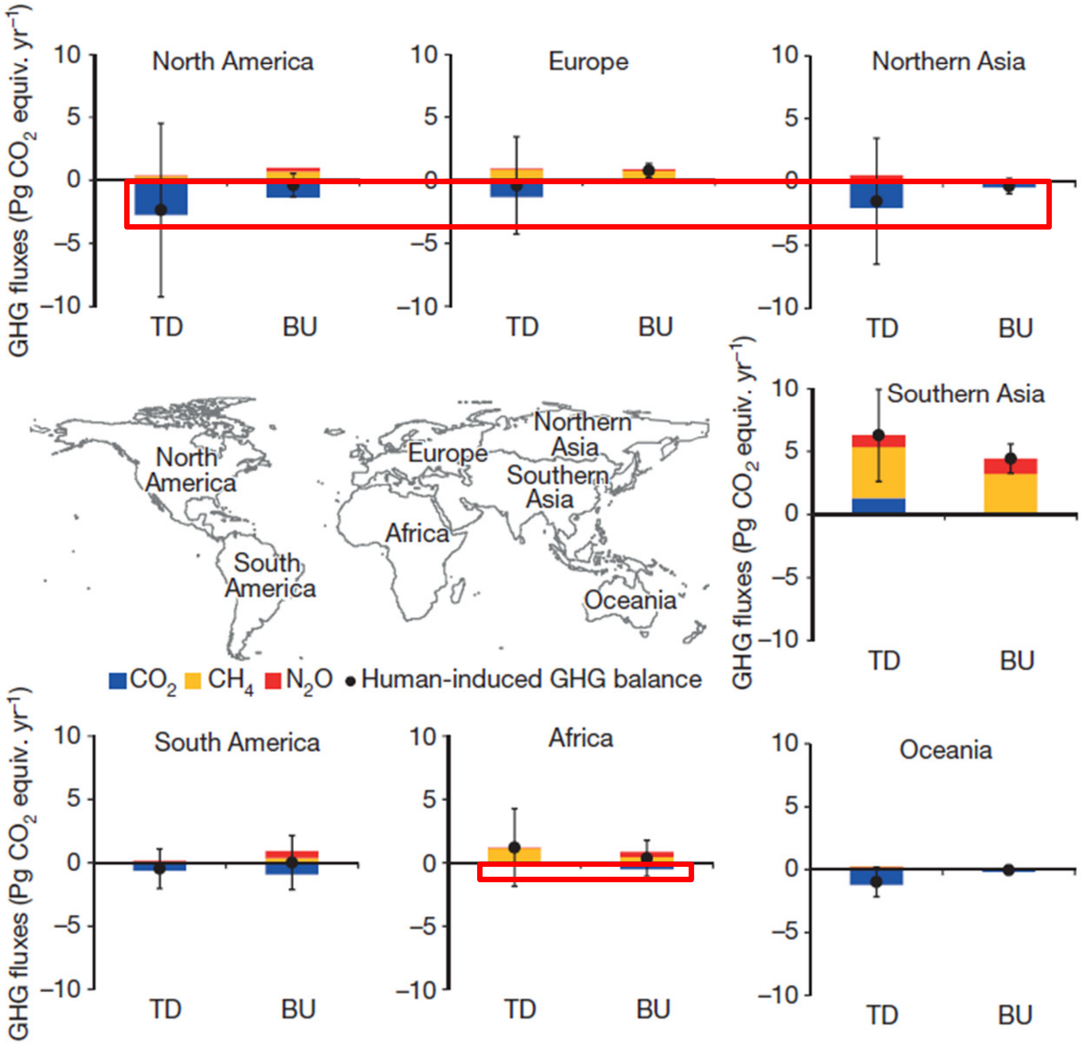

Figure 3 | The balance of human-induced biogenic GHGs for different continents in the 2000s (based on GWP100). Blue bars represent CO_2 flux, yellow CH_4 flux and red for N_2O flux with pre-industrial fluxes removed. Black dots indicate net human-induced GHG balance; error bars, ±s.d. of estimate ensembles.

TD = top-down
BU = bottom-up

Introduction

A full greenhouse gases budget of Africa: synthesis, uncertainties, and vulnerabilities

R. Valentini[1,2], A. Arneth[3], A. Bombelli[2], S. Castaldi[2,4], R. Cazzolla Gatti[1], F. Chevallier[5], P. Ciais[5], E. Grieco[2], J. Hartmann[6], M. Henry[7], R. A. Houghton[8], M. Jung[9], W. L. Kutsch[10], Y. Malhi[11], E. Mayorga[12], L. Merbold[13], G. Murray-Tortarolo[15], D. Papale[1], P. Peylin[5], B. Poulter[5], P. A. Raymond[14], M. Santini[2], S. Sitch[15], G. Vaglio Laurin[2,16], G. R. van der Werf[17], C. A. Williams[18], and R. J. Scholes[19]

The majority of results agree that Africa is a small sink of carbon on an annual scale, with an average value of $-0.61 \pm 0.58\,\mathrm{Pg\,C\,yr^{-1}}$. Nevertheless, the emissions of CH_4 and N_2O may turn Africa into a net source of radiative forcing in CO_2 equivalent terms.

Introduction

Congo river

Congo

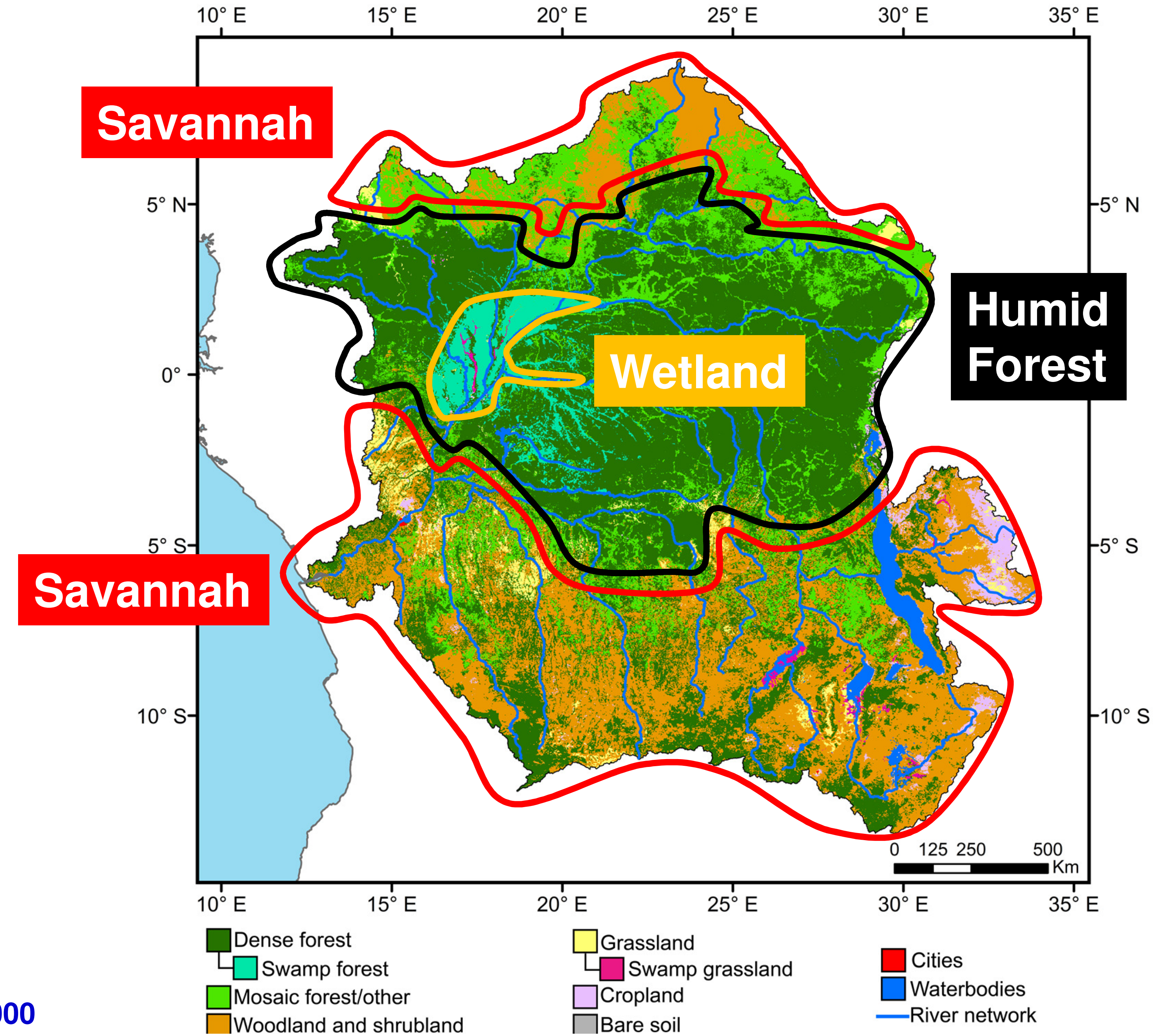

GLC 2000

Congo

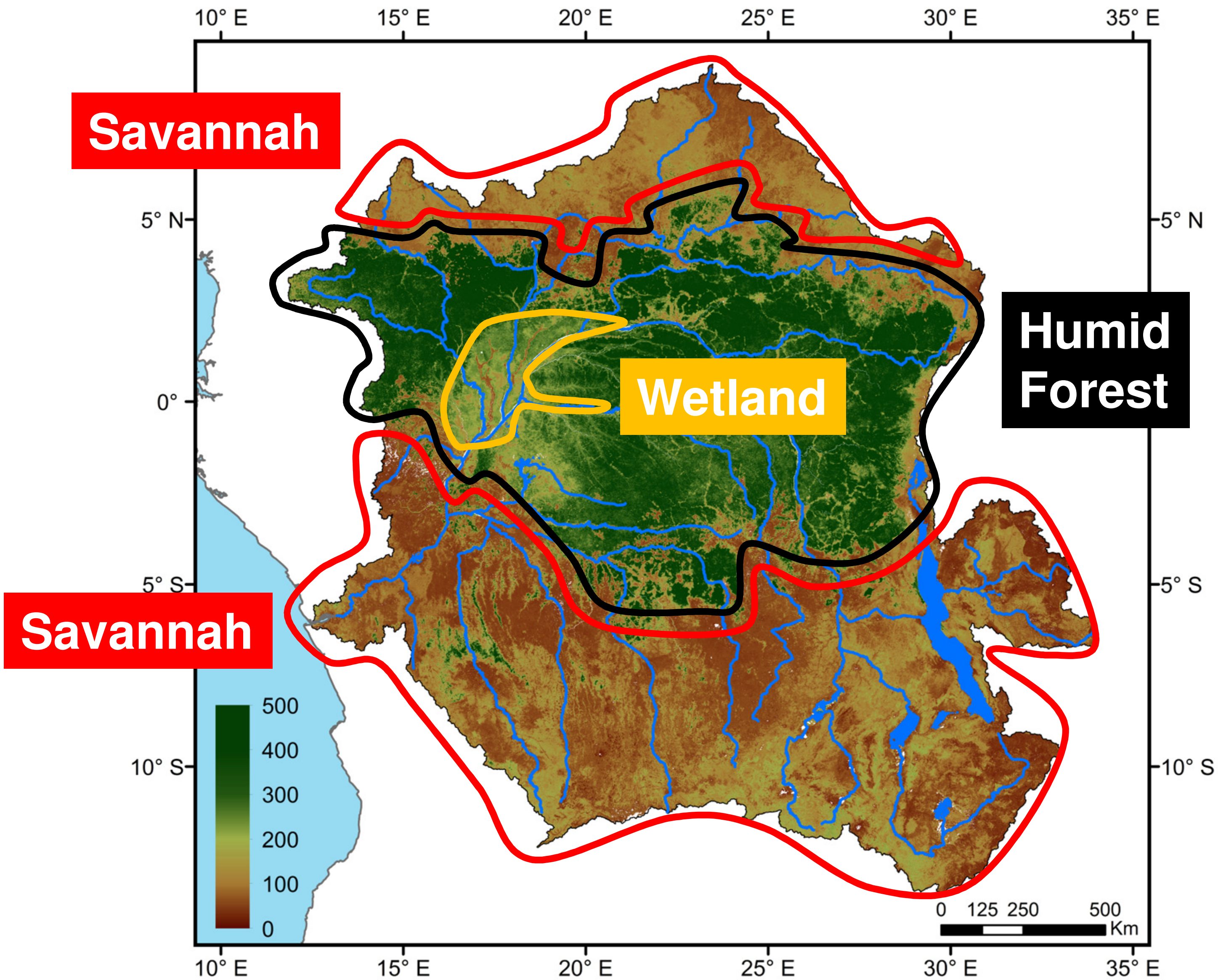

Aboveground live woody biomass (Mg ha^{-1})

WHRC


Wetland
= flooded forest
(Tributary)


Wetland
= floating macrophytes
(Tributary)


Wetland
= floating macrophytes
(Congo mainstem)

Congo

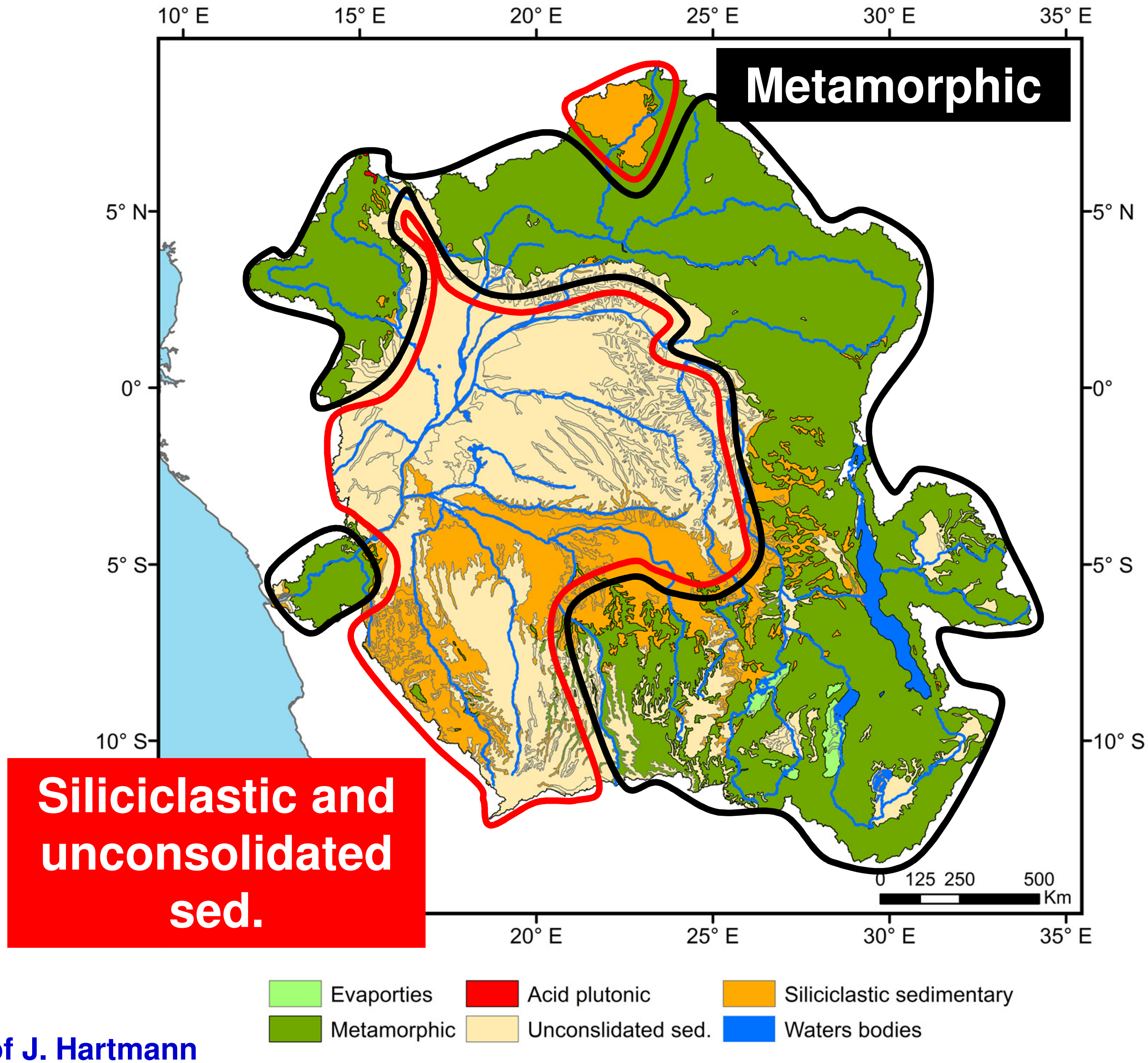

Courtesy of J. Hartmann

Congo

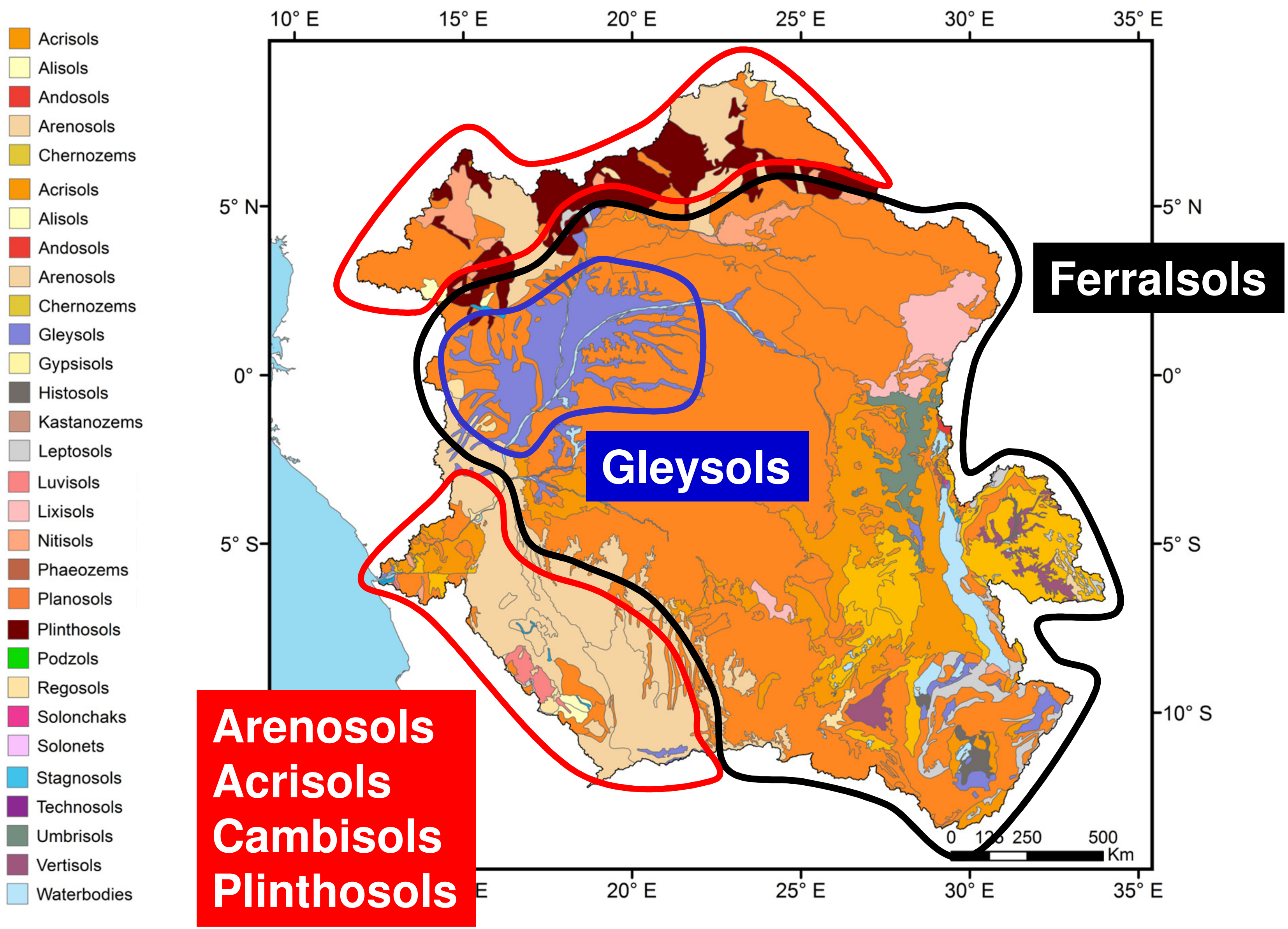

Acrisols
Alisols
Andosols
Arenosols
Chernozems
Acrisols
Alisols
Andosols
Arenosols
Chernozems
Gleysols
Gypsisols
Histosols
Kastanozems
Leptosols
Luvisols
Lixisols
Nitisols
Phaeozems
Planosols
Plinthosols
Podzols
Regosols
Solonchaks
Solonets
Stagnosols
Technosols
Umbrisols
Vertisols
Waterbodies
10° E
15° E
20° E
25° E
30° E
35° E
5° N
0°
5° S
10° S
Ferralsols
Gleysols
Arenosols
Acrisols
Cambisols
Plinthosols
0 125 250 500
Km

Congo

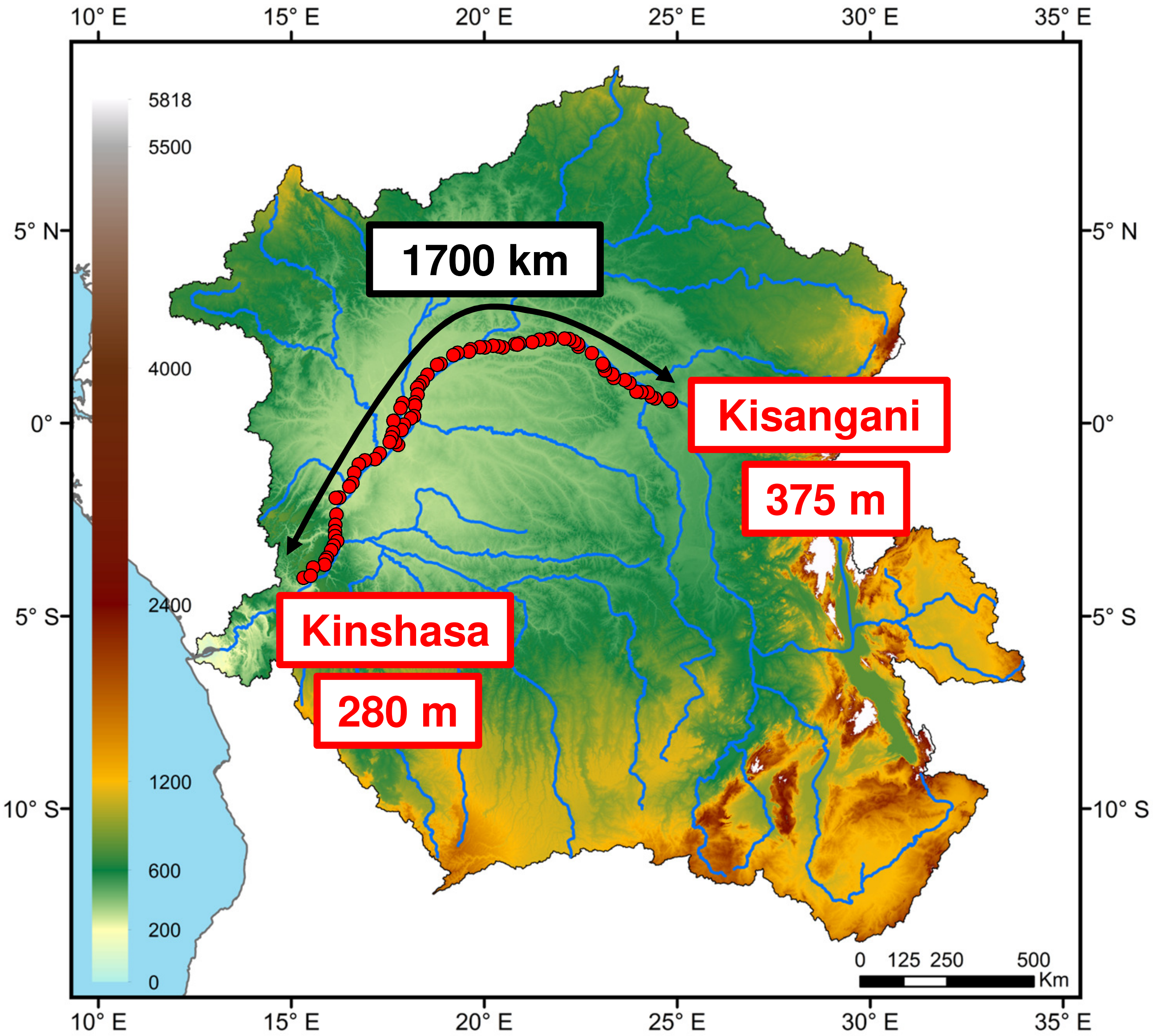

10° E
15° E
20° E
25° E
30° E
35° E
5° N
0°
5° S
10° S
5818
5500
4000
2400
1200
600
200
0
1700 km
Kisangani
375 m
Kinshasa
280 m
0 125 250 500
Km

Cruises & Methods

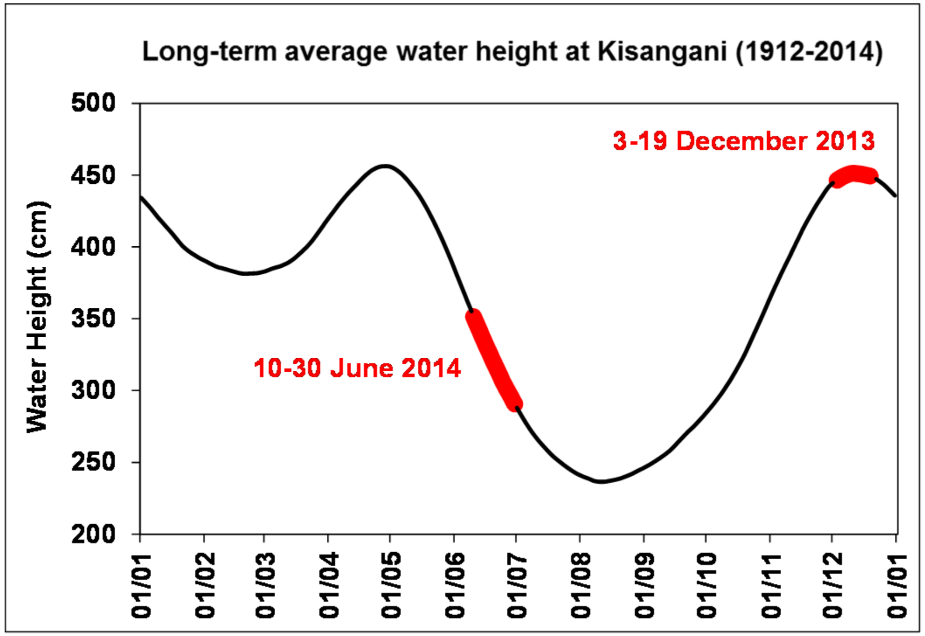

164 stations
29 variables

> 23,000 continuous measurements
pCO_2, cond, temp, pH, O_2, TSM, cDOM

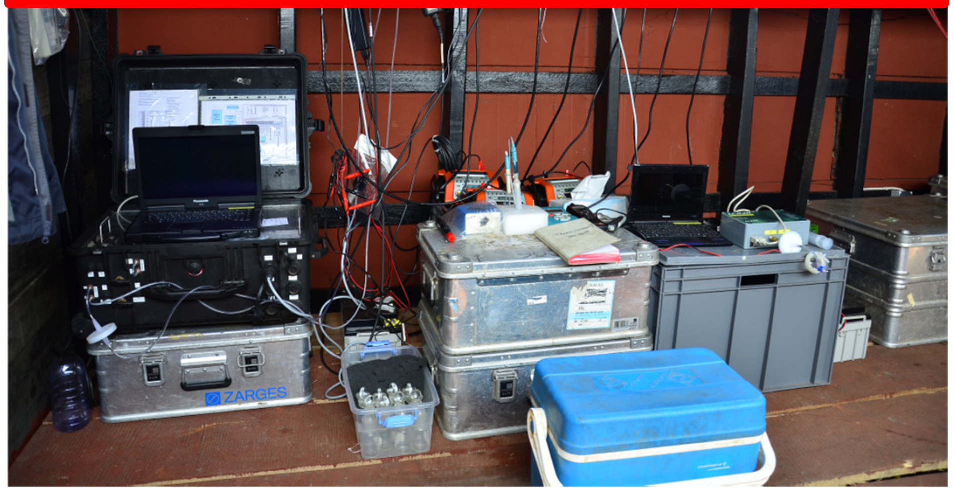

Results

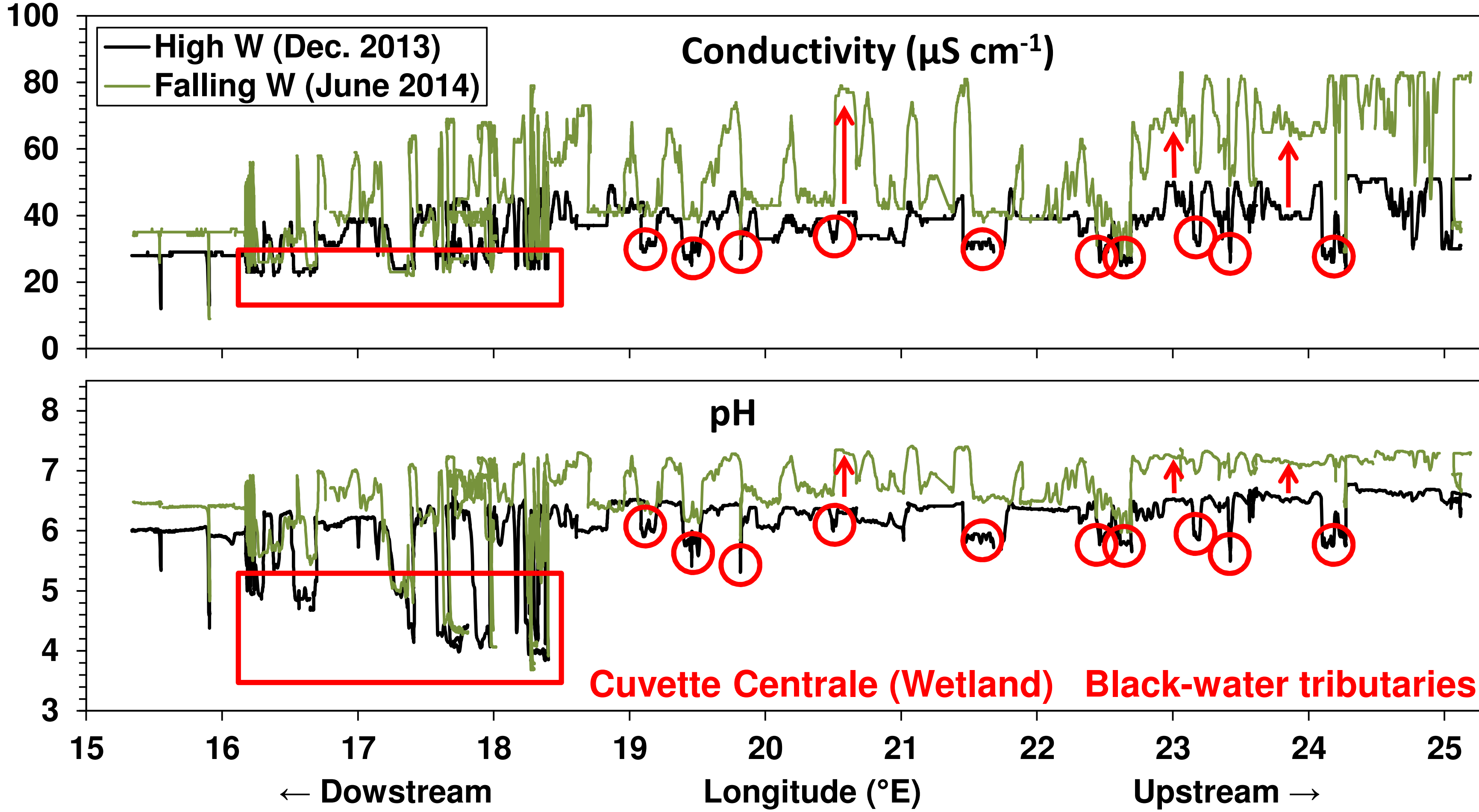

100
80
60
40
20
0
High W (Dec. 2013)
Falling W (June 2014)
Conductivity (µS cm-1)
8
7
6
5
4
3
pH
Cuvette Centrale (Wetland)
Black-water tributaries
15
16
17
18
19
20
21
22
23
24
25
← Dowstream
Longitude (°E)
Upstream →

Results

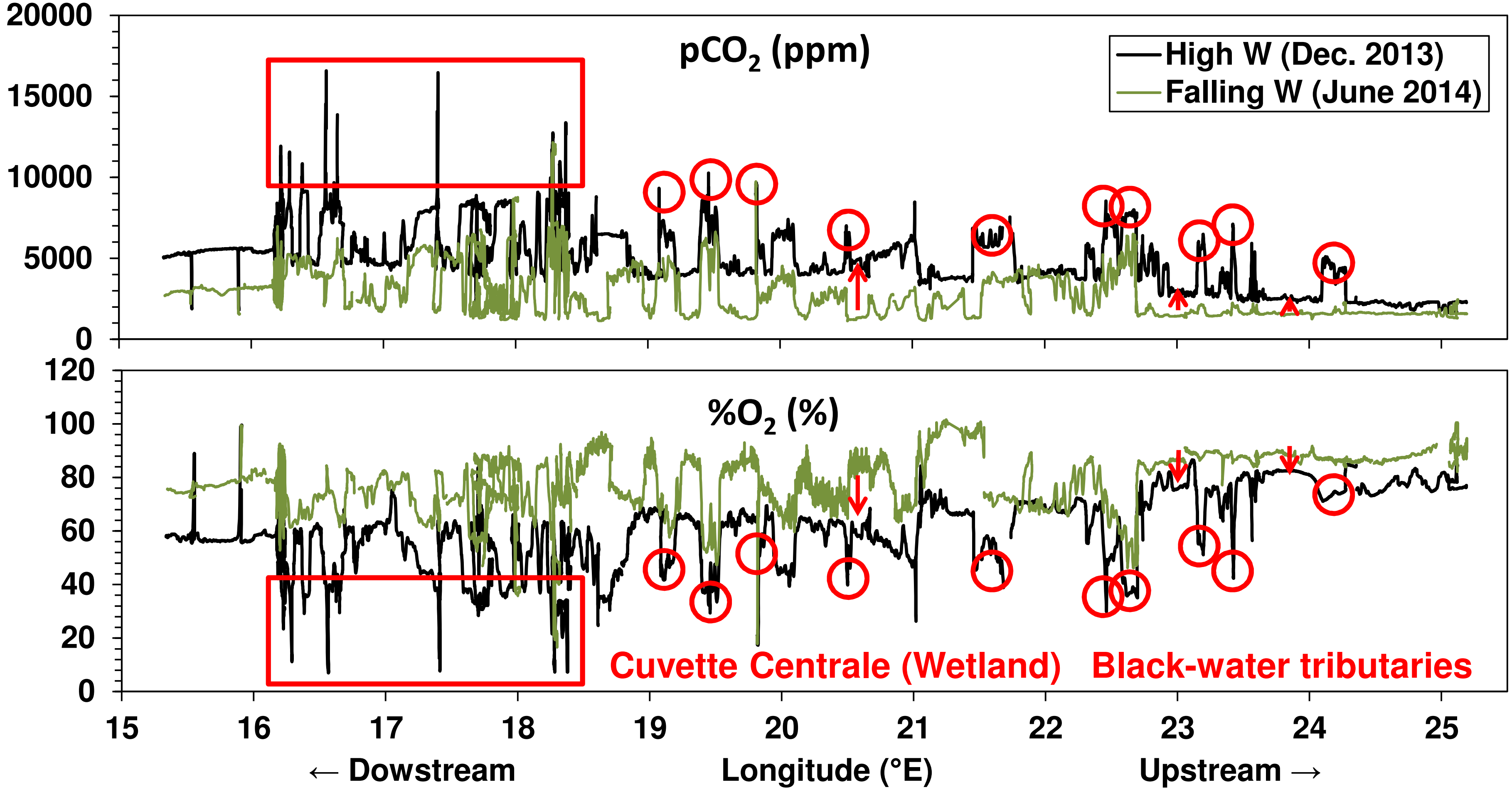

20000
15000
10000
5000
0
pCO$_2$ (ppm)
High W (Dec. 2013)
Falling W (June 2014)
120
100
80
60
40
20
0
%O$_2$ (%)
Cuvette Centrale (Wetland)
Black-water tributaries
15
16
17
18
19
20
21
22
23
24
25
← Dowstream
Longitude (°E)
Upstream →

Results

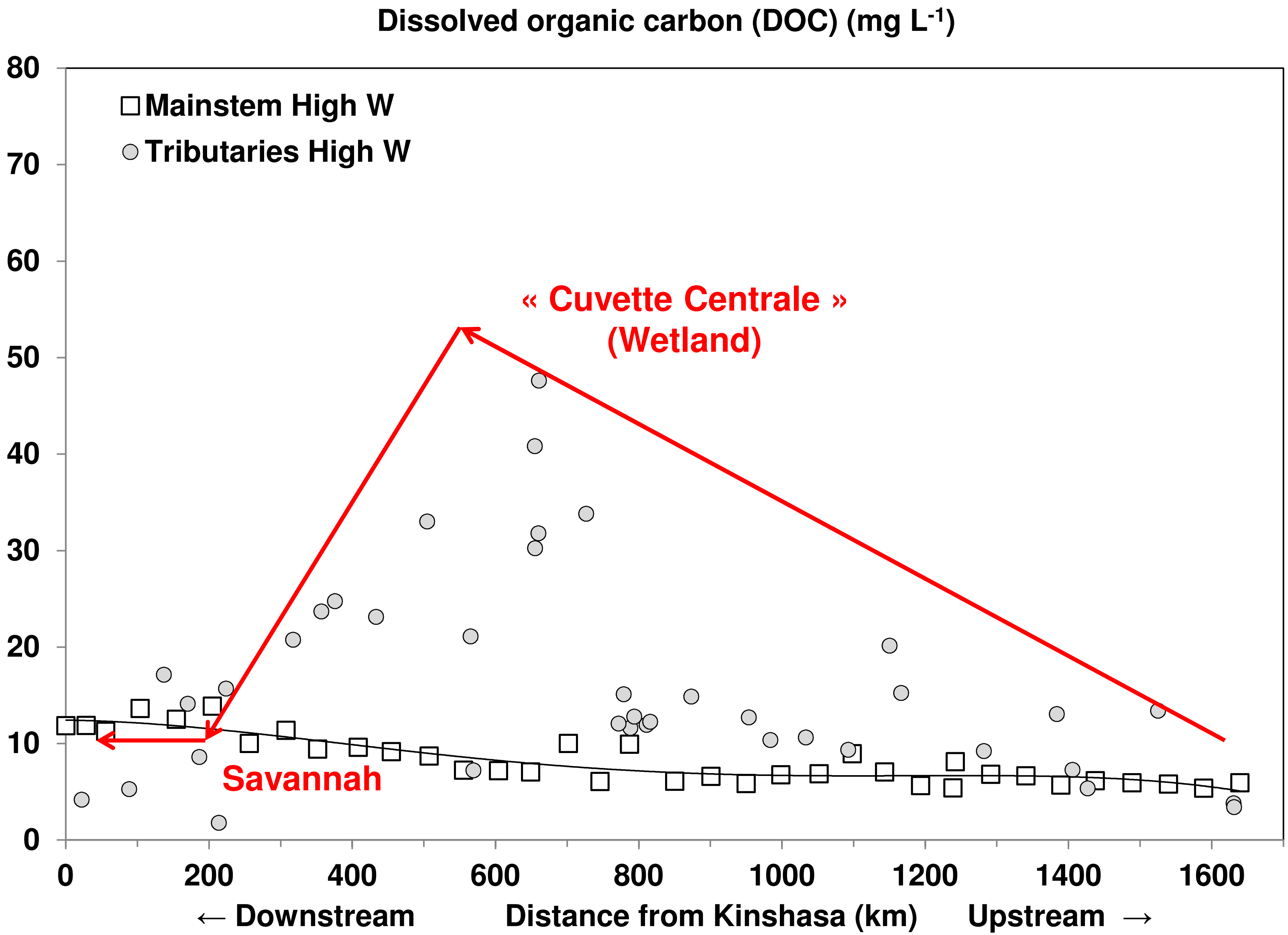

Dissolved organic carbon (DOC) (mg L-1)
Mainstem High W
Tributaries High W
« Cuvette Centrale »
(Wetland)
Savannah
80
70
60
50
40
30
20
10
0
0
200
400
600
800
1000
1200
1400
1600
← Downstream
Distance from Kinshasa (km)
Upstream →

Results

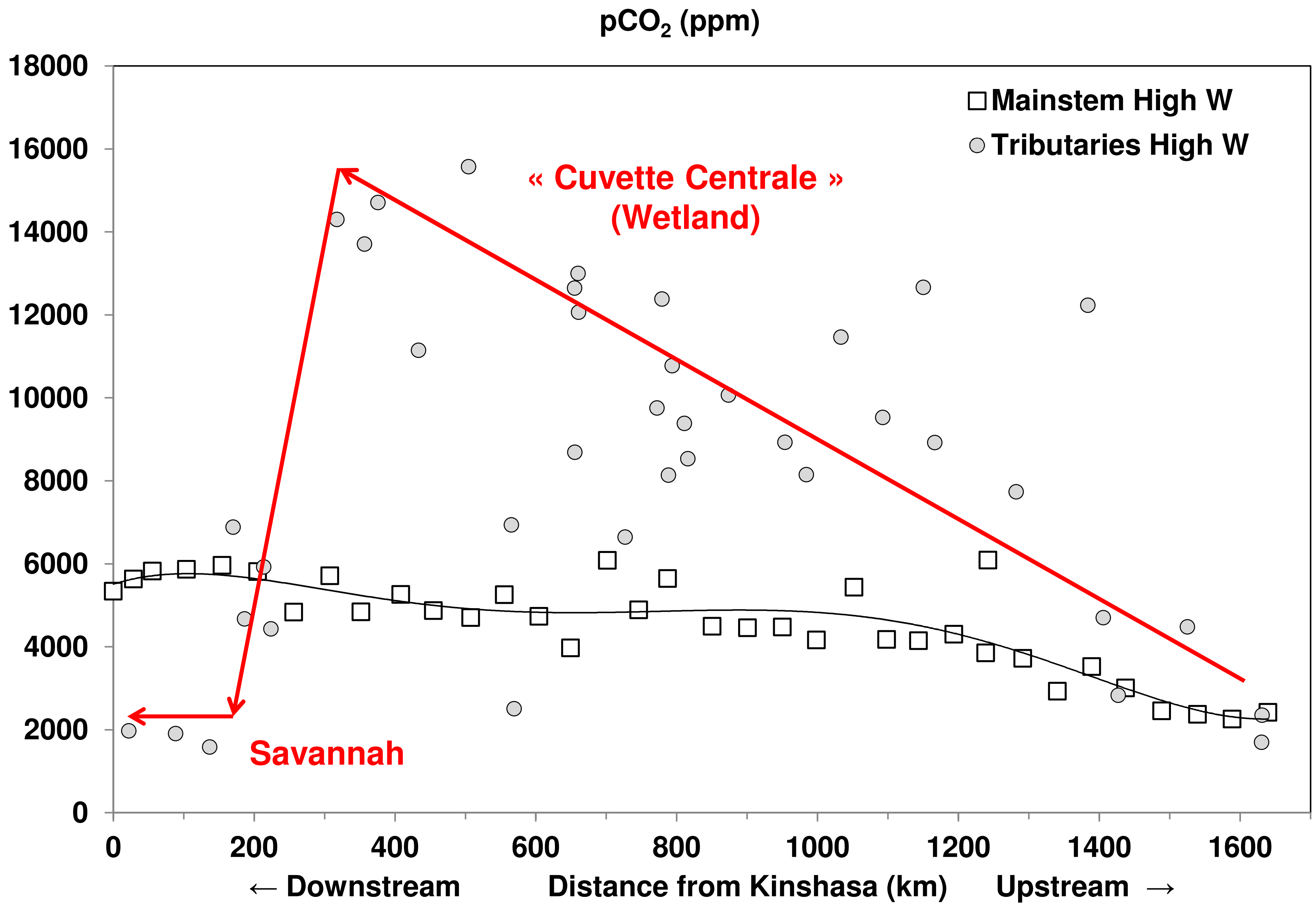

pCO2 (ppm)
18000
16000
14000
12000
10000
8000
6000
4000
2000
0
Mainstem High W
Tributaries High W
« Cuvette Centrale »
(Wetland)
Savannah
0
200
400
600
800
1000
1200
1400
1600
← Downstream
Distance from Kinshasa (km)
Upstream →

Results

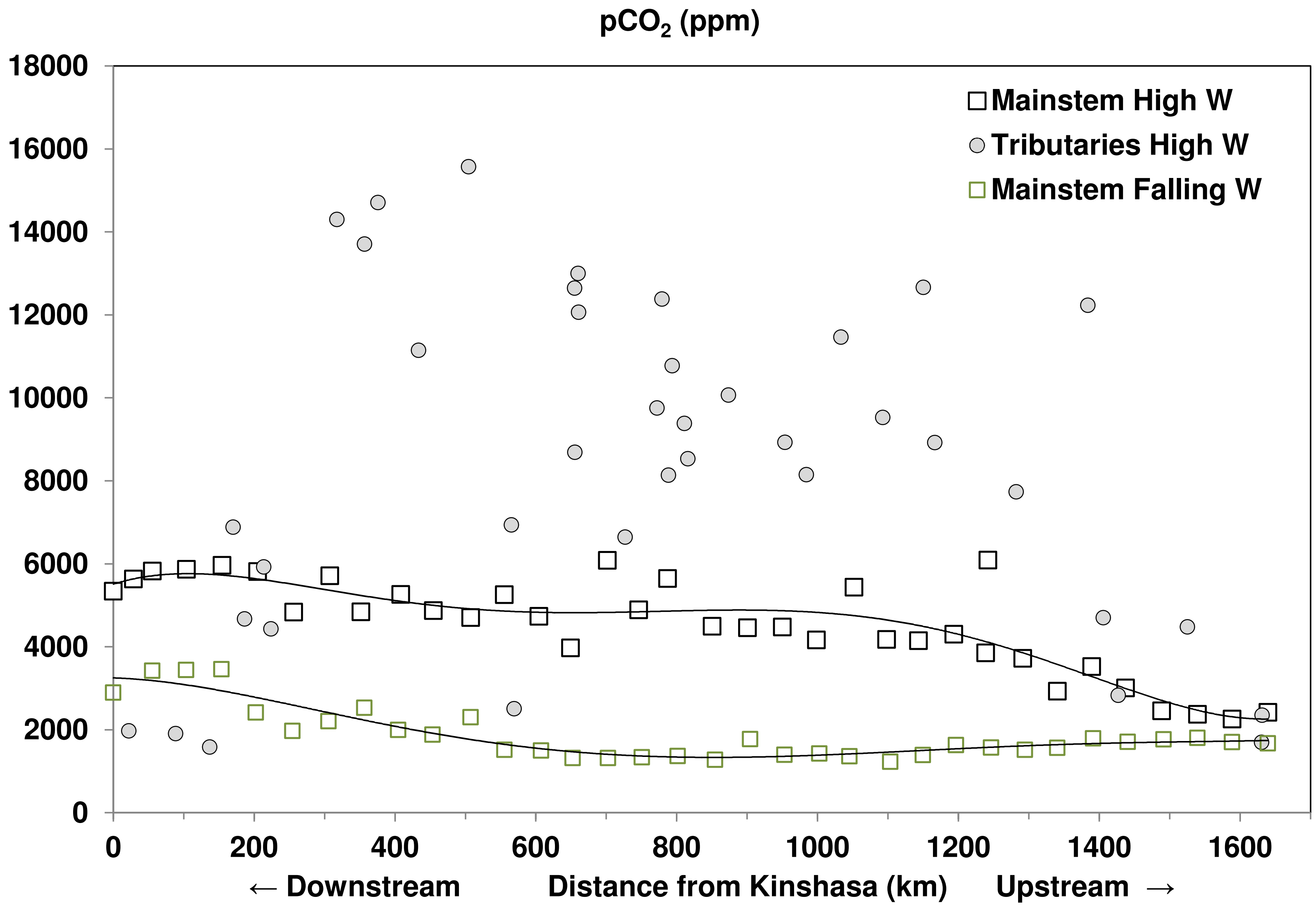

pCO2 (ppm)
18000
16000
14000
12000
10000
8000
6000
4000
2000
0
0
200
400
600
800
1000
1200
1400
1600
← Downstream
Distance from Kinshasa (km)
Upstream →
Mainstem High W
Tributaries High W
Mainstem Falling W

Results

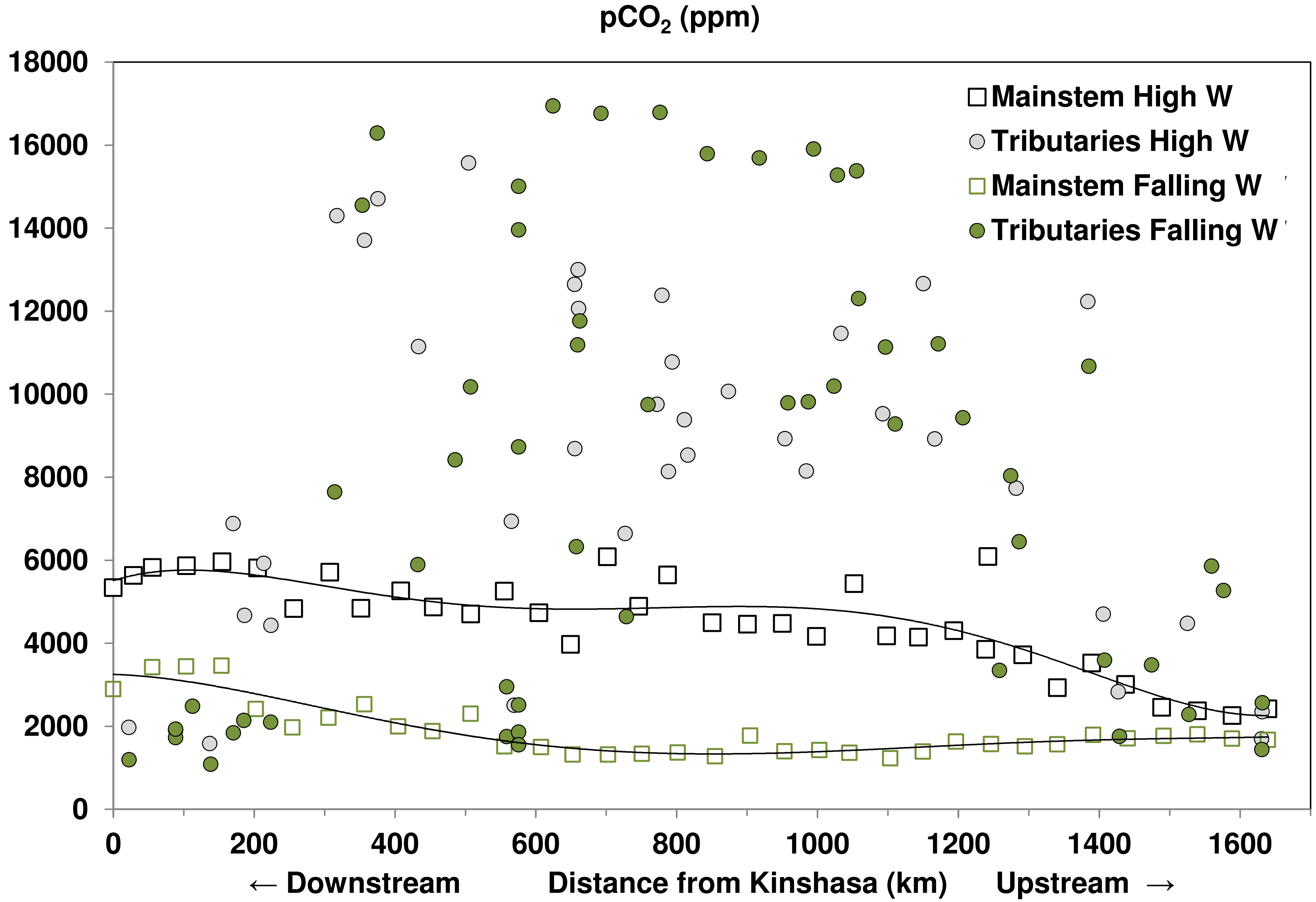

pCO2 (ppm)
18000
16000
14000
12000
10000
8000
6000
4000
2000
0
Mainstem High W
Tributaries High W
Mainstem Falling W
Tributaries Falling W
0
200
400
600
800
1000
1200
1400
1600
← Downstream
Distance from Kinshasa (km)
Upstream →

Results

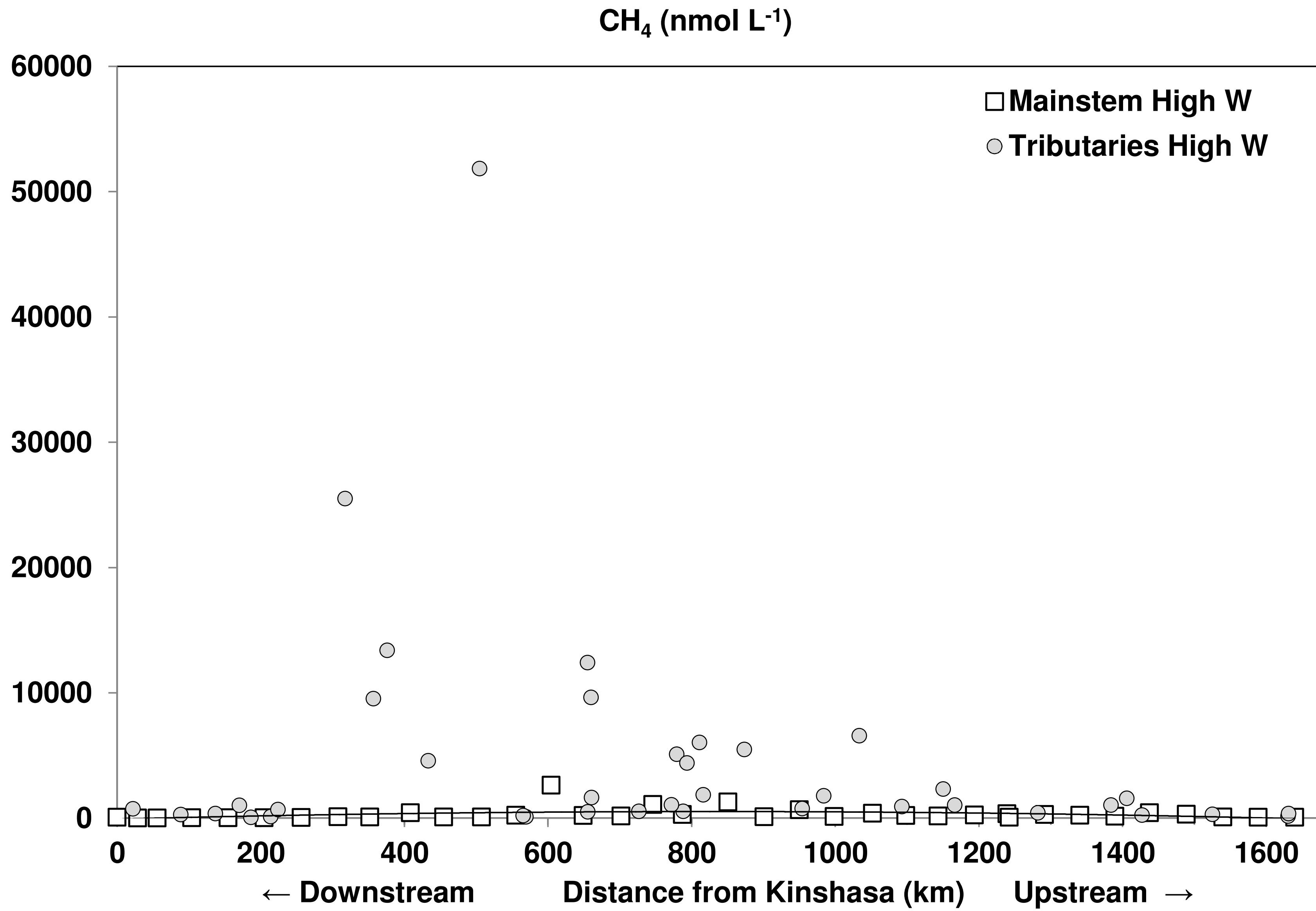

CH4 (nmol L-1)
60000
50000
40000
30000
20000
10000
0
Mainstem High W
Tributaries High W
0
200
400
600
800
1000
1200
1400
1600
← Downstream
Distance from Kinshasa (km)
Upstream →

Results

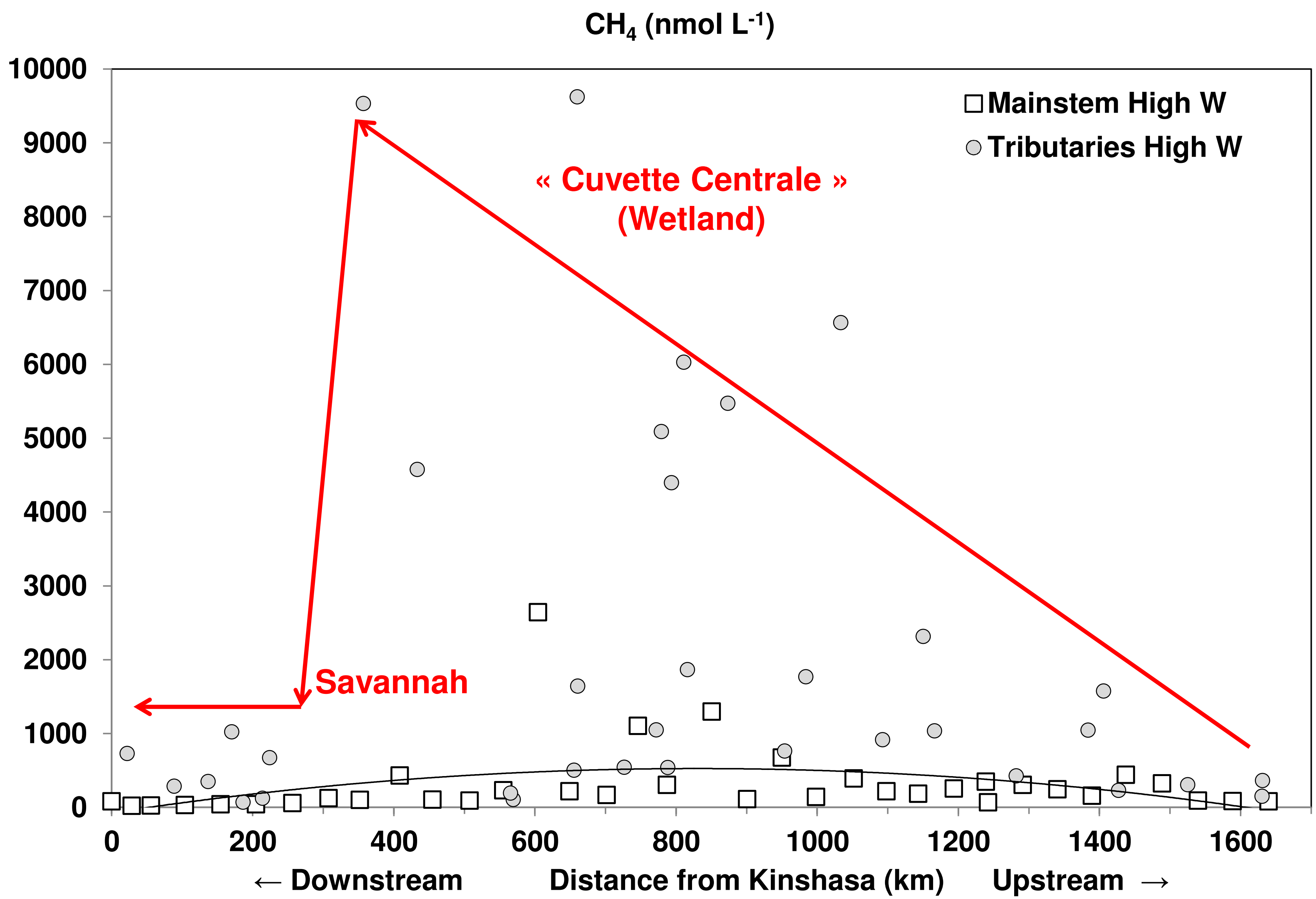

CH4 (nmol L-1)
10000
9000
8000
7000
6000
5000
4000
3000
2000
1000
0
0
200
400
600
800
1000
1200
1400
1600
← Downstream
Distance from Kinshasa (km)
Upstream →
Mainstem High W
Tributaries High W
« Cuvette Centrale »
(Wetland)
Savannah

Results

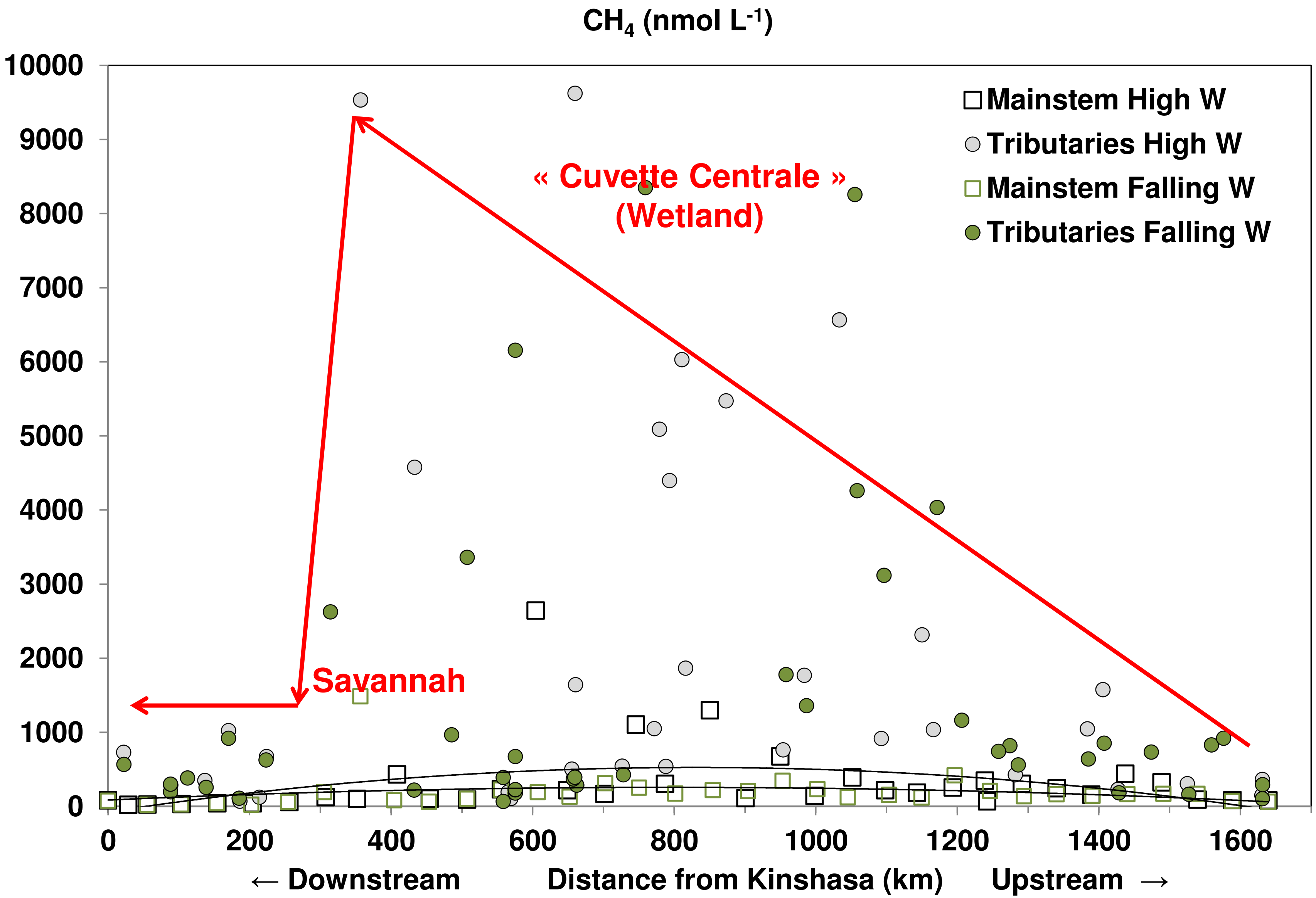

CH_4 (nmol L^{-1})
10000
9000
8000
7000
6000
5000
4000
3000
2000
1000
0
0
200
400
600
800
1000
1200
1400
1600
← Downstream
Distance from Kinshasa (km)
Upstream →
Mainstem High W
Tributaries High W
Mainstem Falling W
Tributaries Falling W
« Cuvette Centrale »
(Wetland)
Savannah

Results

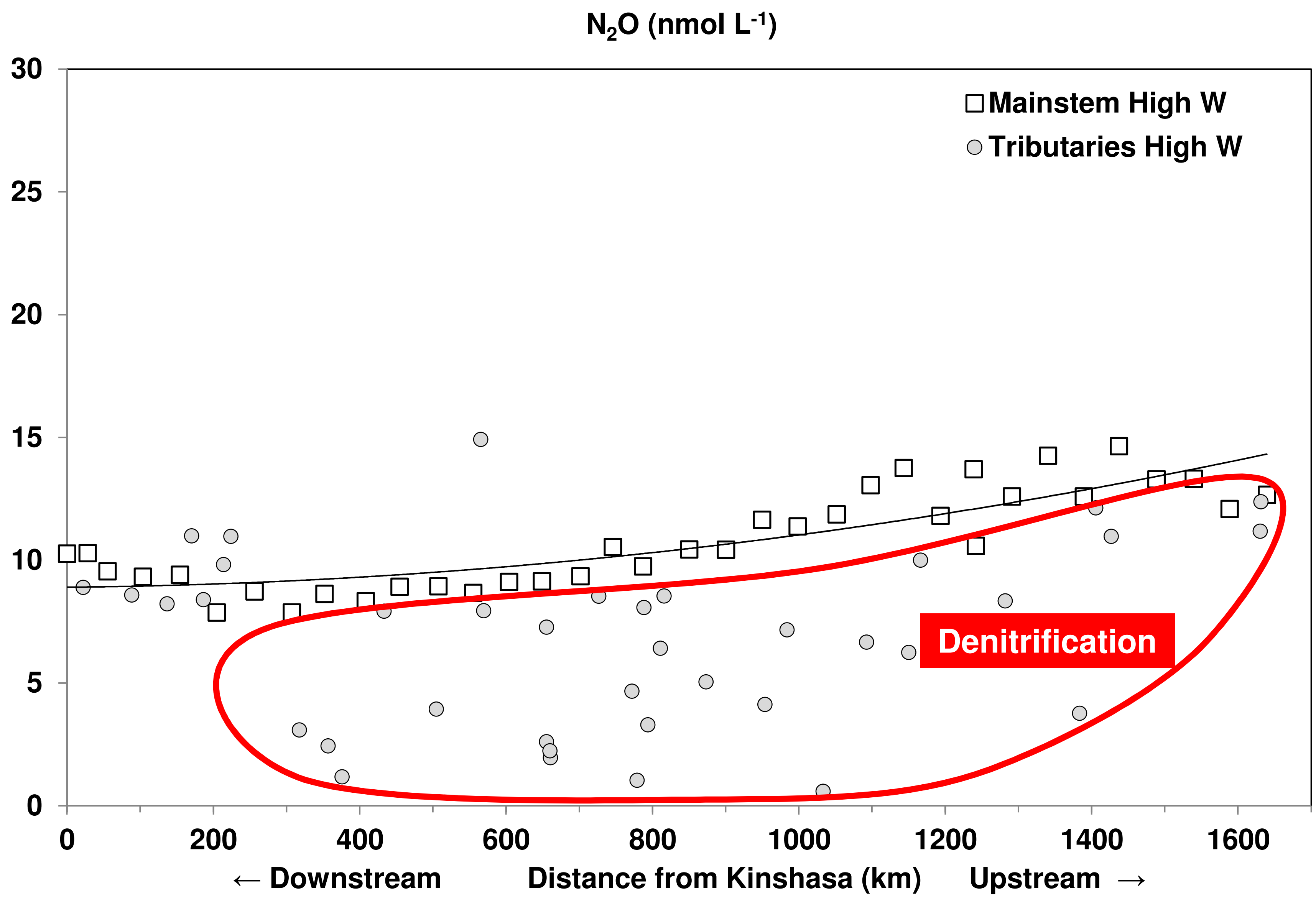

N2O (nmol L-1)
30
25
20
15
10
5
0
Mainstem High W
Tributaries High W
Denitrification
0
200
400
600
800
1000
1200
1400
1600
← Downstream
Distance from Kinshasa (km)
Upstream →

Results

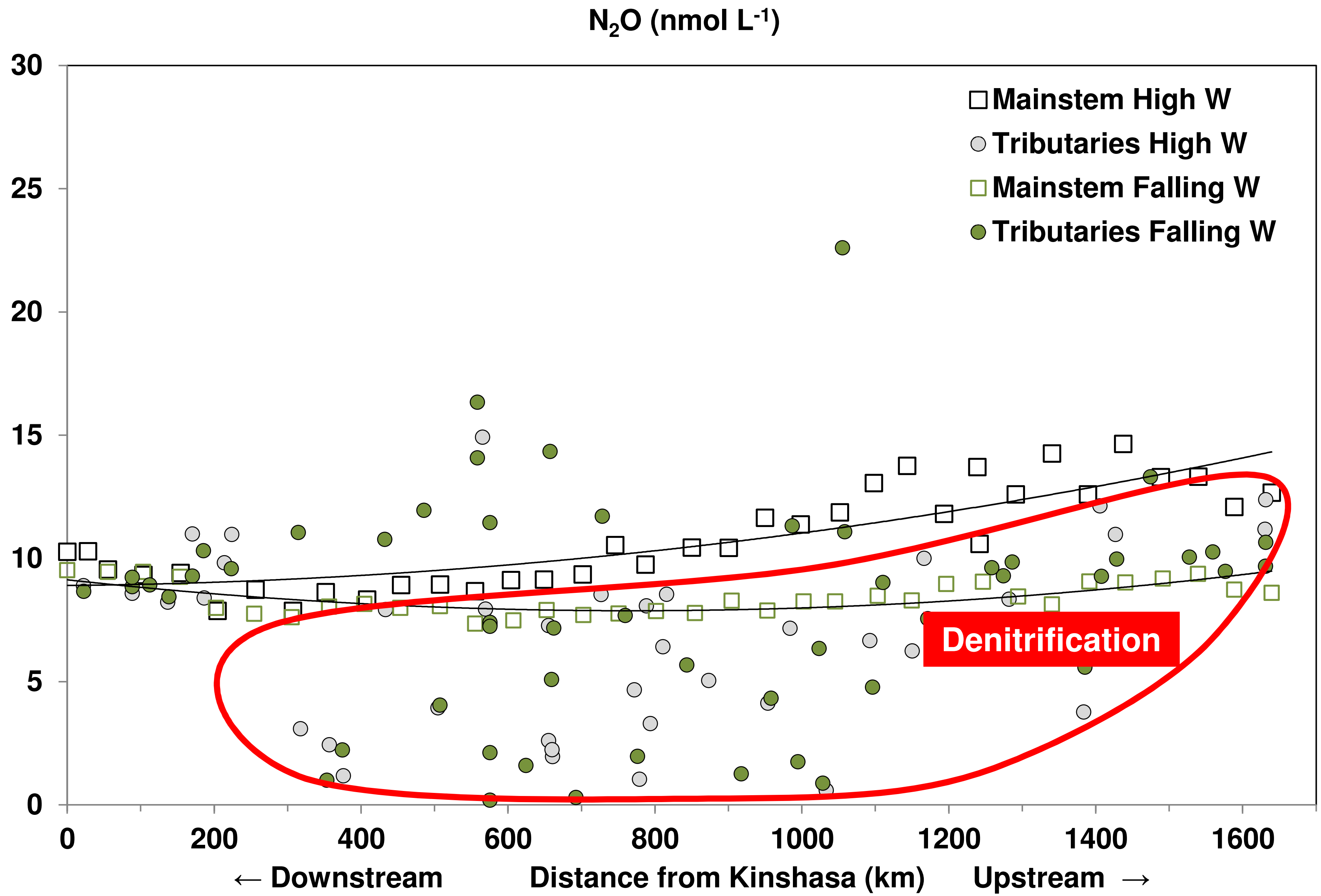

N2O (nmol L-1)
30
25
20
15
10
5
0
Mainstem High W
Tributaries High W
Mainstem Falling W
Tributaries Falling W
Denitrification
0
200
400
600
800
1000
1200
1400
1600
← Downstream
Distance from Kinshasa (km)
Upstream →

Results

All streams/rivers vs catchement characteristics

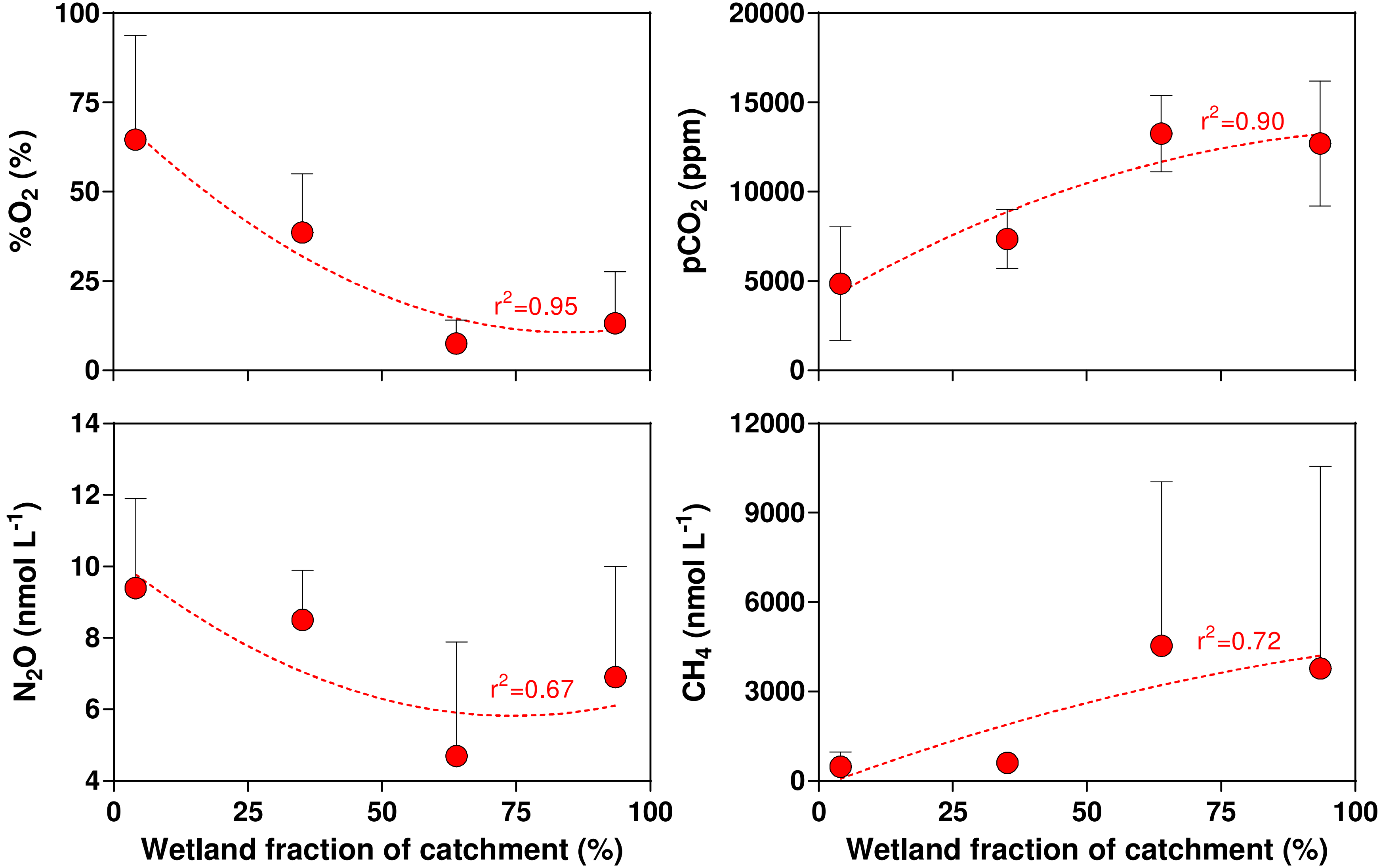

Results

Congo & other African rivers

Results

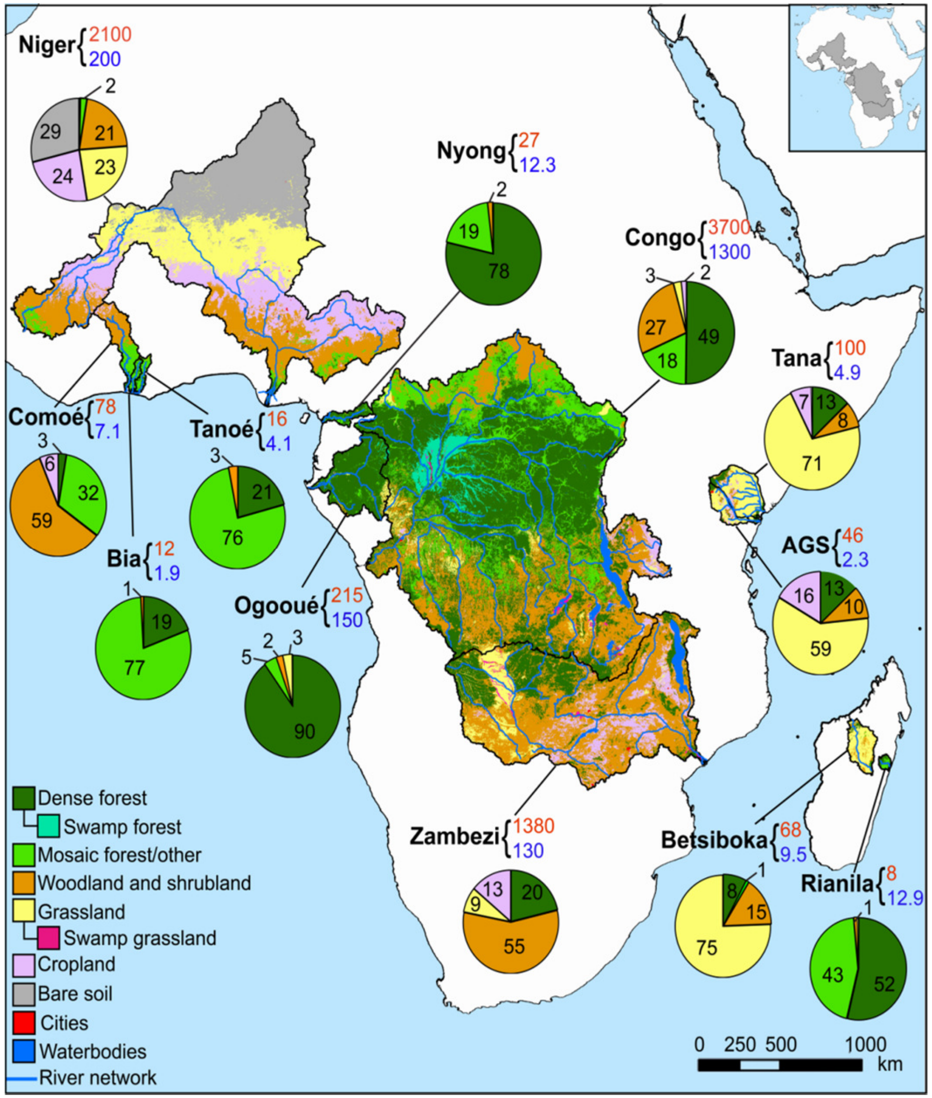
Niger 2100 200
Nyong 27 12.3
Congo 3700 1300
Tana 100 4.9
Comoé 78 7.1
Tanoé 16 4.1
Bia 12 1.9
Ogooué 215 150
AGS 46 2.3
Zambezi 1380 130
Betsiboka 68 9.5
Rianila 8 12.9
Dense forest
Swamp forest
Mosaic forest/other
Woodland and shrubland
Grassland
Swamp grassland
Cropland
Bare soil
Cities
Waterbodies
River network
0 250 500 1000 km

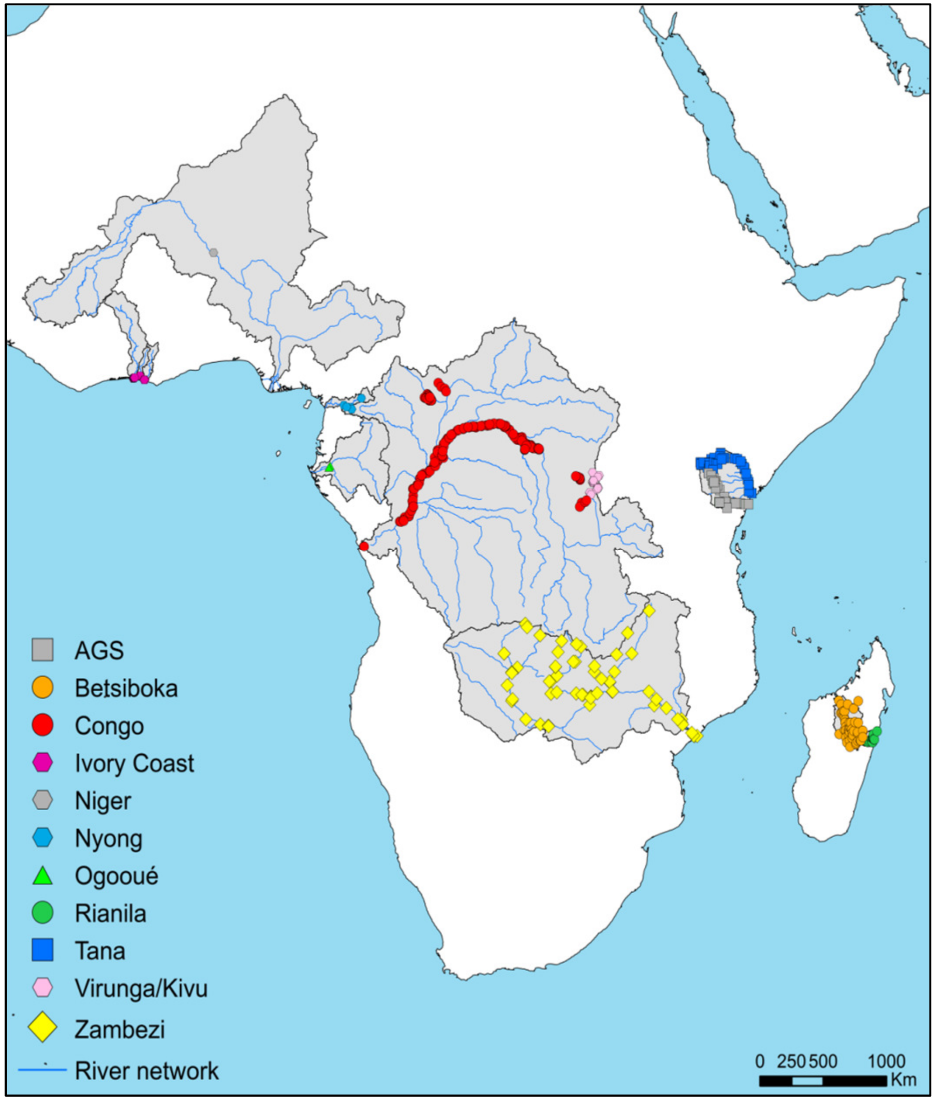
AGS
Betsiboka
Congo
Ivory Coast
Niger
Nyong
Ogooué
Rianila
Tana
Virunga/Kivu
Zambezi
River network
0 250 500 1000 Km

Results

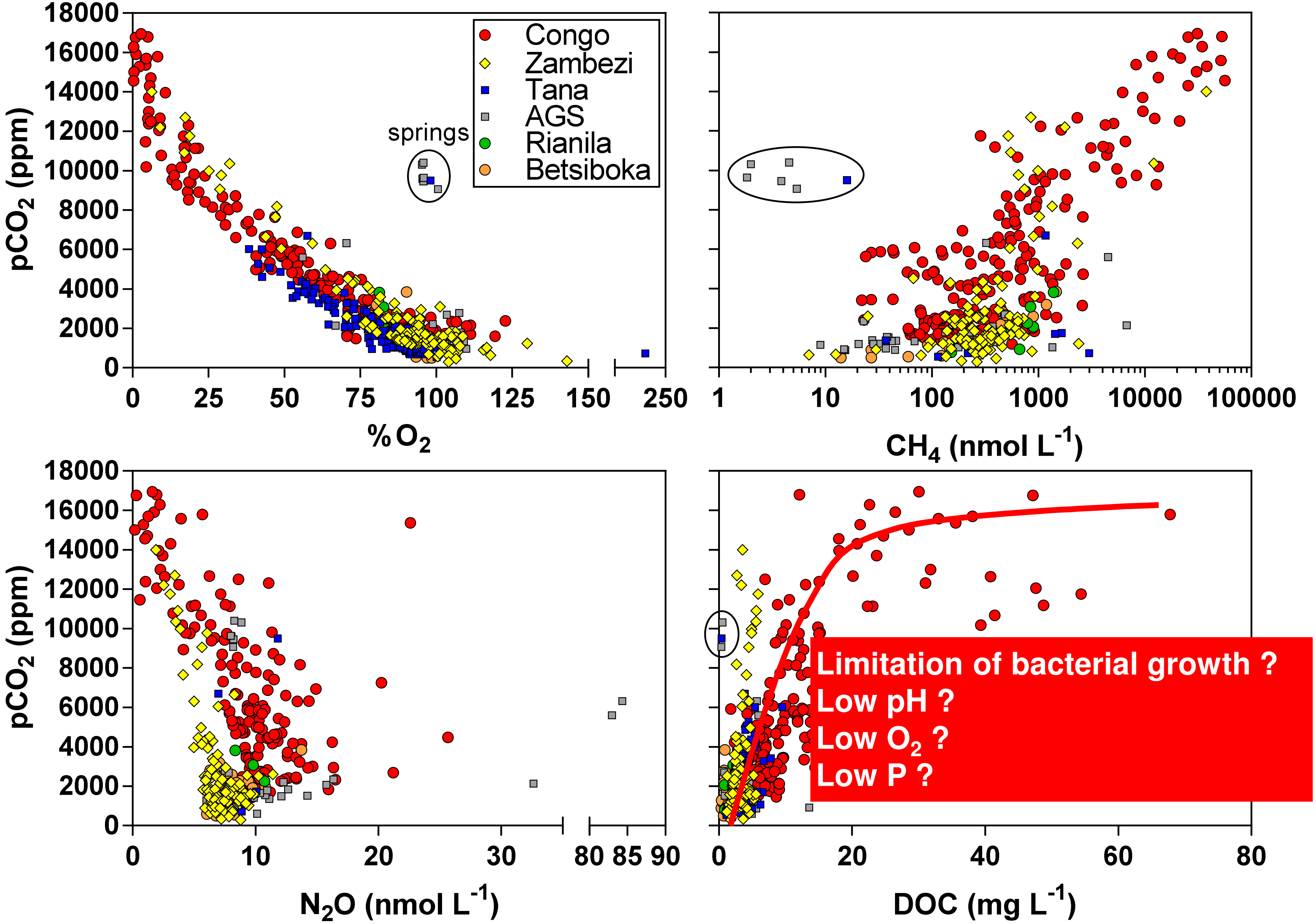

pCO2 (ppm)
% O2
CH4 (nmol L-1)
N2O (nmol L-1)
DOC (mg L-1)
springs
Congo
Zambezi
Tana
AGS
Rianila
Betsiboka
Limitation of bacterial growth ?
Low pH ?
Low O2 ?
Low P ?

Results

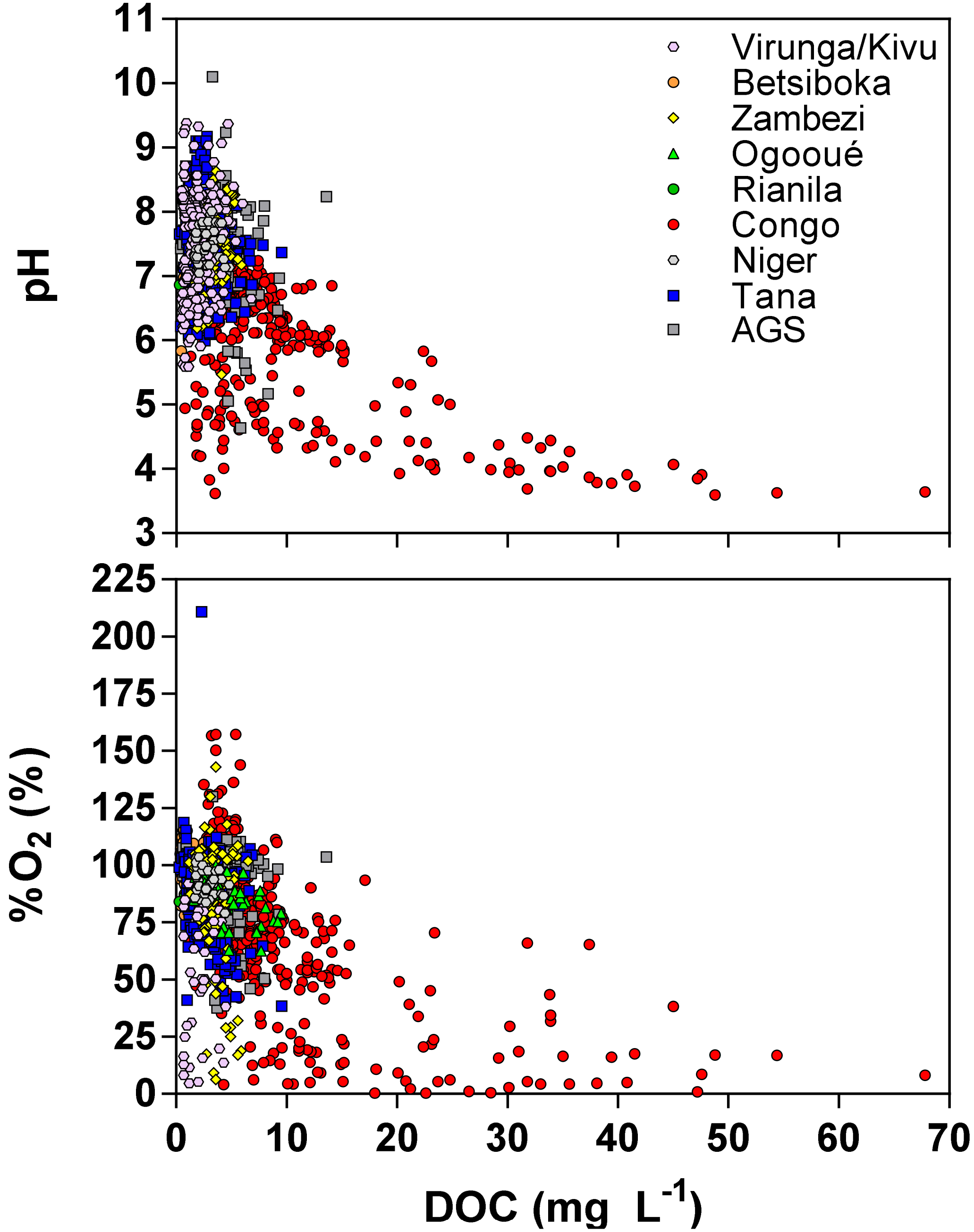

Virunga/Kivu
Betsiboka
Zambezi
Ogooué
Rianila
Congo
Niger
Tana
AGS
pH
11
10
9
8
7
6
5
4
3
%O2 (%)
225
200
175
150
125
100
75
50
25
0
0
10
20
30
40
50
60
70
DOC (mg L-1)

Results

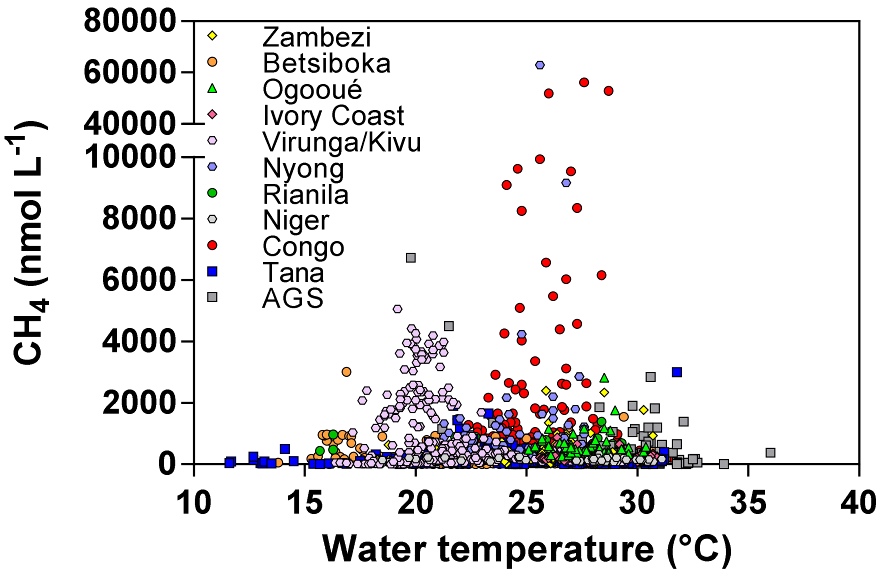
CH4 (nmol L-1)
80000
60000
40000
10000
8000
6000
4000
2000
0
10
15
20
25
30
35
40
Water temperature (°C)
Zambezi
Betsiboka
Ogooué
Ivory Coast
Virunga/Kivu
Nyong
Rianila
Niger
Congo
Tana
AGS

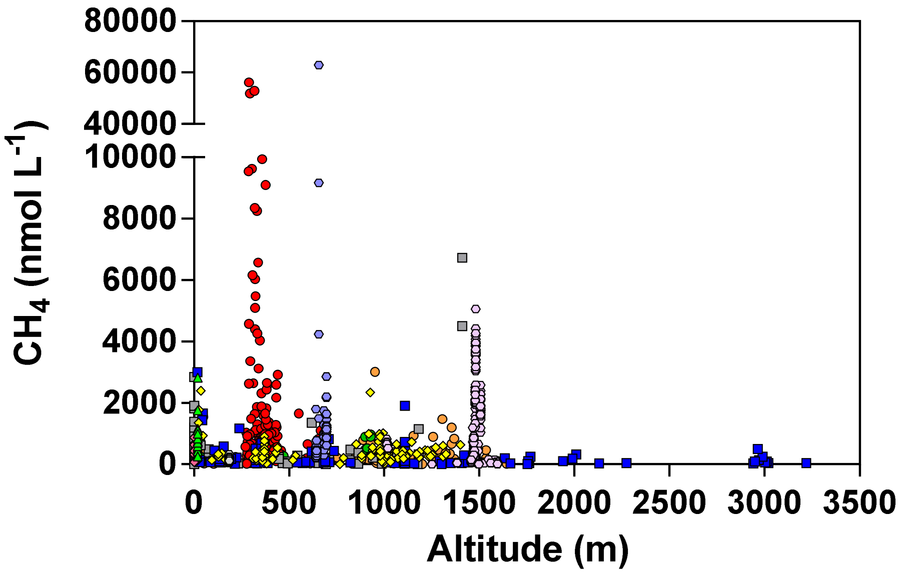
CH4 (nmol L-1)
80000
60000
40000
10000
8000
6000
4000
2000
0
0
500
1000
1500
2000
2500
3000
3500
Altitude (m)

Results

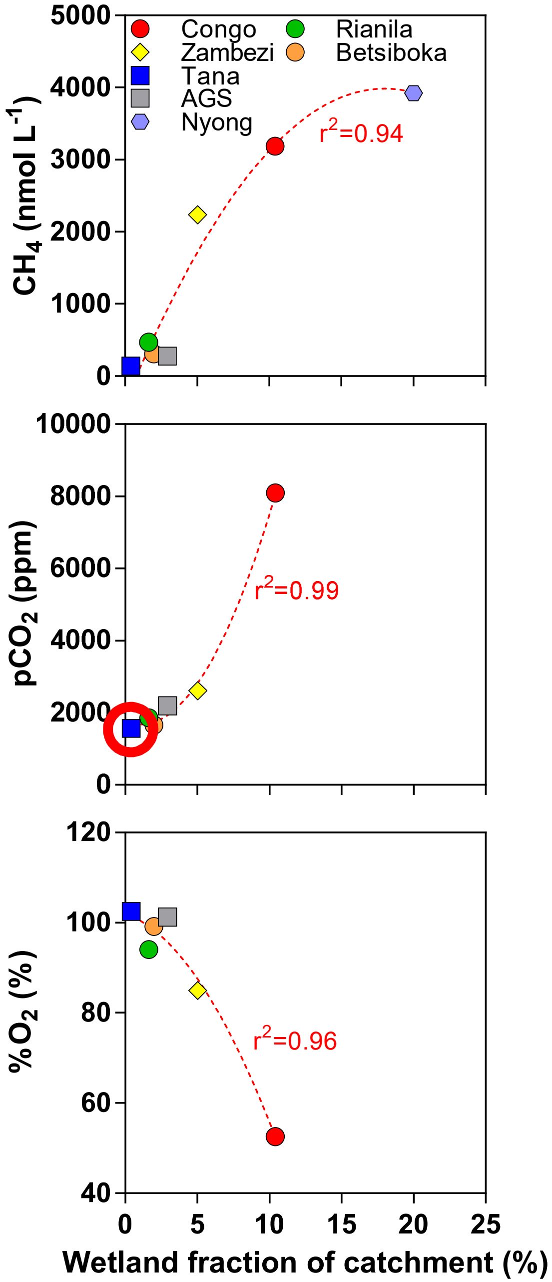

Congo
Zambezi
Tana
AGS
Nyong
Rianila
Betsiboka
r^2=0.94
CH_4 (nmol L^{-1})
5000
4000
3000
2000
1000
0
10000
8000
6000
4000
2000
0
pCO2 (ppm)
r^2=0.99
120
100
80
60
40
$\%O_2$ (%)
r^2=0.96
0
5
10
15
20
25
Wetland fraction of catchment (%)

Results

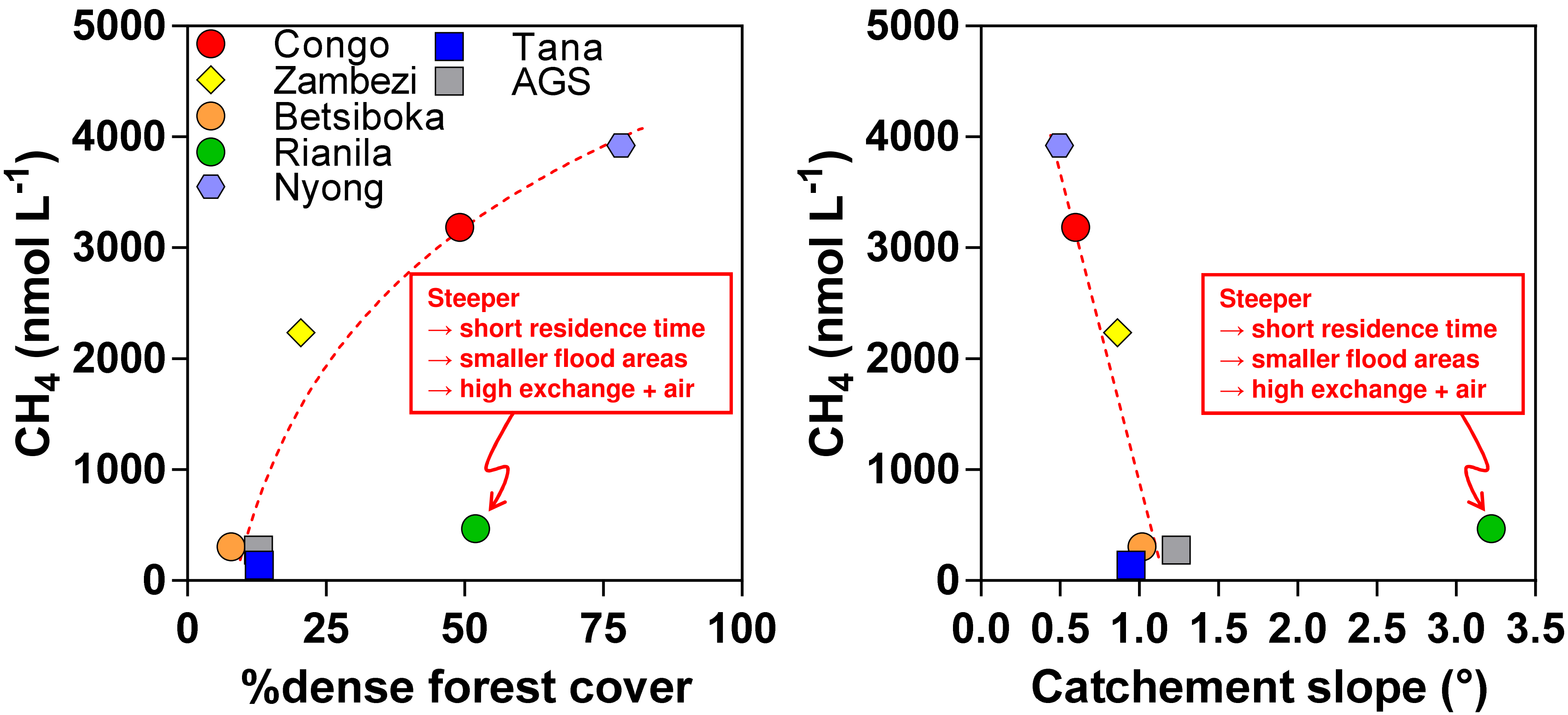
5000
4000
3000
2000
1000
0
CH4 (nmol L-1)
Congo
Zambezi
Betsiboka
Rianila
Nyong
Tana
AGS
Steeper
→ short residence time
→ smaller flood areas
→ high exchange + air
0
25
50
75
100
%dense forest cover
0.0
0.5
1.0
1.5
2.0
2.5
3.0
3.5
Catchement slope (°)

Results

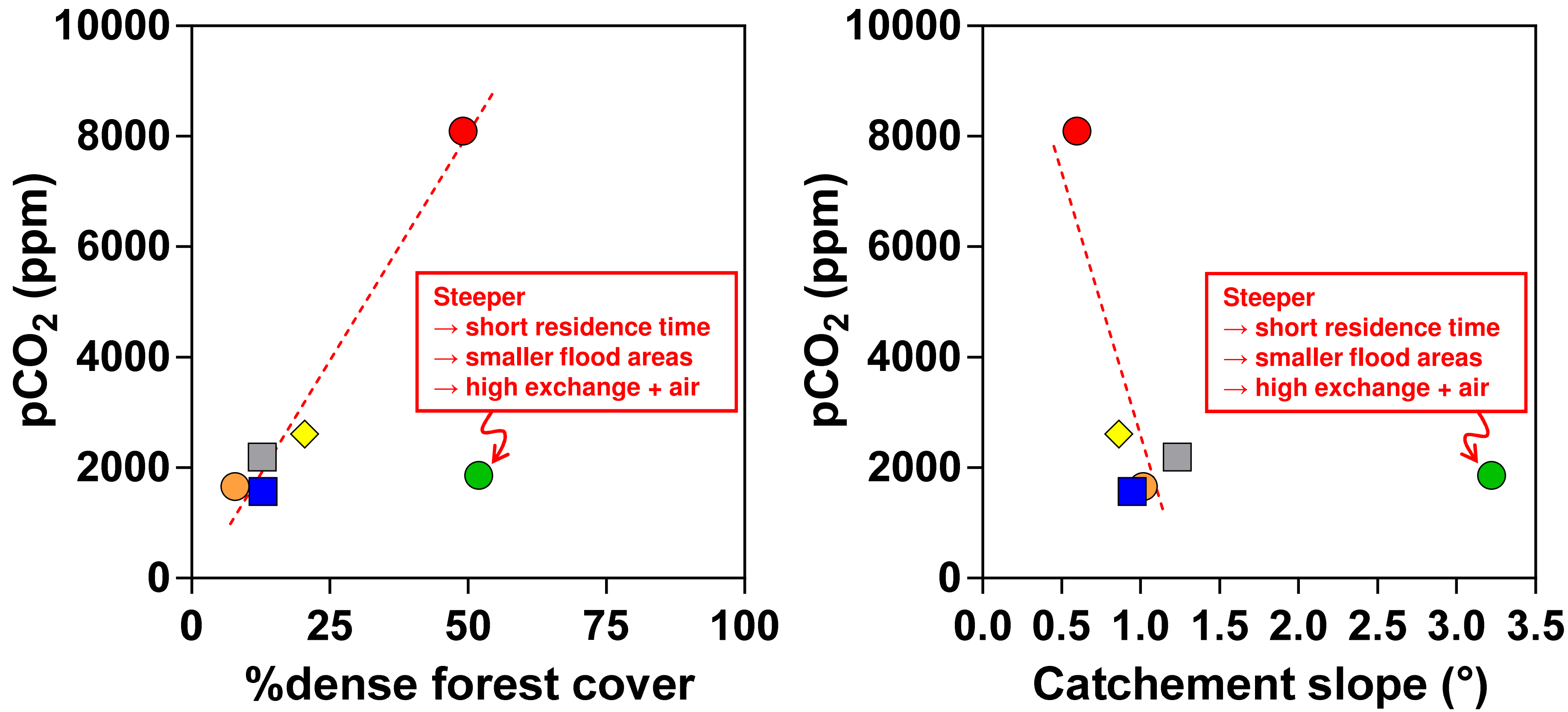
10000
8000
6000
4000
2000
0
pCO2 (ppm)
0
25
50
75
100
%dense forest cover
Steeper
→ short residence time
→ smaller flood areas
→ high exchange + air
10000
8000
6000
4000
2000
0
pCO2 (ppm)
0.0
0.5
1.0
1.5
2.0
2.5
3.0
3.5
Catchement slope (°)
Steeper
→ short residence time
→ smaller flood areas
→ high exchange + air

Results

Congo versus Amazon

Results

	Amazon		Congo
Catchment area (km^2)	6,025,735	>	3,705,222
Slope (°)	1.4		0.6
Discharge ($km^3\ yr^{-1}$)	5,444		1,270
Specific discharge ($L\ s^{-1}\ km^{-2}$)	29	>	11
Precipitation (mm)	2,147	>	1,527
Air temperature (°C)	24.6		23.7
River-stream surface area (km^2)	74,904		26,517
Wetland surface area (%)	14		10
Above ground biomass ($Mg\ km^{-2}$)	909	>	748
Land cover			
Dense Forest (%)	83	>	49
Mosaic Forest (%)	4		18
Woodland and shrubland (%)	4	<	27
Grassland (%)	5		3
Cropland/Bare soil (%)	4		2

Results

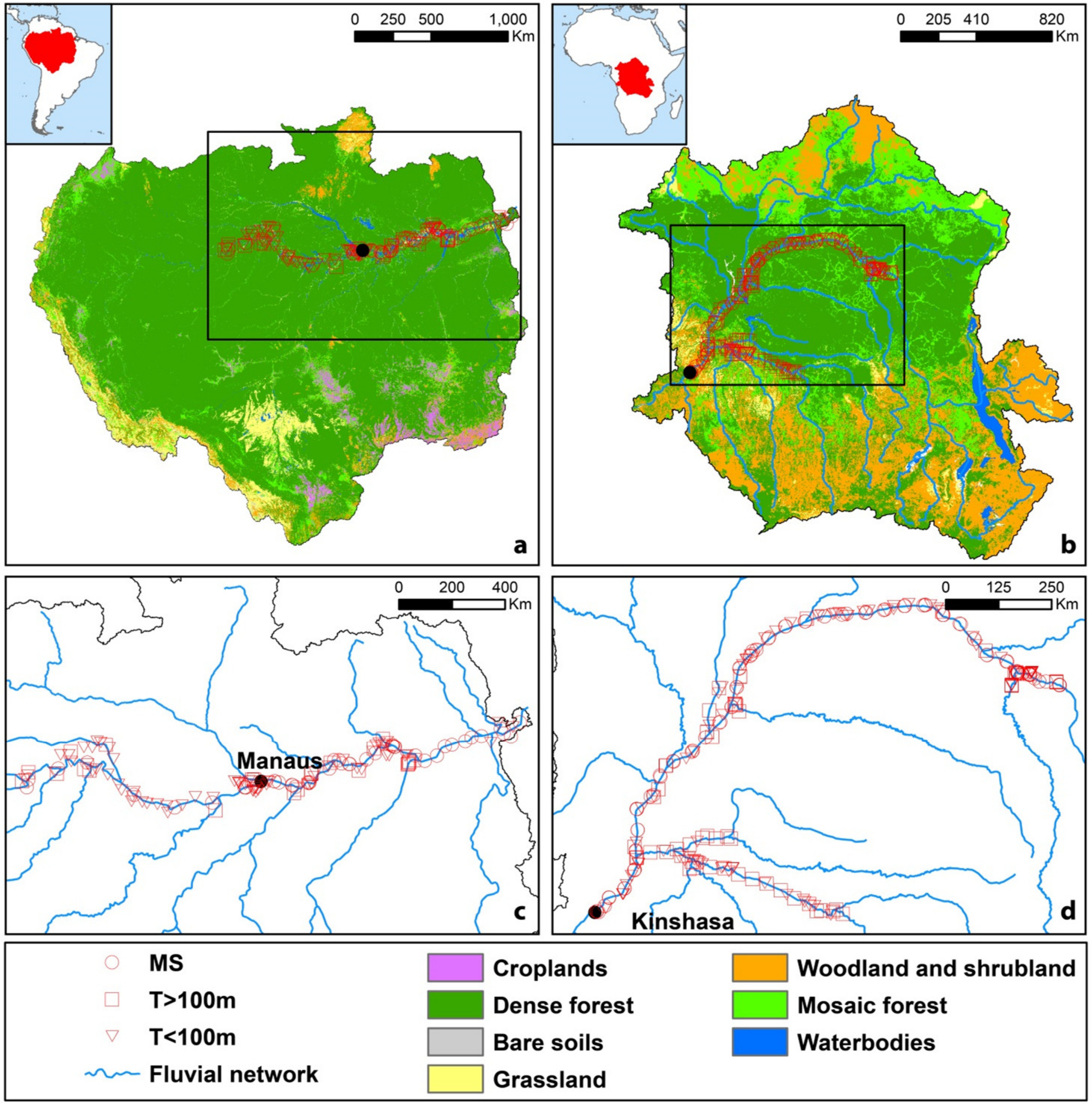

0 250 500 1,000
Km
a
0 205 410 820
Km
b
0 200 400
Km
Manaus
c
0 125 250
Km
Kinshasa
d
MS
T>100m
T<100m
Fluvial network
Croplands
Dense forest
Bare soils
Grassland
Woodland and shrubland
Mosaic forest
Waterbodies

Results

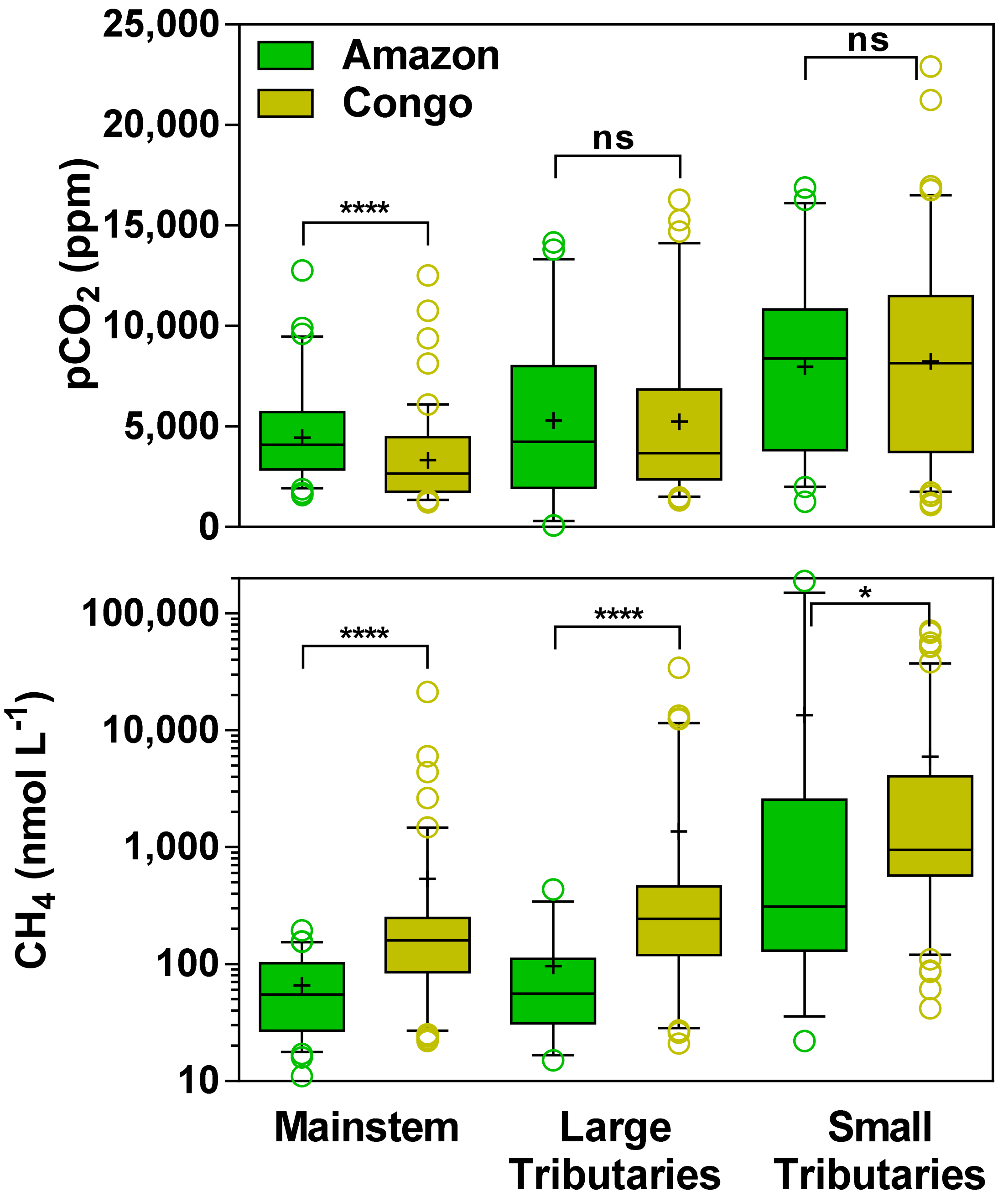

pCO_2 is ± similar

CH_4 is 3-4 times higher in Congo

Results

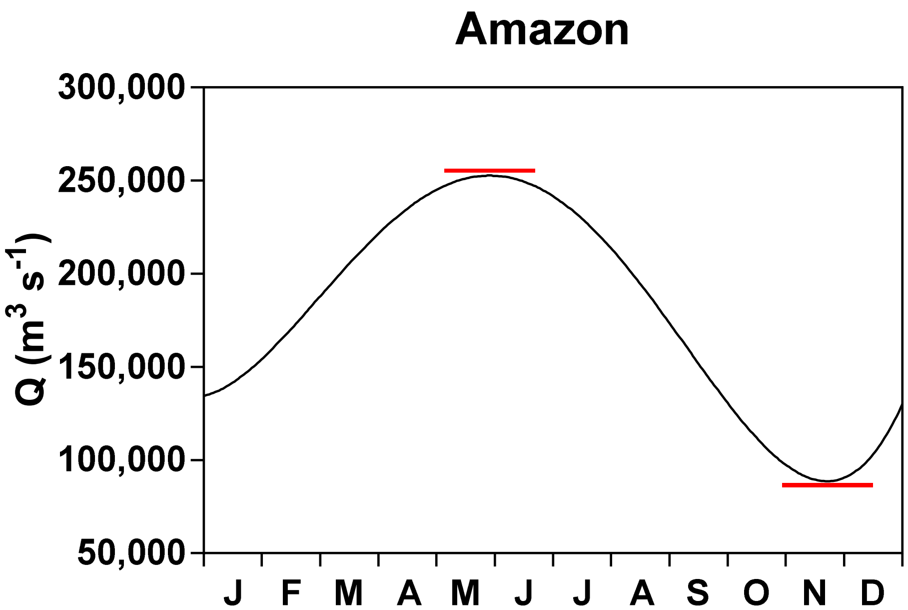

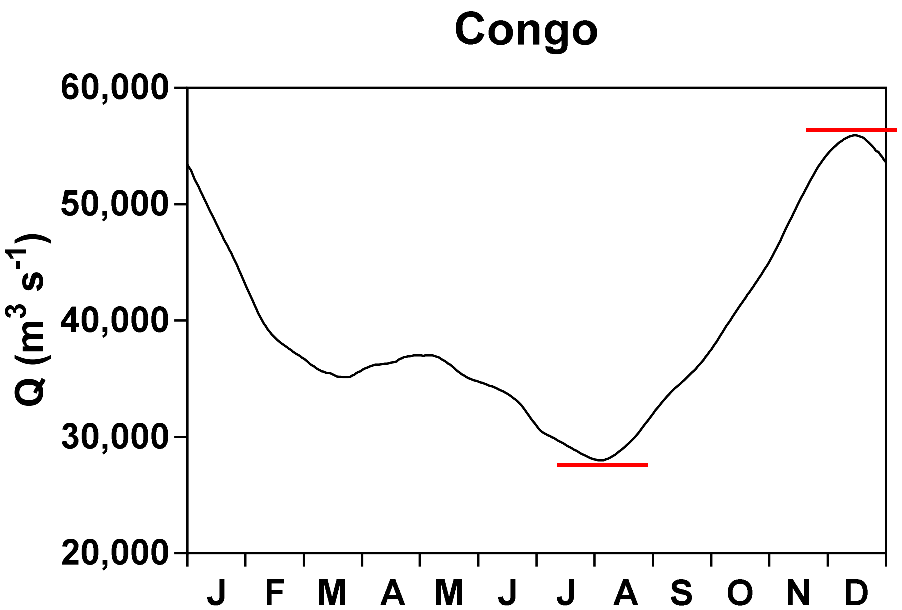

Amazon: $Q_{max}:Q_{min} = 2.85$

$H_{max} - H_{min} = 10\text{-}12$ m

Congo: $Q_{max}:Q_{min} = 1.99$

$H_{max} - H_{min} = 3\text{-}4$ m

Results

Amazon	Congo
Flooded land = 80 % flooded forest Numerous permanent & temporary lakes	Flooded land = 100 % flooded forest Only a few large permanent lakes

Results

Amazon	Congo
Flooded land = 80 % flooded forest Numerous permanent & temporary lakes	Flooded land = 100 % flooded forest Only a few large permanent lakes
Seasonally inundated wetlands	Permanently inundated flooded forest

Results

Amazon	Congo
Flooded land = 80 % flooded forest Numerous permanent & temporary lakes	Flooded land = 100 % flooded forest Only a few large permanent lakes
Seasonally inundated wetlands	Permanently inundated flooded forest
Flooding from river overflow	Wetland water from upland runoff

Results

Amazon	Congo
Flooded land = 80 % flooded forest Numerous permanent & temporary lakes	Flooded land = 100 % flooded forest Only a few large permanent lakes
Seasonally inundated wetlands	Permanently inundated flooded forest
Flooding from river overflow	Wetland water from upland runoff
Macrophytes only present in floodplains	Extensive macrophyte meadows in river channels (mainstem + tributaries)

Explains why CH_4 is 3-4 times higher in Congo

Results

Emissions of greenhouse-gases from Africa & tropics ?

Results

Computation of diffusive CO_2 and CH_4 flux

$F = k\,\Delta CO_2$ or $F = k\,\Delta CH_4$

where *k* is the gas transfer velocity

$k = f\,(\text{turbulence})$

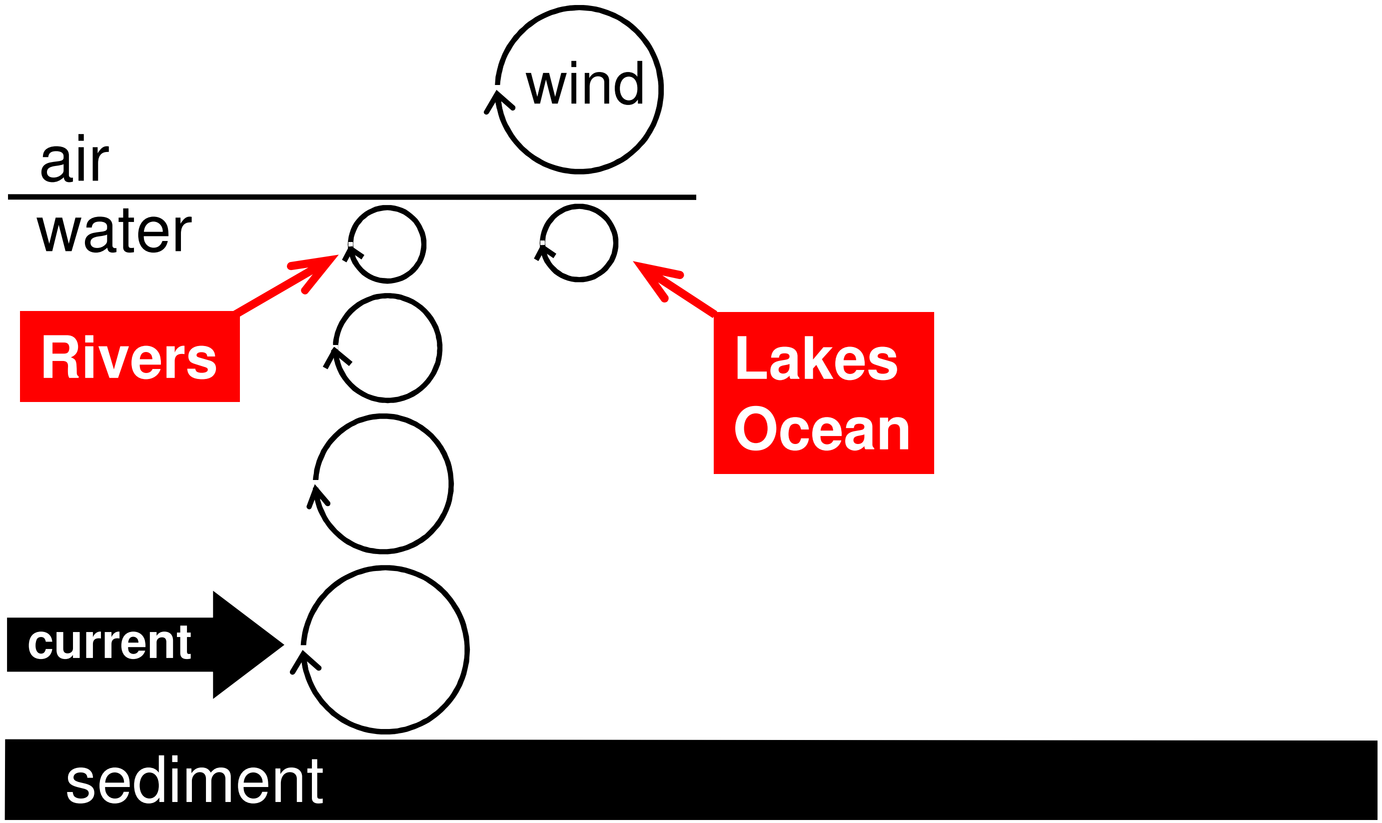

Results

Computation of diffusive CO_2 and CH_4 flux

$F = k\,\Delta CO_2$ or $F = k\,\Delta CH_4$

where k is the gas transfer velocity

Scaling the gas transfer velocity and hydraulic geometry in streams and small rivers

Peter A. Raymond,[1] Christopher J. Zappa,[2] David Butman,[1] Thomas L. Bott,[3] Jody Potter,[4] Patrick Mulholland,[5] Andrew E. Laursen,[6] William H. McDowell,[4] and Denis Newbold[3]

1. $k_{600} = (VS)^{0.89 \pm 0.0.020} \times D^{0.54 \pm 0.030} \times 5037 \pm 604$
2. $k_{600} = 5937 \pm 606 \times (1 - 2.54 \pm 0.223 \times Fr^2) \times (VS)^{0.89 \pm 0.017} \times D^{0.58 \pm 0.027}$
3. $k_{600} = 1162 \pm 192 \times S^{0.77 \pm 0.028} V^{0.85 \pm 0.045}$
4. $k_{600} = (VS)^{0.76 \pm 0.027} \times 951.5 \pm 144$
5. $k_{600} = VS \times 2841 \pm 107 + 2.02 \pm 0.209$
6. $k_{600} = 929 \pm 141 \times (VS)^{0.75 \pm 0.027} \times Q^{0.011 \pm 0.016}$
7. $k_{600} = 4725 \pm 445 \times (VS)^{0.86 \pm 0.016} \times Q^{-0.14 \pm 0.012} \times D^{0.66 \pm 0.029}$

V = stream velocity (m s^{-1})
S = slope
D = depth (m)
Q = discharge ($m^3\ s^{-1}$)
Fr = Froude number = $V/(gD)^{0.5}$

Results

Ebullition of CH_4

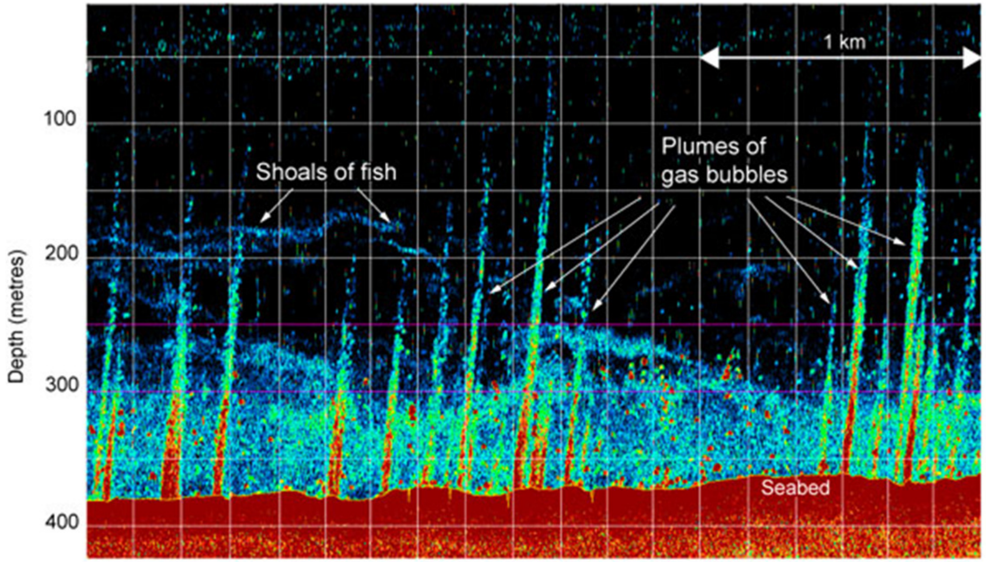

Results

Ebullition of CH_4

Floating chamber

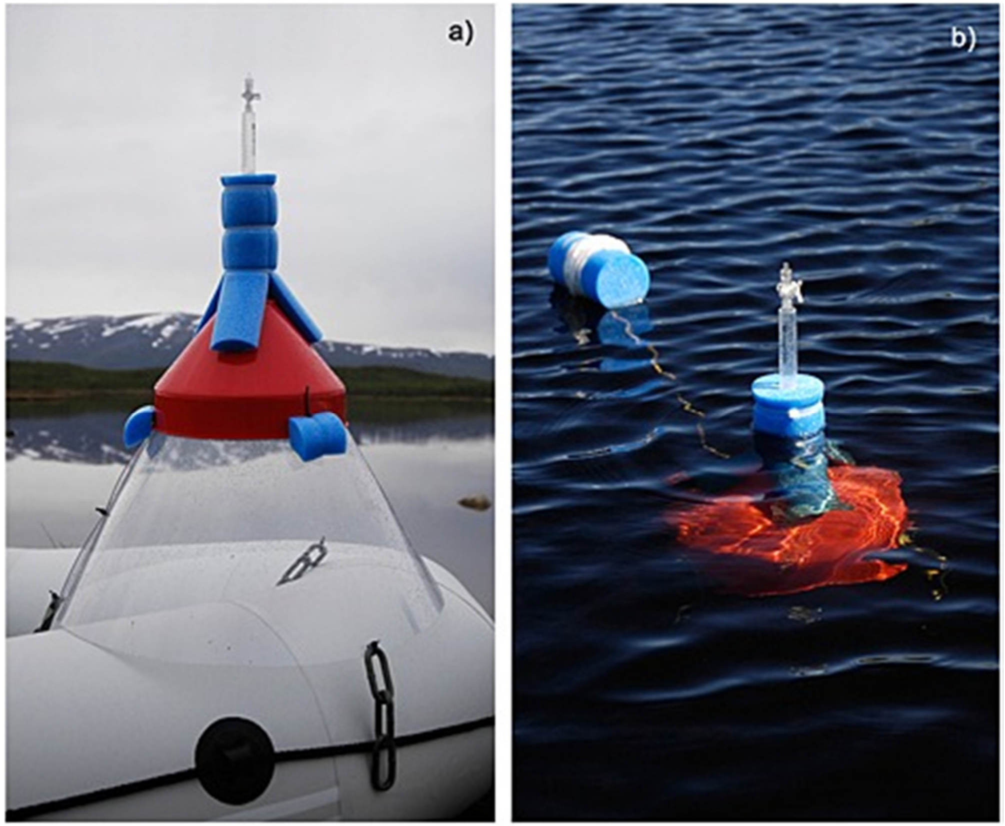

Inverted funnel

Results

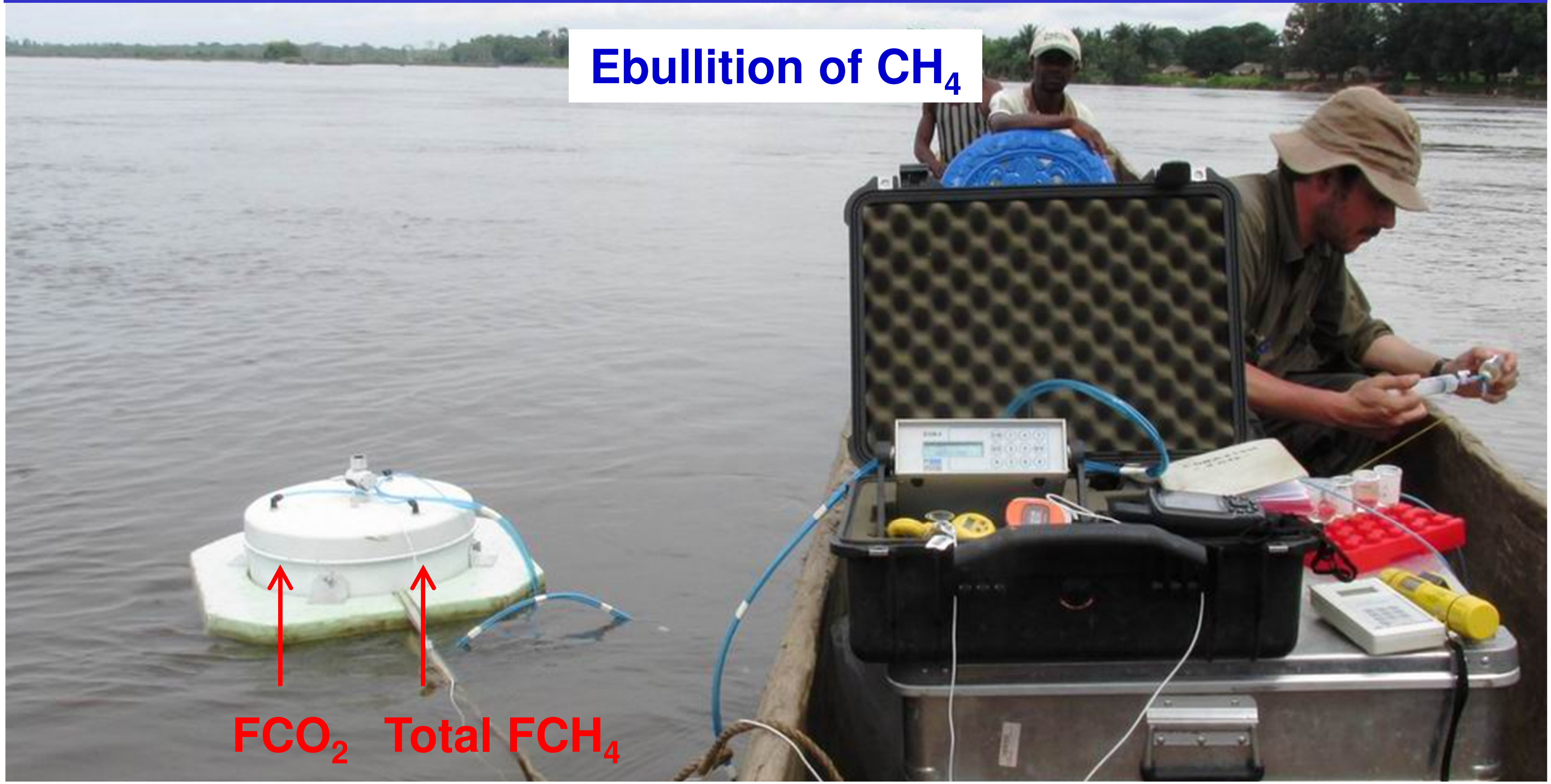

$FCO_2 = k\ \Delta CO_2$

$k = FCO_2 / \Delta CO_2$

Diffusive $FCH_4 = k\ \Delta CH_4$

Total FCH_4 = diffusive FCH_4 + Ebullitive FCH_4

Results

Ebullition of CH_4

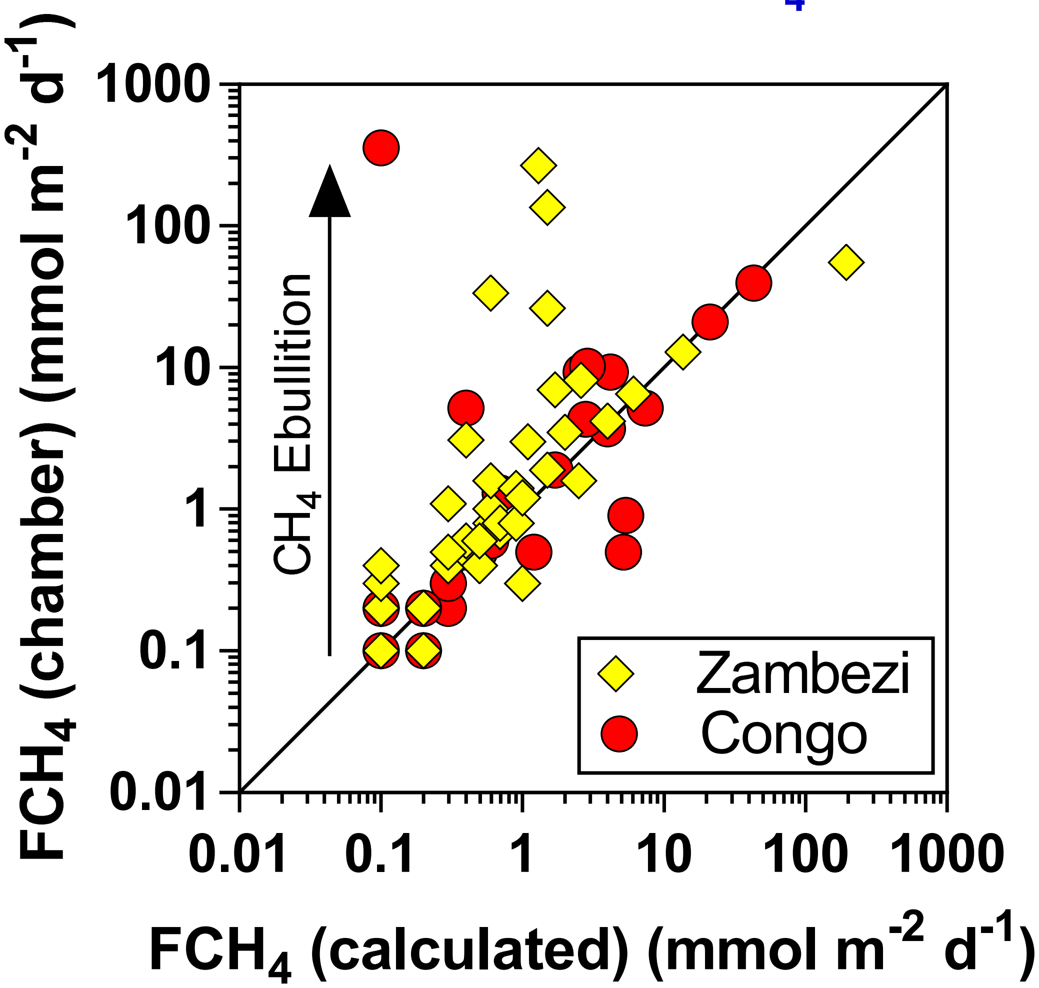

CH_4 ebullition rates = 0.25 x diffusive CH_4 flux (n=68)

Results

Using gas transfer velocity + river/stream areas from GIS of Raymond et al. (2013)

African rivers/streams
CO_2 = 0.27 – 0.36 PgC yr^{-1}
CO_2 + CH_4 = 0.31 – 0.42 PgC yr^{-1} ($CO_{2\ equivalents}$)

A full greenhouse gases budget of Africa: synthesis, uncertainties, and vulnerabilities

R. Valentini[1,2], A. Arneth[3], A. Bombelli[2], S. Castaldi[2,4], R. Cazzolla Gatti[1], F. Chevallier[5], P. Ciais[5], E. Grieco[2], J. Hartmann[6], M. Henry[7], R. A. Houghton[8], M. Jung[9], W. L. Kutsch[10], Y. Malhi[11], E. Mayorga[12], L. Merbold[13], G. Murray-Tortarolo[15], D. Papale[1], P. Peylin[5], B. Poulter[5], P. A. Raymond[14], M. Santini[2], S. Sitch[15], G. Vaglio Laurin[2,16], G. R. van der Werf[17], C. A. Williams[18], and R. J. Scholes[19]

Sink of C = 0.6 PgC yr^{-1}
Off-set by 2/3 !

Results

Using gas transfer velocity + river/stream areas from GIS of Raymond et al. (2013)

African rivers/streams

$CO_2 = 0.27 – 0.36$ PgC yr^{-1}

$CO_2 + CH_4 = 0.31 – 0.42$ PgC yr^{-1} ($CO_{2\ equivalents}$)

Cuvette Centrale Congolaise (wetland)

$CO_2 = 0.39$ PgC yr^{-1}

$CO_2 + CH_4 = 0.62$ PgC yr^{-1} ($CO_{2\ equivalents}$)

Cuvette Centrale Congolaise + rivers/streams

$CO_2 + CH_4 = 0.93 – 1.04$ PgC yr^{-1} ($CO_{2\ equivalents}$)

Results

Global anthropogenic CO_2 fluxes in 2010 ($PgC\ y^{-1} = 10^{15}\ gC\ y^{-1}$)

9.1±0.5 $PgC\ y^{-1}$

0.9±0.7 $PgC\ y^{-1}$ +

5.0±0.2 $PgC\ y^{-1}$
50%

2.6±1.0 $PgC\ y^{-1}$
26%
Calculated as the residual of all other flux components

24%
2.4±0.5 $PgC\ y^{-1}$
Average of 5 models

www.globalcarbonproject.org/

Results

African rivers/streams

CO_2 = 0.27 – 0.36 PgC yr^{-1}

Where's the CO_2 coming from ?

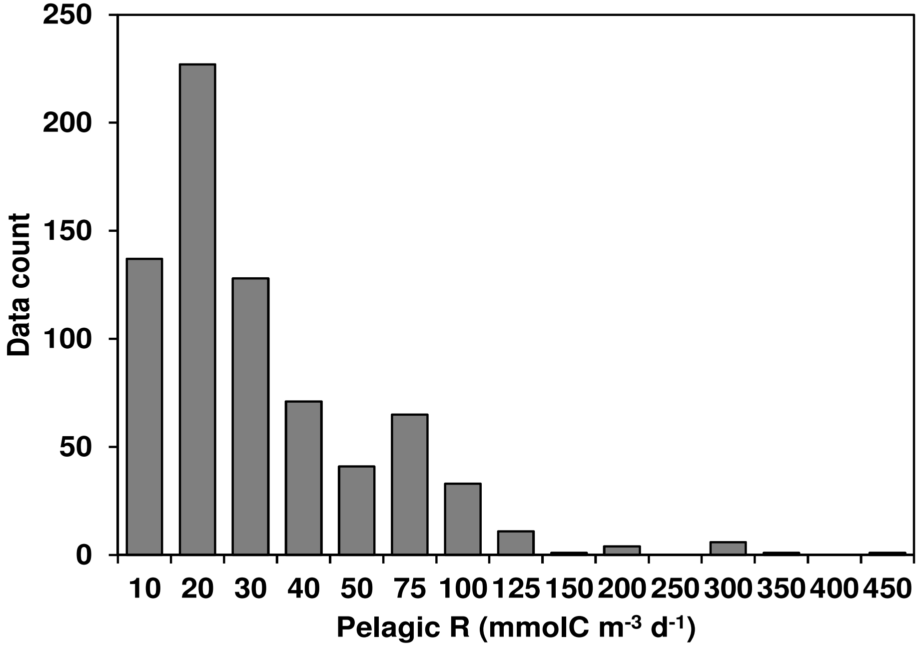

>800 aquatic community respiration (R)

median R was 99.4 mmolC m^{-2} d^{-1}

Upscaled → 11% of the CO_2 emission from rivers

CO_2 emission from rivers sustained by external CO_2 inputs (wetlands or soils)

Results

Using gas transfer velocity + river/stream areas from GIS of Raymond et al. (2013)

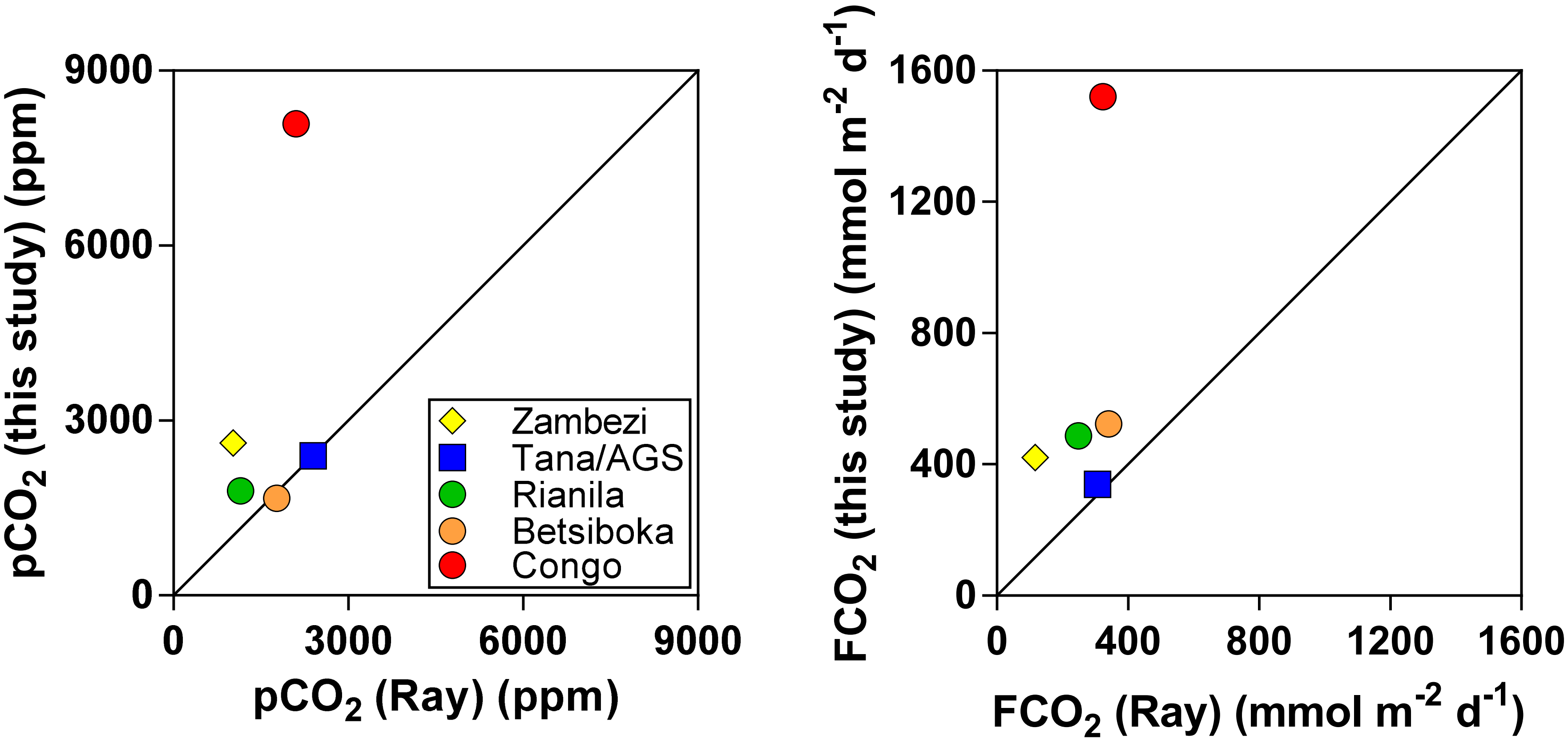

Results

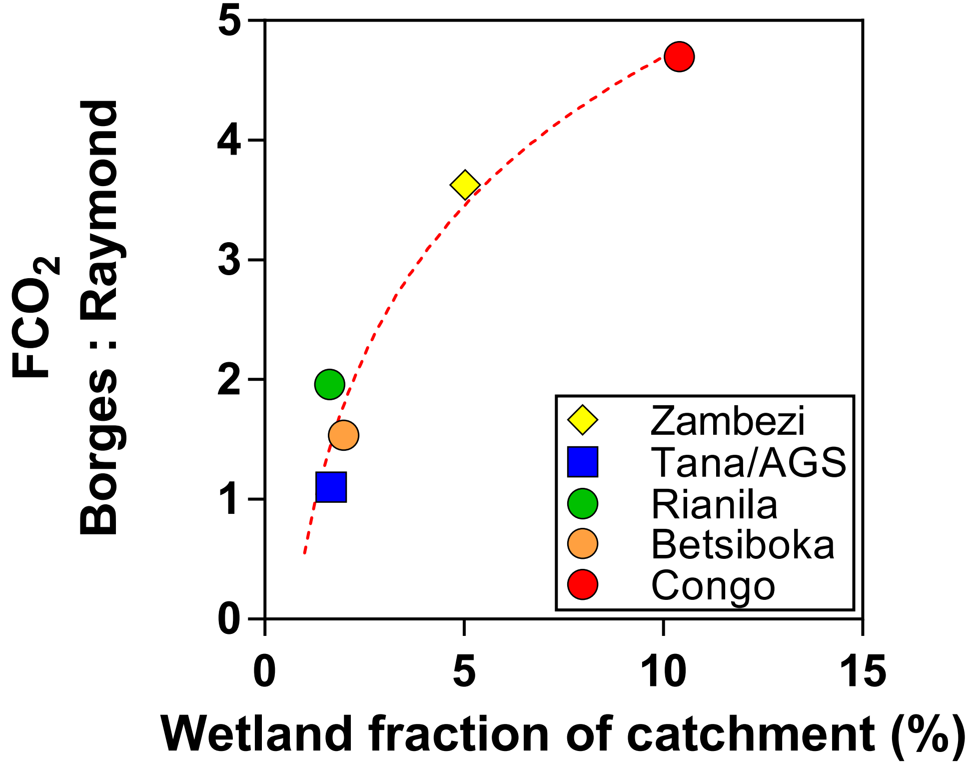

FCO2
Borges : Raymond
5
4
3
2
1
0
0
5
10
15
Wetland fraction of catchment (%)
Zambezi
Tana/AGS
Rianila
Betsiboka
Congo

Field versus model data in the Congo River

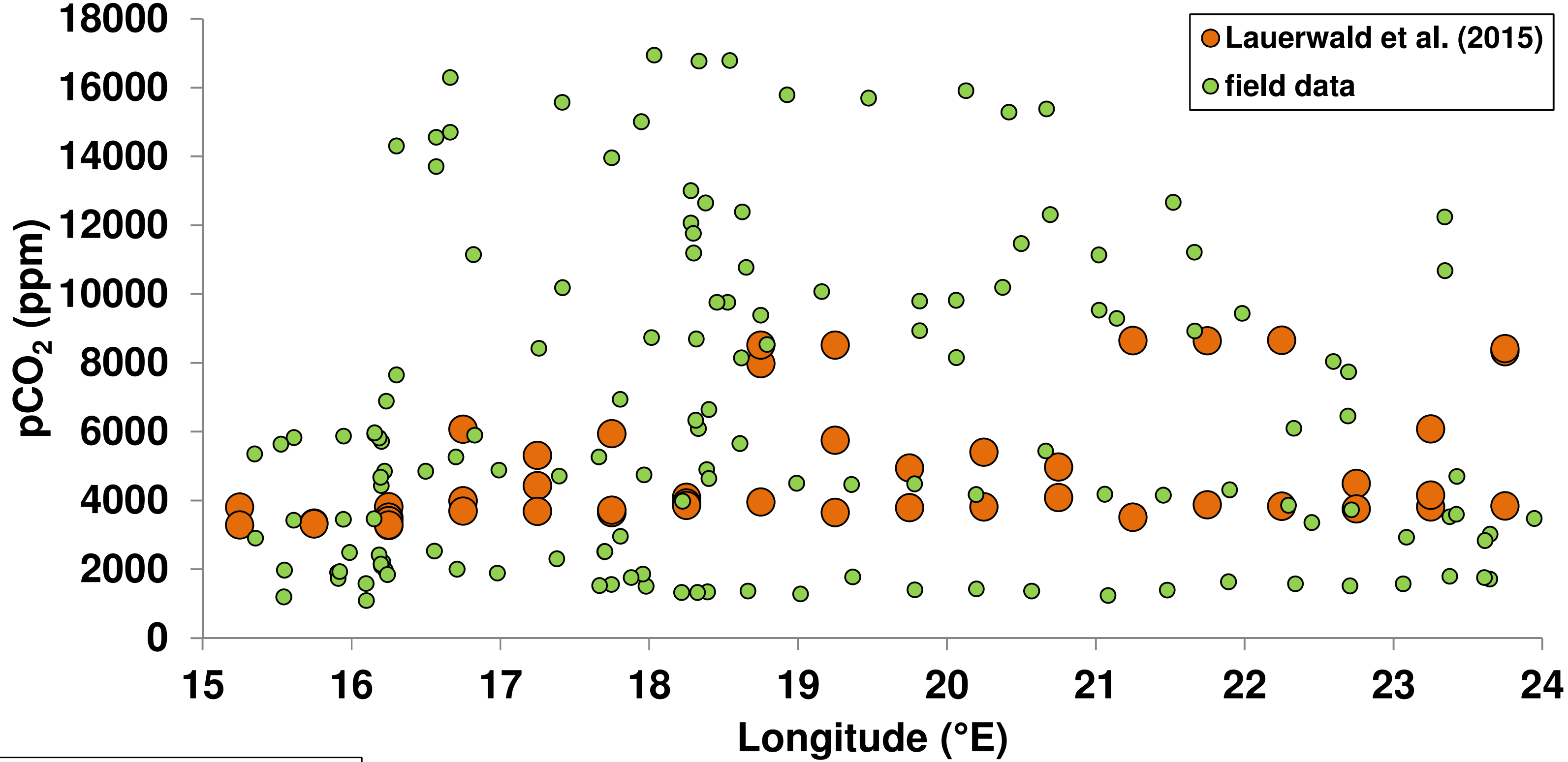

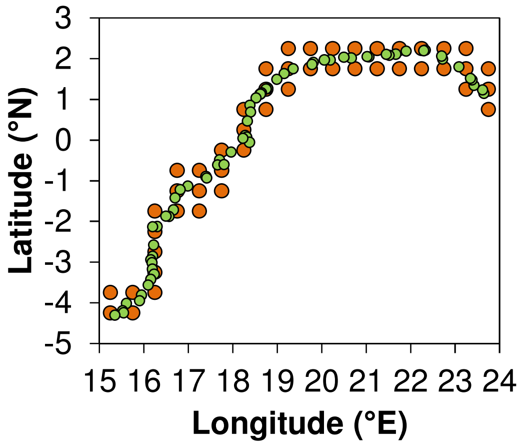

Model $\overline{pCO_2}$ = 4850 ppm

Field $\overline{pCO_2}$ (mainstem) = 1870 – 4500 (FW – HW)

Field $\overline{pCO_2}$ (tributaries) = 7925 – 8250 (FW – HW)

Results

Using gas transfer velocity + river/stream areas from GIS of Raymond et al. (2013) + GLWD (Lehner & Döll 2003)

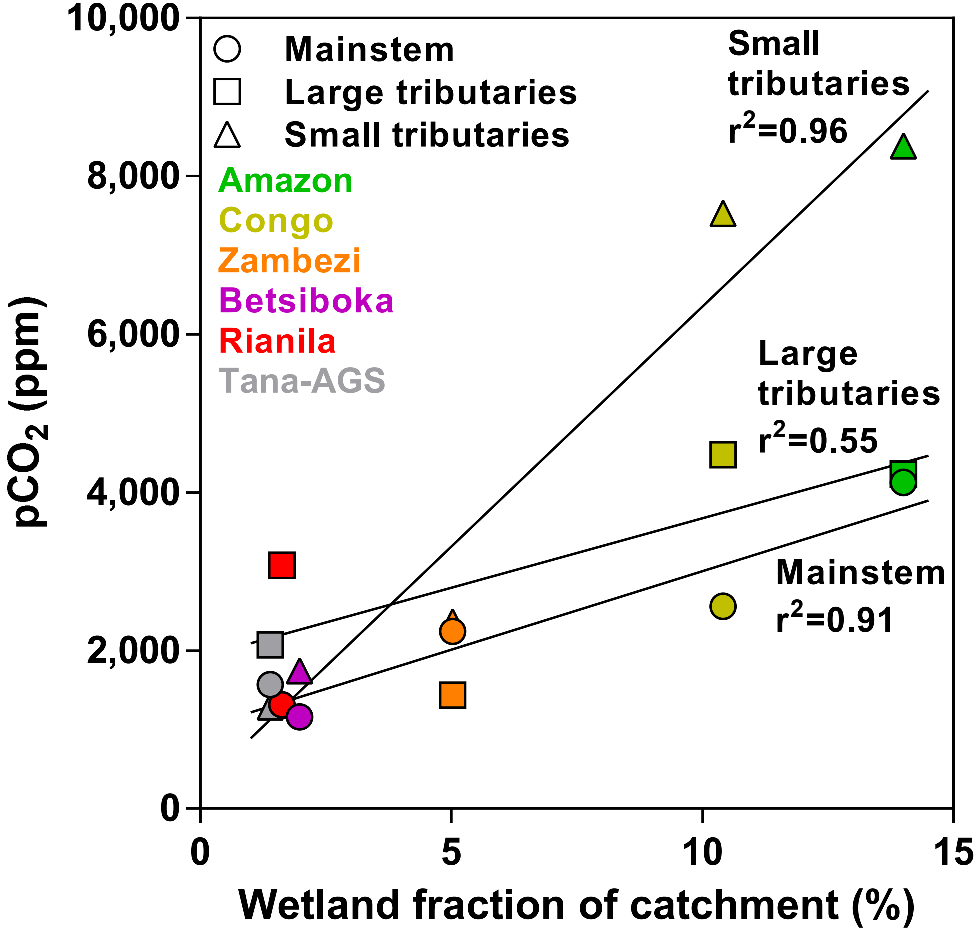

CO_2 emissions from tropical rivers = 1.8 PgC yr^{-1}

Raymond et al. (2013) 1.4 PgC yr^{-1}

Lauerwald et al. (2015) 0.5 PgC yr^{-1}

Further Reading

nature geoscience
ARTICLES
PUBLISHED ONLINE: 20 JULY 2015 | DOI: 10.1038/NGEO2486

Globally significant greenhouse-gas emissions from African inland waters

Alberto V. Borges[1]*, François Darchambeau[1], Cristian R. Teodoru[2], Trent R. Marwick[2], Fredrick Tamooh[2,3], Naomi Geeraert[2], Fredrick O. Omengo[2], Frédéric Guérin[4], Thibault Lambert[1], Cédric Morana[2], Eric Okuku[2,5] and Steven Bouillon[2]

www.nature.com/scientificreports

SCIENTIFIC REPORTS

OPEN

Divergent biophysical controls of aquatic CO_2 and CH_4 in the World's two largest rivers

Received: 07 July 2015
Accepted: 29 September 2015
Published: 23 October 2015

Alberto V. Borges[1], Gwenaël Abril[2,3], François Darchambeau[1], Cristian R. Teodoru[4], Jonathan Deborde[2], Luciana O. Vidal[5], Thibault Lambert[1] & Steven Bouillon[4]

Acknowledgments

François Darchambeau, Thibault Lambert
University of Liège (Belgium)

Steven Bouillon, Cristian R. Teodoru, Trent R. Marwick, Fredrick Tamooh, Naomi Geeraert, Fredrick O. Omengo, Cédric Morana, Eric Okuku
KULeuven (Belgium)

Frédéric Guérin
IRD (France)

Gwenaël Abril
CNRS, IRD, UFF

Acknowledgments

European Research Council (ERC)

Fonds National de la Recherche Scientifique (FNRS)

Federal Public Planning Service Science Policy (BELSPO)